Vitamin A Modulation of Hepatic Retinoid and Triglyceride Metabolism

by

Emily Sarah Sugars

A thesis submitted in partial fulfillment of the requirements for the degree of

Master of Science

Department of Physiology
University of Alberta

Abstract

Introduction: Vitamin A is an essential dietary micronutrient and its active metabolite all-*trans* retinoic acid is a key regulator of both hepatic retinoid and hepatic lipid homeostasis. Retinoic acid is a potent transcriptional regulator with more than 500 proposed target genes, however the tissue, dose, and sex-dependent variation in these genes remains unclear. A protective effect has been proposed for retinoic acid on metabolic-dysfunction associated steatotic liver disease, a disease characterised by the pathophysiological accumulation of triacylglycerol in the liver. This study aims to develop a more holistic understanding of retinoic acid responsive genes in the liver and the interaction between hepatic retinoid and lipid metabolism.

Methods: Changes in mRNA expression were quantified by whole-genome microarray in male C57BL/6 mice, four hours after a 30 mg/kg dose of retinoic acid. The most up and downregulated genes and key retinoid metabolic genes were then assessed by RT-qPCR in female and male mice following another 30 mg/kg dose of retinoic acid, and female and male mice after long term dietary vitamin A manipulation. The effects of obstructed retinoic acid signalling on gene expression, retinoid, and triacylglycerol homeostasis were examined through a hepatocyte specific, dominant negative retinoic acid receptor mice (Alb-cre$^{+/-}$:RARdn$^{fl/-}$).

Results and Conclusions: Three-hundred and thirty one genes were identified by microarray as differentially expressed following retinoic acid administration, with downregulation of lipogenic genes. The retinoic acid specific hydrolase CYP26A1 was upregulated by retinoic acid and high dietary vitamin A in both females and males, and downregulated when the retinoic acid receptor was obstructed. Alb-cre$^{+/-}$:RARdn$^{fl/-}$ mice had increased circulating retinol, decreased circulating triacylglycerol, and did not accumulate triacylglycerol in the liver when fasted.

Preface

This thesis is an original work by Emily Sugars. The research project, of which this thesis is a part, received research ethics approval from the University of Alberta Research Ethics Board, Project Name “Experimental manipulation of vitamin A homeostasis No. 2966”. The RNA Microarray in Chapter 4: Microarray Analysis of Hepatic Gene Expression in Response to Acute Retinoic Acid Exposure was completed in collaboration with the Alberta Transplant Applied Genomics Centre. Some of the work in Chapter 5: Sex Differences in Hepatic Response to Acute Retinoic Acid Exposure and Long Term Dietary Vitamin A Manipulation was conducted by Nicole Applin. Quantification of retinoids and triacylglycerol in Chapter 5: Sex Differences in Hepatic Response to Acute Retinoic Acid Exposure and Long Term Dietary Vitamin A Manipulation and Chapter 6: Hepatocyte Specific Knock-in of Dominant Negative Retinoic Acid Receptor Alters Retinoid and Triacylglycerol Homeostasis was completed by Samantha Kinney. No part of this thesis has been previously published.

Dedication

For Addison, who joined me in utero for the completion of much of this research.

Acknowledgements

This research was generously funded by the Canada Graduate Scholarship – Master's program Natural Sciences and Engineering Research Council of Canada. This thesis would not have been possible without support from many people.

Thanks to my supervisor, Dr. Robin Clugston, for nearly five years of patient and knowledgeable mentorship.

Thanks to all the members, past and present, of the Clugston laboratory, with particular thanks to Samantha Kinney and Nicole Applin who supported the continuation of this project while I was on maternity leave.

Thanks to my committee members Dr. Elaine Leslie and Dr. Rene Jacobs for their valuable advice, feedback, and flexibility.

Finally, thanks to my family for unwavering encouragement.

Table of Contents

List of Tables

List of Figures

Chapter 1: General Introduction

1.1 Vitamin A

Vitamin A, or all-*trans*-retinol (retinol), is an essential micronutrient with critical importance in several physiological processes. Specifically, evidence has recently emerged suggesting an important role for vitamin A in liver disease, although exactly how this happens is unclear (1). Vitamin A is obtained through the diet as either preformed vitamin A in animal products, or provitamin A carotenoids – mainly beta-carotene – in brightly coloured fruits and vegetables (2). Both in Canada and globally, vitamin A deficiency persists despite overall advances in nutrient availability (3, 4). Upwards of $500 million USD is spent world-wide annually in attempt to address vitamin A deficiency, primarily through universal supplementation and staple-food fortification programs (5).

Vitamin A exerts its effects through the active metabolite all-*trans*-retinoic acid (RA), a potent transcriptional regulator. RA acts by binding to the retinoic acid receptor (RAR), which dimerizes with the retinoid X receptor (RXR) and binds to retinoic acid response elements (RAREs) in the promoter regions of target genes (6). RA binding to RAR recruits a co-activator or co-repressor protein complex, thereby inducing or suppressing transcription of the target gene. Three isoforms of RAR – alpha, beta, and gamma – work together to drive RA signalling with tissue and developmental specificity.

More than 500 genes have been proposed as regulatory targets of RA (7). This, as well as the variety of processes affected by RA signalling, necessitates that cellular levels of RA are tightly regulated through negative feedback. Excess RA is broken down by cytochrome P450 26 family enzymes (CYP26). Two isoforms, CYP26A1 and CYP26B1, are responsible for the majority of RA breakdown in the adult. The enzymes in the retinoid catabolic pathway are some

of the most significant transcriptional targets of RA. RA directly induces *Cyp26* expression through the RAR, maintaining cellular RA levels under tight homeostatic control (6).

The liver is the central hub for whole body vitamin A metabolism. More than 80% of whole body vitamin A is stored as retinyl esters (RE), an inactive storage form, in hepatic stellate cells (HSCs); a specialized cell type that make up less than 10% of cells in the liver but contain more than 90% of the liver's vitamin A stores. When dietary vitamin A is abundant, excess retinol is converted to RE by lecithin:retinol acyltransferase (LRAT). Conversely, when dietary vitamin A is insufficient the liver mobilizes these stores to maintain a steady supply of vitamin A to the body (9).

1.2 Metabolic Dysfunction Associated Steatotic Liver Disease

Metabolic dysfunction associated steatotic liver disease (MASLD, previously known as non-alcoholic fatty liver disease or NAFLD) is characterized by increased lipid accumulation in hepatocytes and is associated with a variety of health complications (10,11). MASLD is the most common chronic liver disease in the world, affecting an estimated 24% of the global population, and its prevalence has continued to increase over recent years (12). The current paradigm involves a combination of overnutrition and increased adiposity with genetic predisposition and susceptibility to oxidative stress and inflammation (13). Although often discussed specifically in the context of obesity – as many as 90% of morbidly obese individuals may present with MASLD and obesity is associated with a 7-fold increase in its incidence – the disease also has prevalence in the non-obese population, particularly in those with pre-existing metabolic conditions (14).

Initially, simple steatosis of the hepatocytes is relatively benign as the liver is physiologically evolved for ectopic lipid storage. However, when left unchecked lipotoxic, non-esterified fatty acids cause oxidative stress and inflammation, leading to fibrosis and disease progression from simple steatosis to metabolic dysfunction-associated steatohepatitis (MASH) and, eventually, cirrhosis or hepatocellular carcinoma (HCC; 15, 16). A hallmark of MASLD progression is the loss of hepatic vitamin A stores, as HSCs are activated by lipotoxic extracellular vesicles leading to the excessive extracellular matrix production that causes fibrosis (17, 18). Previous research has proposed a protective role for retinoic acid against the development and progression of MASLD, although the mechanism remains unclear (19, 20, 21).

1.3 Hypothesis and Goal

The overall objective of this research is to gain a more holistic understanding of hepatic retinoid signalling and its potential impact on lipid metabolism and liver disease. This will be investigated through two specific research aims. Aim 1 is to develop a knowledgebase of hepatic RA responsive genes, testing the hypothesis that RA will alter a variety of genes involved in vitamin A and lipid metabolism. Aim 2 is to describe the phenotype of a transgenic mouse model expressing a hepatocyte-specific dominant negative retinoic acid receptor, to test the hypothesis that impairing RA signalling will alter hepatic retinoid status, which may subsequently affect both whole-body retinoid homeostasis and hepatic lipid homeostasis.

1.4 Experimental Plan

1.4.1 Aim 1 – Building a knowledgebase of hepatic retinoic acid responsive genes

While many genes have been identified as responsive to RA, tissue specificity, dose dependency, discrimination between directly and indirectly responsive genes, and sex differences are yet to be elucidated (7). To address this, we assessed the liver-specific changes in gene expression, *in vivo*, across a variety of RA signalling models in female and male mice. Firstly, we used an RNA microarray to capture an unbiased view of genes responsive to an acute pharmacological dose of RA (Chapter 4). We then contrasted the acute pharmacological response with a model of long term, dietary vitamin A manipulation (Chapter 5), quantifying changes in gene expression with real time quantitative polymerase chain reaction (RT-qPCR). Finally, we established a transgenic mouse model expressing a dominant negative retinoic acid receptor in hepatocytes (Chapter 6) to gain insight on the differences between activating and inhibiting RAR signalling, and begin to isolate genes directly versus indirectly regulated by the retinoic acid receptor.

Many of the genes previously identified *in vitro* as responsive to RA are important in lipid metabolism. This, along with the correlation between hepatic vitamin A and MASLD, founded our hypothesis that RA will alter a variety of genes involved in both vitamin A and lipid metabolism.

1.4.2 Aim 2 – Phenotypic Description of Alb-cre$^{+/-}$:RARdn$^{fl/-}$ mouse

It has been more than thirty years since the original RAR transgenic mice were developed (22, 23). Since then, genetic interference of RAR signalling has been studied in various germline,

adult-onset, whole-body, and tissue-specific models. To further investigate the phenotypic effects of impaired RAR signalling, we employed a novel application of RARaT403 – a potent dominant negative isoform of RARα (24). By expressing RARaT403 exclusively in the hepatocytes of mice, we quantified the changes in whole body retinoid and triacylglycerol homeostasis driven specifically by hepatic RAR signalling, in contrast to the effects of RARaT403 expressed in adipose that have been previously reported (25).

1.5 Rational and Significance

The overall goal of building a more holistic understanding of hepatic vitamin A signalling will address several limitations in the current body of research. By integrating multiple modalities for testing RA signalling – acute and chronic, stimulation and inhibition, females and males – we can begin to isolate tissue, dose, and sex specific effects. Despite increased effort in recent years to consider biological sex as an important variable, the inclusion of female subjects in research remains inadequate. Limited research supports that retinoid signalling and its regulation may be different in females and males (26). Further, prevalence, clinical presentation, and disease progression of MASLD varies between sexes (27).

Genome-wide RNA microarray provides a powerful tool for unbiased analysis of responsive genes, allowing for both identification of novel RA responsive genes and application to pathway analysis for novel physiological insight, which may support the hypothesised interaction between retinoid and lipid metabolism.

There are significant health implications to this research highlighted by three facts: *i*) Vitamin A deficiency persists as a significant global health problem. *ii*) There is an emerging

link between vitamin A deficiency, abnormal vitamin A signalling, and MASLD. *iii*) Health care systems world-wide are largely unprepared for the increasing prevalence of chronic diseases, and treatments remain limited – particularly in low and middle income countries that are both more recently adapting to the epidemiological transition with limited resources and where vitamin A deficiency is more common. Thus, improving our understanding of fundamental vitamin A metabolism and its interaction with lipid metabolism and metabolic disease could have a significant impact on human health.

Chapter 2: Literature Review

2.1 Review of Vitamin A Metabolism

2.1.1 Dietary retinoids, Absorption, and Uptake

Vitamin A is the most commonly known in a class of structurally and functionally related molecules called retinoids. Strictly speaking, vitamin A refers to all-*trans*-retinol (retinol), a fat-soluble compound first discovered more than 100 years ago (28). Retinoids exist in several forms due to the variable stability, solubility, and potency of the compounds, and must be obtained through the diet as *de novo* synthesis is not possible in animals. The fundamental principle of retinoid physiology is the dynamic cycling between forms to uphold homeostasis (Figure 1). Excessive retinoic acid (RA) must be avoided due to its potency and free retinol degrades too rapidly for long term storage, yet sufficient intracellular levels must be maintained for functionality. Consequently, less than 0.01% of total dietary retinoid is RA (29).

Pro-vitamin A carotenoids, primarily beta-carotene, are the most abundant retinoid source in plants. Beta-carotene is absorbed by intestinal enterocytes and packaged into postprandial chylomicrons either directly or after conversion to retinyl esters (RE), the main storage form in animals. Conversely, when dietary vitamin A is obtained through animal sources it is found preformed as either retinol or RE. Intestinal lumen RE are first converted to retinol by retinyl ester hydrolases for absorption across the plasma membrane, then re-esterified alongside dietary retinol for chylomicron packaging. Chylomicron remnants reach the liver after exocytosis into the lymphatic system and subsequent entry into the circulation (30). Approximately 75% of dietary retinoids are absorbed by the liver for hepatic use and storage.

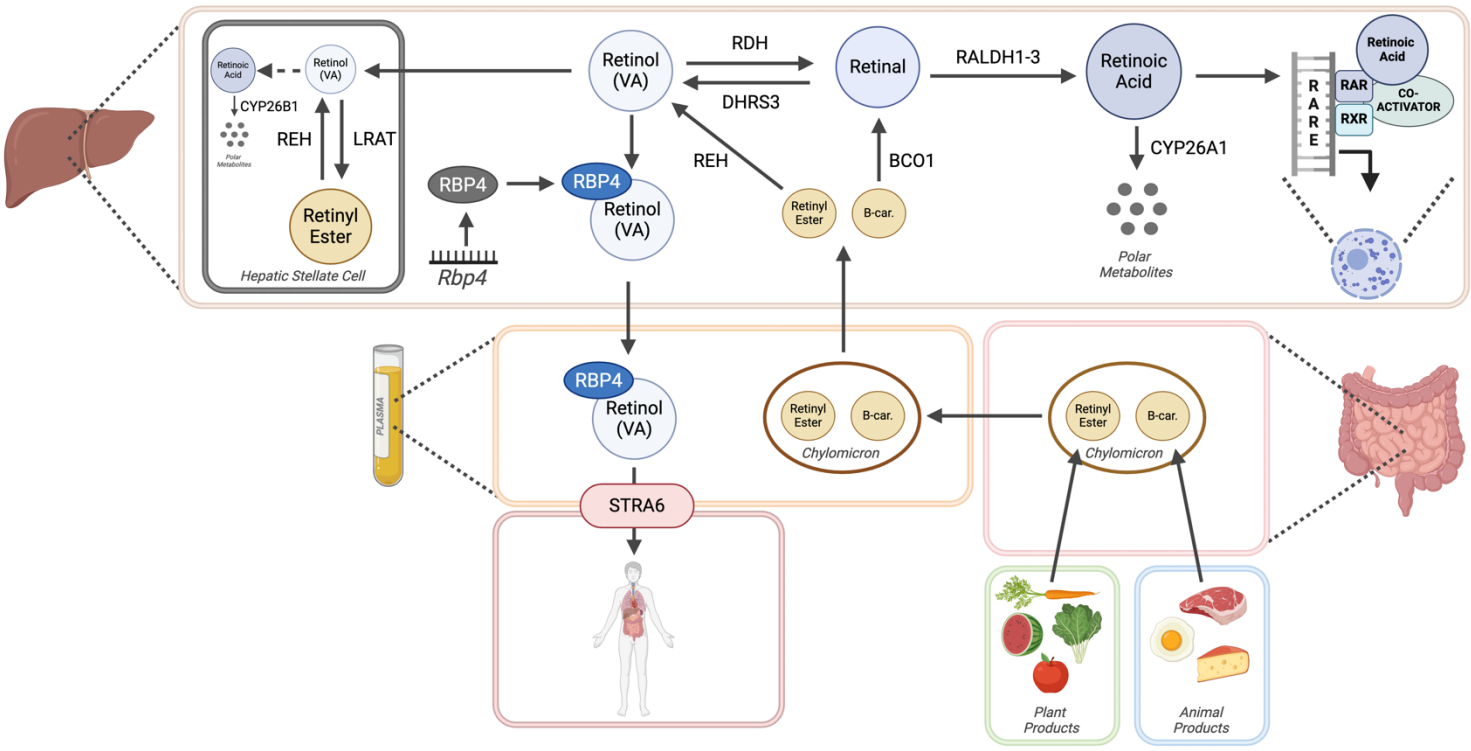

Figure 1. Schematic overview of vitamin A metabolism. Dietary retinoids are packaged into chylomicrons and taken up by the liver from the circulation. Vitamin A (retinol) is converted into the active metabolic retinoic acid (RA) through a two-step process involving retinaldehyde (retinal) as an intermediate. RA binds to the retinoic acid receptor (RAR) in the nucleus to exert its effects on gene expression. Retinol is either exported bound to retinol binding protein 4 (RBP4) for use by extrahepatic tissues, or transported to hepatic stellate cells (HSCs) for storage as retinyl ester (RE). Excess retinoids are disposed of by CYP26 hydrolysis of RA.

2.1.2 Hepatic Vitamin A Metabolism

The liver is the central hub for whole body vitamin A homeostasis. In rodents fed vitamin A sufficient diets 80 - 90% of whole-body retinoid is found in the liver, although this decreases drastically with vitamin A deficiency when hepatic supplies are mobilised to meet the needs of peripheral tissues (31). Within the liver, retinoids are first taken up by hepatocytes and liberated from chylomicron remnants. RE are hydrolyzed to retinol by retinyl ester hydrolase and β-carotene is cleaved by beta-carotene oxygenase 1 (BCO1), forming two molecules of retinaldehyde that can be reduced to retinol (32, 33).

Intracellular retinol has several fates, dictated by proliferative and metabolic need and substrate availability (Figure 1). A family of binding proteins exist to carry the liposoluble retinoids in aqueous environments such as the cytoplasm or blood. Notably, retinol binding protein 4 (RBP4) binds retinol and is secreted into the plasma for circulation to extrahepatic tissues (34). Retinol is also converted to RA for transcriptional regulation within hepatocytes by a two-step process: reversible oxidation to retinaldehyde by retinol dehydrogenase (RDH) followed by irreversible oxidation to RA by retinaldehyde dehydrogenase (RALDH). Excess retinol is transferred to hepatic stellate cells (HSCs) and esterified with long chain fatty acids by lecithin retinol acyl transferase (LRAT) to form RE for storage. Although seemingly redundant, dietary RE must be first hydrolyzed to retinol before shuttling to HSCs and subsequent re-esterification; the mechanism of hepatocyte-HSC retinol transport is unknown (35).

The HSC is a specialized cell type that make up less than 10% of cells in the liver but contain more than 90% of the liver's vitamin A stores (9). Large cytoplasmic lipid droplets are the distinctive feature of HSCs, which contain a significantly larger retinoid proportion and

lower triglyceride proportion than adipocyte or hepatocyte localised droplets (36). When needed, RE are hydrolyzed and retinol is transferred back to hepatocytes and mobilised bound to RBP4. It is through this key mechanism that whole-body vitamin A homeostasis is maintained during times of low vitamin A availability. Several candidate retinyl ester hydrolases have been proposed in HSCs, but clear evidence of substantial RE hydrolysis *in vivo* is yet to be achieved for any enzyme (37, 38, 39).

RA itself is irreversibly degraded by cytochrome P450 (CYP) enzymes. While some non-specific CYPs are capable of RA catabolism, three isoforms of CYP26 family enzymes – CYP26A1, CYP26B1, CYP26C1 – are retinoic acid-specific hydrolases (6, 40). CYP26A1 and CYP26B1 are responsible for the majority of RA clearance in the adult, while CYP26C1 is primarily expressed embryonically (41). Knock-out mouse models *Cyp26a1*$^{-/-}$ and *Cyp26b1*$^{-/-}$ are gestationally and neonatally lethal, clearly demonstrating the necessity of strict RA regulation (42, 43). Within the liver, it is hypothesised that CYP26A1 functions primarily in hepatocytes and CYP26B1 in HSCs due to the cell-type specific expression pattern of the isoforms (44).

2.1.3 Retinoic Acid Signalling

All-*trans*-RA is the endogenous ligand for the retinoic acid receptor (RAR), a nuclear receptor and transcription factor for more than 500 target genes (7). Three isoforms of RAR – alpha, beta, and gamma – work together to drive RA signalling with tissue and developmental specificity (8). The canonical mechanism of RA signalling is as follows: Unliganded RAR is localized to the nucleus, heterodimerized with the retinoid X receptor (RXR) and bound to conserved sequences in the promoters of target genes termed retinoic acid response elements

(RAREs; 45). RA enters the nucleus and binds RAR, inducing a conformational change that recruits a co-activator or co-repressor protein complex to induce or suppress transcription of the target gene (46).

The proteins in the retinoid metabolic pathway themselves are highly regulated by RA. *Cyp26a1* and *Cyp26b1* induction is particularly critical to the maintenance of cellular RA levels because the RALDH reaction is irreversible. Similarly, *Lrat* is upregulated and *Raldh1* – which encodes the major RALDH isoform – is downregulated to direct retinol to storage and away from excess RA synthesis (47, 48, 49).

The RARs are widely expressed and function with physiologic redundancy. Knockout of any single RAR causes only mild to moderate phenotypic changes in a mouse model (50, 51, 52), and knockdown of RARα triggers compensatory upregulation of RARβ and RARγ (53). As a result, a comprehensive understanding of RAR signalling in specific tissues remains elusive, representing an important niche for the application of a dominant negative RAR.

2.2 Review of Lipid Metabolism

To understand the proposed link between RA and MASLD, a basic understanding of lipid metabolism is necessary. More than 95% of dietary lipids are triacylglycerol (TG): an ester of glycerol and three fatty acids (54). Free fatty acids (FFA), in addition to serving as an energy source, are signalling molecules and can be lipotoxic. Hence, the body stores fatty acids as TG to combat this (16). As with retinoids, TG and FFA exist in a dynamic state that rapidly responds to nutritional changes through coordinated action by liver and adipose tissues.

Insulin signalling in the fed state drives TG uptake and storage. Dietary fats are emulsified by bile acids in the small intestine, where TG is digested into monoacylglycerol and two fatty acids for uptake by enterocytes, then reformed into TG (55). Since vitamin A is liposoluble, the absorption of TG follows the same pathway: chylomicron packaging and exocytosis into the lymphatic system before entering the bloodstream at the thoracic duct (30). TG circulating in chylomicrons is broken down into FFA by lipoprotein lipase on the luminal surface of cells, which are absorbed and oxidized for energy or reformed and stored as TG (56).

In the fasted state, low insulin triggers lipolysis and TG is mobilized for energy. Adipose triglyceride lipase (ATGL) and hormone sensitive lipase (HSL) hydrolyze TG stored in adipocyte lipid droplets into FFA, which are transported bound to albumin in the circulation to muscle, heart, liver, and other tissues that oxidize fatty acids for ATP production during fasting (57, 58). The liver, which is the body's main metabolic buffer for the fed to fasting transition, accumulates TG during fasting because of significant uptake from the plasma of FFA released from adipocyte lipolysis; a phenomenon known as fasting induced hepatic steatosis (59). This is an evolutionary adaptation to ensure adequate substrate availability for ketogenesis and very low density lipoprotein (VLDL) secretion, which are necessary to meet the energy demands of the body during starvation (60).

Overall, hepatic TG levels are the result of the balance of four major processes: 1) Uptake; 2) *de novo* Lipogenesis; 3) β-oxidation; and 4) VLDL secretion. MASLD, defined as abnormal hepatic TG accumulation without significant alcohol consumption or other specific aetiology, is associated with alterations in all of these processes (10, 11). High dietary fat consumption and elevated plasma FFA – due to large adipose mass (which directly increases fatty acid release) and peripheral insulin resistance (which phenotypically mimics fasting) –

increase TG and FFA uptake by the liver via chylomicron endocytosis and protein mediated uptake, respectively (61, 62). Hepatic *de novo* lipogenesis is promoted by hyperglycemia and hyperinsulinemia via transcriptional upregulation of lipogenic genes (63). The paradoxical induction of lipogenesis despite prevalent insulin resistance in MASLD has been coined "selective insulin resistance", and may be due to divergence of the insulin signalling pathways for glucose and lipid metabolism or increased lipogenic substrate availability (64, 65, 66). Mitochondrial β-oxidation is induced by glucagon and inhibited by insulin in a healthy liver, and may increase or decrease with MASLD (67 - 70). While impaired β-oxidation would contribute to steatosis, increased mitochondrial activity may also promote disease progression through oxidative stress (71). Finally, VLDL secretion is regulated by both TG availability and protein capacity for lipoprotein assembly, which are in turn affected by insulin, metabolic state, and other signalling pathways (72). Interestingly, RA has been shown to reduce hepatic VLDL TG secretion in mice (73). MASLD is associated with overproduction of VLDL particles, likely driven by increased substrate availability with steatosis, leading to hypertriglyceridemia (74). In total, an estimated 74% of hepatic TG in MASLD is from uptake and 26% from induced *de novo* lipogenesis (75); increased VLDL secretion and possibly increased β-oxidation are not sufficient to prevent steatosis and may in fact worsen health outcomes. Thus, intrahepatic lipid metabolism is a promising area for MASLD treatment and may be a potential application for RA.

2.3 Proposed Link Between Retinoic Acid and Steatotic Liver

Although early retinoid research focused primarily on RA's effects on differentiation and proliferation – often in the context of cancer – the identification of RA as a potent inhibitor of

adipogenesis, and subsequent discovery of several master regulators of lipid metabolism as RA responsive, led researchers to hypothesize a link between obesity, insulin resistance, MASLD, and aberrant retinoid signalling (76, 77, 78). A hallmark of MASLD progression is the loss of hepatic vitamin A stores. Research with human liver biopsies found direct, negative correlation between severity of MASLD and amount of vitamin A in the liver, along with altered expression of vitamin A metabolic genes (17, 79). Further, dietary provitamin A carotenoid intake is inversely associated with MASLD risk (80). However, the specific mechanism and therapeutic potential for vitamin A remain unknown. Review of recent evidence suggests RA may have a protective effect against MASLD pathogenesis and disease progression through two general pathways: 1) Decreasing adipocyte FFA efflux and hepatocyte lipogenesis, while increasing fatty acid oxidation; and 2) Antioxidant and anti-inflammatory effects.

2.3.1 Pro-Fatty Acid Oxidation and Anti-Lipogenic Effects of Retinoic Acid

RA treatment in mice decreased hepatic expression of sterol regulatory element-binding transcription factor 1 (*Srebf1*) – a key driver of lipogenesis – and its target gene fatty acid synthase (*Fasn*); increased fatty acid oxidation genes peroxisome proliferator activated receptor alpha (*Ppara*), uncoupling protein 2 (*Ucp2*), carnitine palmitoyltransferase 1 (*Cpt1-L*), and carnitine/acylcarnitine carrier (*Cac*); and decreased hepatic TG (81). Ablation of adipose RAR signalling via adipocyte-specific expression of a dominant negative RAR increased FFA flux and caused marked hepatic steatosis in mice (25). When a dominant negative RAR was expressed in hepatocytes, mitochondrial β-oxidation was down-regulated and mice developed microvesicular steatosis on chow diet; high dietary RA reversed these effects (82). Similarly, hepatocyte specific

knockout of RARα increased hepatic TG accumulation in chow fed mice (21). Despite these observations, full mechanistic details of RA's pro-fatty acid oxidation and anti-lipogenic effects are yet to be elucidated. Kim et al. demonstrated that peroxisome proliferator activated receptor gamma (*Pparγ*) mediated lipogenesis is inhibited by RA via downstream effects of hairy and enhancer of split 6 (*Hes6*), however *Pparγ* is predominantly expressed in adipose tissue (20). Berry and Noy proposed RA's effects are largely mediated by peroxisome proliferator activated receptor beta/delta (PPARβ/δ); RA treatment induced adipose *Parβ/δ* expression, promoting adipocyte lipolysis and fatty acid oxidation without increasing circulating FFA, and reversed hepatic steatosis in obese mice (19). PPARβ/δ has an emerging role in energy metabolism, although the correlation between RA treatment and PPARβ/δ expression may be a secondary effect of weight loss, rather than a key mechanistic driver of RA's anti-steatotic affect (83).

2.3.2 Anti-inflammatory and Antioxidant Effects of Retinoic Acid

A lesser talked about, yet potentially significant, pathway by which vitamin A may protect against MASLD is reduction of oxidative stress and inflammation. Inflammation and HSC activation – the process in which HSCs differentiate into myofibroblasts, losing their vitamin A stores and producing excess extracellular matrix – ultimately drive disease progression from simple steatosis to steatohepatitis and cirrhosis (17, 18). β-carotene supplementation decreased histological signs of inflammation and expression of proinflammatory cytokines tumor necrosis factor-alpha (TNF-α) and transforming growth factor-β1 (TGF-β1) in the livers of high fat diet fed rats (84). The synthetic provitamin A carotenoid β-cryptoxanthin decreased Kupffer cell infiltration and prevented fibrosis in a mouse model of MASH (85). RAREs have been

identified in the thioredoxin (*Trx*) gene, a key player in cellular management of oxidative stress (86). However, the clinical significance of vitamin A's antioxidant anti-inflammatory actions is debated (87). Although frequently grouped with vitamins C and E in discussion of 'the antioxidant vitamins', vitamin A is primarily an indirect antioxidant working through RA's transcriptional upregulation of antioxidant genes as opposed to direct capture of free radicals (88).

Importantly, therapeutic treatment with all-*trans*-RA in humans is problematic because its potency imposes potentially toxic and teratogenic side effects. Thus, for both proposed pathways, achieving a clear mechanistic understanding is needed to identify viable targets for pharmaceutical intervention.

2.4 Sex Differences in Retinoic Acid Signalling

Sex differences are prevalent in both RA signalling and hepatic lipid metabolism yet remain under-investigated in the literature. A diet rich in provitamin A carotenoids is associated with a greater reduction in coronary heart disease risk in women compared to men (89). Female mice also appear more resistant to the metabolic consequences of mutations in the retinoid metabolic pathway than males. Knockdown of RDH – the enzyme responsible for the rate-limiting step in RA synthesis – decreases the steady state concentration of RA in the liver of both female and male mice, but only males develop insulin resistance on a high fat diet (90). This was linked to increased β-oxidation in females versus decreased in males, relative to wild-type mice for each sex. It has also been hypothesised that estrogen may induce the expression of retinoid metabolic enzymes, comprising a compensatory response to RDH knockdown, but this has not

been investigated in the liver (91). Further, dietary vitamin A supplementation decreased some proinflammatory cytokines in obese female, but not obese male, mice (92). These data align with the fact that sex-specific differences in white adipose deposition – namely, a propensity for subcutaneous over visceral fat accumulation in females – are protective against metabolic disease; something Yasmeen et al. propose is related to retinoid signalling (93, 94). In their mouse model, estrogen inhibited RALDH expression in the visceral fat of females, increasing retinaldehyde accumulation which subsequently increased ATGL expression through a non-genomic mechanism (95). This aligns with the increased risk for visceral fat deposition in women with low estrogen, such as polycystic ovarian syndrome or post-menopause (96). Collectively, these data suggest that cross-talk between retinoid, sex-hormone, and lipid metabolic signalling may be an important factor in understanding their associated diseases and highlight the necessity of including female subjects in future studies.

2.5 Effect of Fasting on Retinoic Acid Metabolism

In addition to the dramatic effects the fed-fasting transitions have on macronutrient metabolism, vitamin A homeostasis is also modulated by feeding status. Since RA is predominantly catabolic it makes sense that counterregulatory mechanisms exist between RA and insulin signalling to maximize insulin's postprandial anabolic actions (26). In fact, the concentration of RA in the liver decreases with re-feeding as a downstream effect of insulin receptor activation (97). Insulin binding to its cell surface receptor activates the phosphatidylinositol-3-kinase (PI3K)/protein kinase B (PKB) pathway, which results in inhibition of forkhead box protein O1 (FOXO1) mediated transcription (98). Although this has

the primary effect of inhibiting gluconeogenesis and glycogenolysis, it also decreases RDH expression and thus decreases RA synthesis in the fed state (97).

In the absence of insulin, active FOXO1 induces RDH expression to increase RA synthesis. Breakdown of RA during fasting is balanced between CYP26A1 induction by RA itself and CYP26A1 downregulation by glucagon and cortisol. The net effect is moderately decreased CYP26A1 so RA levels are elevated to support the body's catabolic state, yet regulated to prevent toxicity (99). Upon re-feeding glucagon and cortisol decrease and CYP26A1 induction becomes dominant; subsequent breakdown returns RA to fed-state levels. However in a CYP26A1 knockdown mouse model, RA remained elevated after re-feeding and gluconeogenesis inhibition was impaired (105).

Chapter 3: Materials and Methods

3.1 Animals

All animals experiments were approved by the University of Alberta's Animal Care and Use Committee, in accordance with the guidelines established by the Canadian Council of Animal Care. Animals were housed by the Health Sciences Laboratory Animal Services at the University of Alberta. Unless otherwise stated, all animal experiments used C57BL/6 (Jackson Labs) mice, ad lib fed a standard chow diet (5L0D* PicoLab® Laboratory Rodent Diet, LabDiet, St.Louis, MO).

3.2 Acute Retinoic Acid

Mice were given a dose of 30mg/kg of all-trans-retinoic acid (atRA; R2625, Sigma-Aldrich, St. Louis, MO) via intraperitoneal (i.p.) injection in alignment with the dosage used in previous studies (73). atRA was dissolved in dimethylsulfoxide (DMSO) and emulsified in phosphate buffered saline 1:10 (PBS) to generate a 10mg/mL solution of atRA for injection and injection volume was calculated from each mouse's body weight to achieve the 30mg/kg dose. Control mice were given a 10% DMSO/PBS i.p. injection as a vehicle. Tissues (blood, liver, subcutaneous white adipose, visceral white adipose, brown adipose, lung, intestine) were collected four hours post injection in accordance with previous data showing the peak response to retinoic acid after four hours (Clugston Lab; unpublished). Mice were ad lib fed, with free access to food and water until anesthetized with isoflurane and euthanized by cervical dislocation prior to tissue collection. Tissues were snap frozen in liquid nitrogen and stored at -80°C until analysis.

3.3 Dietary Vitamin A

To compare the effect of acute retinoic acid exposure to the effects of chronic dietary vitamin A manipulation, and probe for potential sex differences, thirty one C57BL/6 mice (18 females, 13 males) were weaned onto purified diets with differing vitamin A content. Seven females and four males received a diet containing 0 IU/g vitamin A; five females and five males received a diet containing 4 IU/g vitamin A; and six females and four males received a diet containing 25 IU/g vitamin A. Purified diets were purchased from Bio-Serv (Flemington, NJ, USA) and were standard chow AIN-93 diet aside from the vitamin A content modifications (100). Mice remained on diets for 120 days prior to tissue collection. The amounts of vitamin A and 120 day duration were selected based on a previously established model of vitamin A manipulation (101). Tissue was collected and frozen as per the protocol used in the acute RA study; mice were ad lib fed with free access to food and water until anesthetized.

3.4 Microarray

Liver samples for microarray were collected following the acute RA protocol. Whole livers were dissected into the distinct lobes; 5-10mg samples were extracted from the left lobe by punch biopsy for use on the array. Affymetrix Clariom D (Thermo-Fisher Scientific, Waltham, MA) whole transcript and micro RNA (miRNA) arrays were completed by the Alberta Transplant Applied Genomics Centre transcriptomics core.

3.5 Generation of Gene Lists and Pathway Analysis

Data from the array were first processed in Transcriptome Analysis Console (TAC) software (Thermo-Fisher Scientific) to analyse the differential expression between the experimental and control groups, and generate the list of genes to be used for the pathway analysis. Raw signal data from microarray were imported to TAC software and normalized by robust multi-array average with signal space transformation (RMA-SST). To remove erroneous or weak signals, probe signals were filtered by detection above background (DABG) whereby a p value was calculated for the comparison of the strength of each probe versus the background noise. Genes were considered 'not expressed' and the corresponding probe set data was removed from analysis if less than 50% of samples has a DABG p value < 0.05. Differentially expressed genes were identified by empirical Bayes statistical test. From the 64 354 total probes on the chip, a significance threshold was selected as the cut-off to identify differentially expressed genes (DEGs) on the gene list. The significance threshold was selected with two goals: firstly, to reduce the size of the gene list to a digestible length for pathway analysis and, secondly, to not reduce the list so much such that no new scientific insight could be obtained. Based on this, the cut-off was initially set to genes with a false discovery rate less than 0.05 ($FDR < 0.05$), however the resulting list of 28 genes provided no novel scientific insight after pathway analysis. Thus, the cut-off was recessed to genes that had a significant fold-change of at least 1.5 ($FC \geq 1.5 \mid FC \leq -1.5$; $p < 0.05$), producing a list of 801 DEGs. To accommodate for inadequate annotation of non-coding and pseudogenes in the gene databases, only genes recognised as coding and complex were selected to generate the final list of 332 genes to be used for pathway analysis.

To evaluate the potential regulation of gene expression by RA through micro RNAs (miRNAs), a list of differentially expressed ($FC \geq 1.5 \mid FC \leq -1.5$; $p < 0.05$) miRNAs was generated by TAC. Twenty-seven predicted miRNAs were excluded due to inadequate

annotation; literature searches of the 8 remaining differentially expressed miRNAs were conducted. The name of each miRNA plus "liver" and the name plus "retinoic acid" were searched in PubMed to probe for links between the differentially expressed miRNAs and hepatic retinoic acid signalling.

Pathway analysis was done with WebGestalt (WEB-based Gene SeT AnaLysis Toolkit) software using gene set enrichment analysis (GSEA) and network topology analysis (NTA). The analyses were run with the default parameters, as per the recommendations in the WebGestalt manual.

3.6 Transgenic Mouse Model

3.6.1 Mouse Strains and Genotyping

The floxed retinoic acid receptor dominant negative ($RARdn^{fl/fl}$) mice, from a C57BL/6 background, were generously donated by Dr. William Blaner (Colombia University Institute of Human Nutrition). The mice possess a truncated form of human retinoic acid receptor alpha (RARaT403) downstream of a *loxP*-flanked STOP sequence. RARaT403 lacks the carboxyl terminus of the protein which effectively inhibits transcriptional activation by the endogenous RARs in a dose dependent manner (24). The *loxP*-STOP RARaT403 gene was inserted into the ROSA26R locus – an established genomic integration site in mice – by electroporation of embryonic stem (ES) cells. ES cells confirmed to possess the mutation were subsequently injected into mouse blastocysts, and the resulting chimeric pups were bred to generate a mouse line carrying a dormant RARaT403 (henceforth called $RARdn^{fl/fl}$; 102).

Hepatocyte specific expression of RARaT403 was achieved by breeding heterozygous RARdn$^{fl/-}$ mice with heterozygous *albumin-Cre* (Alb-cre$^{+/-}$; Jackson Labs JAX stock #003574) mice. In Alb-cre$^{+/-}$:RARdn$^{fl/-}$ offspring, cre recombinase excises the floxed STOP sequence upstream of RARaT403. Expression of the cre recombinase enzyme is under control of the serum albumin promoter, and thus RARaT403 is solely expressed in hepatocytes. Alb-cre$^{-/-}$:RARdn$^{fl/-}$ and Alb-cre$^{+/-}$:RARdn$^{-/-}$ littermates (hereafter simplified to RARdn$^{fl/-}$ and Alb-cre$^{+/-}$ respectively) were used as controls.

Genotyping was done by PCR of the ear notch using primers 5'-ACCTGAAGATGTTCGCGATTATCT-3' and 3'- ACCGTCAGTACGTGAGATATCTT -5' for Alb-cre and 5'-ATGGTGTACACGTGTCACC-3' and 3'-CACCTTCTCAATGAGCTCC-5' for RARaT403, producing 374bp and 210bp products respectfully, visible by DNA electrophoresis. Genotypes were verified by RT-qPCR of cre recombinase and RARaT403 mRNA.

3.6.2 Diets, Fasting, and Tissue Collection

Two cohorts of mice were studies: one 'unfasted' with free access to food and water until tissue collection, and one fasted 18 hours overnight prior to tissue collection midmorning. Mouse body weights were recorded, and tissues (blood, WAT, liver, and lung) were collected, frozen, and stored as described above. To confirm the absence of extrahepatic RARaT403 expression, brown adipose (BAT), kidney, heart, intestine, stomach, muscle, spleen, and brain were additionally collected from Alb-cre$^{+/-}$:RARdn$^{fl/-}$ mice and RARaT403 mRNA was measured by qPCR.

3.7 Real-time Quantitative Polymerase Chain Reaction (RT-qPCR)

Tissues were homogenized in TRIzol reagent (Invitrogen, Waltham, MA) and total RNA was extracted with the Qiagen RNAeasy Plus Mini Kit (Quiagen, Germantown, MD) according to manufacturer instructions. Concentration and purity of RNA were measured using the Take3 Micro-Volume Plate in the Epoch 2 Microplate Spectrophotometer (Agilent Technologies, Santa Clara, CA).

cDNA was synthesized with the High-Capacity cDNA Reverse Transcription kit (Applied Biosystems, Waltham, MA) and Proflex PCR thermal cycler (Applied Biosystems); each RNA sample was uniquely diluted to produce exactly 2000ng of cDNA per sample. cDNA was stored at -20°C and thawed on ice immediately prior to use for RT-qPCR.

mRNA levels were quantified by RT-qPCR using Taqman master mix (Thermo Fisher) for RARaT403 and PowerUP SYBR Green Master Mix (Thermo Fisher) for all other genes. Gene specific forward and reverse primers were designed in NCBI Primer Blast software, and unique amplification of the gene of interest was tested by melt-curve and DNA gel electrophoresis analysis. *Cyclophilin A (CYA), β-Actin, 18S* served as stable reference genes.

Cycle thresholds (CT) were detected by the QuantStudio™ 3 Real-Time PCR System and analysed in QuantStudio™ Design and Analysis Software v1.5.1 according to the $2^{-\Delta\Delta CT}$ relative quantification method. Triplicates were averaged, compared against a stable reference gene, and expressed as fold-change relative to control (the vehicle treated group for acute RA experiences; the 4 IU/g group in the dietary model; or the $RARdn^{fl/-}$ in the transgenic mouse model).

3.8 High-performance Liquid Chromatography

Quantification of retinol and retinyl esters was accomplished using reverse-phase HPLC in plasma, liver, lung, and white adipose, as previously described (103). In brief, 100mg of solid tissues were homogenized in 1mL of phosphate buffered saline (PBS) (or 100µL in 400µL for plasma) and an equal volume of 100% ethanol for protein denaturation, with a known amount of retinyl acetate internal standard. Three mL of hexanes were used to extract total retinoids (separated from PBS by centrifugation at 3000rpm for 10 minutes; repeated twice) and then evaporated with nitrogen gas blow-down. The remaining lipid residue, containing both retinol and retinyl esters, was dissolved in a 70% acetonitrile; 15% methylene; 15% methanol solution and column separated and analysed by a 1260 Infinity II LC analytic HPLC system (Agilent Scientific). Retinoids were separated based on retention time and concentration of retinol and retinyl esters were calculated from the area under the absorbance peaks at 325nm and adjusted for the amount of internal standard. Measurements from solid tissues were normalized to sample mass for reporting per gram of tissue.

3.9 RBP4 ELISA

Plasma RBP4 concentration was determined by Enzyme-linked immunosorbent assay (ELISA) specific to mouse RBP4 (Sigma-Aldrich RAB1860). Unfasted Alb-cre$^{+/-}$:RARdn$^{fl/-}$ and control plasma samples were thawed on ice and diluted such that the concentrations fell within the detectable range of the kit (based on preliminary data): 1:30 000 dilution for Alb-cre$^{+/-}$:RARdn$^{fl/-}$ samples and 1:20 000 for Alb-cre$^{+/-}$ and RARdn$^{fl/-}$ samples. The standard curve was generated by diluting 12 ng/mL standard provided by the manufacturer with the included buffer

to achieve 6, 3, 1.5, 0.75, 0.376, 0.188 , and 0 (buffer only) ng/mL standards. ELISA was completed according to manufacturer instructions and read by Epoch 2 Microplate Spectrophotometer (Agilent Technologies). Samples were run in duplicate, and the background noise (calculated by the average optical density from 2 blank wells) was subtracted from each readout prior to averaging the duplicates. Standard curve was plotted as a 2^{nd} order polynomial (quadratic). Concentrations were interpolated, multiplied by the dilution factor, and reported as μM based on RBP4's molecular weight of 21kDa.

3.10 TG Assays

3.10.1 Folch Extraction for Hepatic Triacylglycerol

Total lipids from solid tissues were extracted by Folch extraction (104). In brief, approximately 100mg of liver sample was homogenized in 1M NaCl and half was added to 4 volumes of Folch solution (2:1 Chloroform:Methanol). Following phase separation by centrifugation (3000rpm for 10 minutes; repeated twice), Folch solution was evaporated by nitrogen gas blow-down. Lipid residue was redissolved with 2% triton X-100 in chloroform, which was again evaporated by nitrogen gas blow-down. Extracted lipids were dissolved in ddH_2O, made possible by triton emulsification. Samples were diluted 1/5 with ddH_2O prior to colorimetric assay.

3.10.2 Colorimetric Assay

Plasma and liver TG in transgenic mice were quantified by colorimetric assay. Standard curve was constructed from 2.5mg/mL glycerol standard and stepwise dilutions in 1M NaCl to generate 1.25, 0.625, 0.3125, 0.156, 0.078, 0.039 mg/mL glycerol standards, as well as a 1M NaCl blank (0 mg/mL glycerol standard). Plasma samples or Folch extraction product and assay reagent were added to a 96-well flat bottom plate in a 1:100 ratio, oscillated for 1 minute, and incubated at 37°C for 5 minutes prior to read. Readout was taken at 500nm wavelength. Triplicates were run across two separate 96-well plates due to the number of samples (n = 48). A specific standard curve was constructed for each plate and the blank average (background noise) was subtracted from all wells. Interpolated TG concentrations were determined by non-linear regression and multiplied by the dilution factor. For liver samples, concentration was normalized to the mass of liver homogenized for Folch extraction (~50mg) to report concentrations as mg TG/g Liver.

3.11 Calculations and Statistical Analyses

All statistical analyses were completed with GraphPad Prism software and data are reported as means ± SEMs. Groups were compared by either one or two-way ANOVA with Sidak's multiple comparisons test, or by unpaired T-test. Statistical significance was set at $p < 0.05$.

Chapter 4: Microarray Analysis of Hepatic Gene Expression in Response to Acute Retinoic Acid Exposure

4.1 Overview

To capture an unbiased view of the liver's genetic response to retinoic acid (RA), ten adult male mice were injected with either all-*trans*-RA (n = 5) or vehicle (n = 5) and gene expression after four hours was compared by RNA microarray. We hypothesised that a variety of genes involved in both vitamin A and lipid metabolism would be differentially expressed, based on the feedback regulation by RA and its links with lipolysis, lipogenesis, and fatty acid oxidation. However, we did not know exhaustively which genes would be altered, if micro RNA (miRNA) changes would be significant, or the prevalence of interaction between different signalling pathways. We employed pathway analysis to address these knowledge gaps and gain mechanistic insight on the proposed link between RA and hepatic lipid metabolism.

4.2 Microarray Results

4.2.1 Retinoic Acid Modulation of Hepatic Gene Expression

A total of 64 354 probes were analysed by Affymetrix Clariom D microarray. Based on the selected cut-off of $FC \geq 1.5 \mid FC \leq -1.5$; $p < 0.05$, 801 genes were differentially expressed in response to acute RA treatment: 532 genes upregulated and 269 downregulated (Figure 2A). The DEGs were divided by TAC software into 7 classifications based on the RefSeq (NCBI Reference Sequence) database for *mus musculus* (Figure 2B). Class 1 was **non-coding** genes, comprising 49% or 395 of the DEGs, and represented genes without a known protein product. Non-coding genes largely lacked functional annotation, and thus were removed prior to pathway analysis. The second class, **multiple complex**, was designated to genes for which more than one locus type was reported and included 195 DEGs in this dataset.

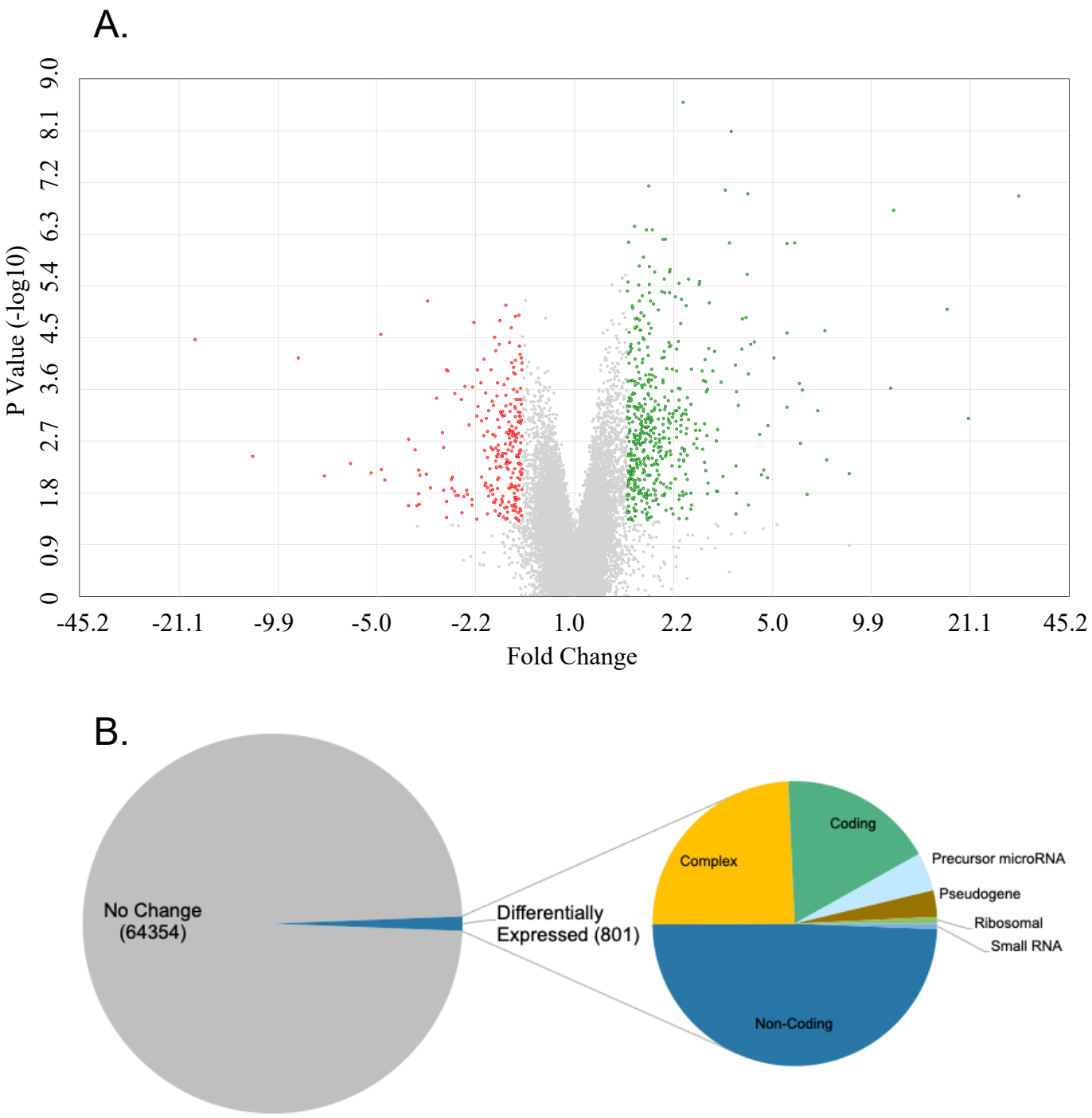

Figure 2. Microarray of differentially expressed genes following acute retinoic acid treatment. A) Volcano plot showing distribution of up and downregulated genes. B) Of the 64 354 probes on the array, 801 were differentially expressed with $p < 0.05$ and fold change < -1.5 or >1.5; subsequently characterised into different categories.

Notably, many genes in this class were predicted genes based on computerized analysis of the mouse genome. One hundred forty-one **coding genes** (class 3) – genes that produce a protein coding transcript – were differentially expressed, including key drivers of retinoic acid metabolism *Cyp26a1* and *Cyp26b1*. Class 4 was **precursor micro RNAs**, describing genes transcribed into miRNA products. Analysis of the 35 differentially expressed miRNAs is described below. The remaining classes: **pseudogenes**, **ribosomal**, and **small RNA** contained 24, 6, and 5 genes respectively. As was the case with non-coding genes, these 35 genes were inadequately annotated and thus removed from pathway analysis.

The complete list of 336 coding and complex genes used for pathway analysis is provided in Table 1. RT-qPCR was used to validate the 3 most up and downregulated genes from the array with expression levels high enough for analysis: *Cyp26a1* (array FC 30.62); chemokine (C-X-C motif) ligand 1 (*Cxcl1*, array FC 20.81); lipocalin 2 (*Lcn2*, array FC 17.69); and *Cyp7a1* (array FC -18.63); hydroxy-delta-5-steroid dehydrogenase 3 beta (*Hsd3b2*, array FC -2.33); sterol regulatory binding element transcription factor 1 (*Srebf1*, array FC -2.33). All 6 genes tested by RT-qPCR corroborated the expression changes seen on the array (Figure 3).

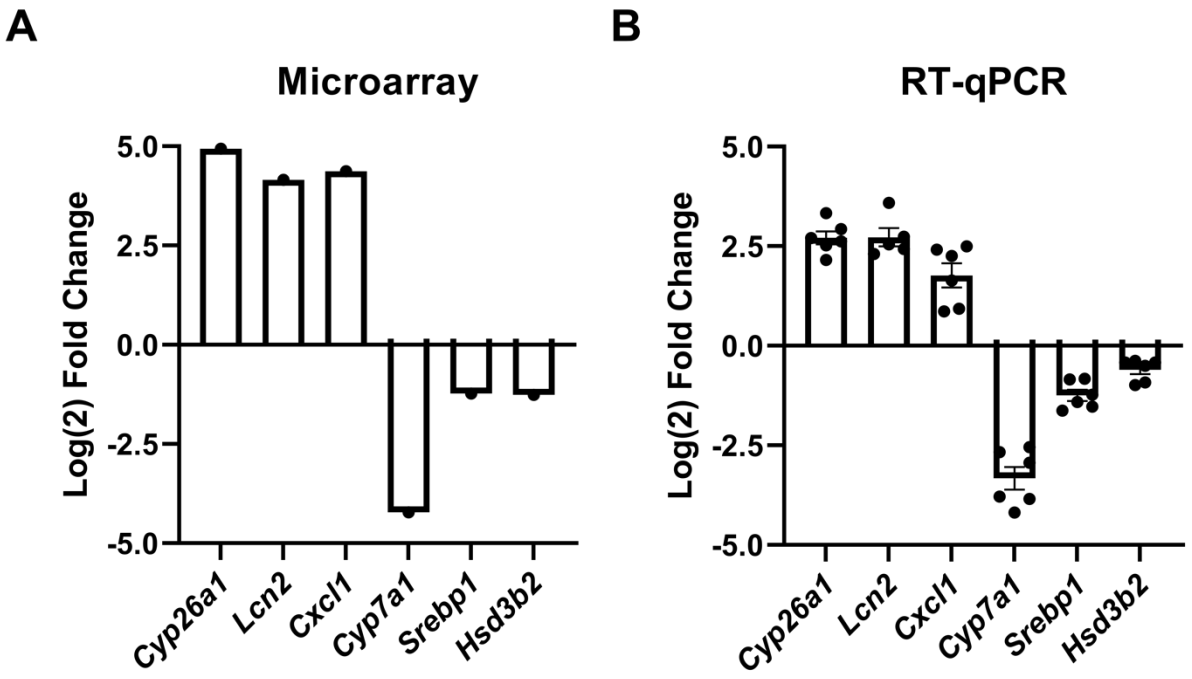

Figure 3. Validation of the top up and down regulated genes from microarray by RT-qPCR. A) Expression fold-change of the 3 most upregulated (*Cyp26a1*, *Lcn2*, *Cxcl1*) and downregulated (*Cyp7a1*, *Srebp1*, *Hsd3b2*) genes identified by microarray. B) Fold-change of the same 6 genes tested by RT-qPCR to validate expression change four hours after 30mg/kg dose of retinoic acid (RA) in mice.

4.2.2 Link Between Retinoic Acid Responsive miRNAs and Hepatic Metabolism

Due to increasing evidence supporting the physiological significance of miRNAs, yet the exclusion of miRNA functional annotation from the pathway analysis database, miRNAs were analysed through literature data mining as described in 3.4. The microarray detected 35 precursor microRNAs as differentially expressed. Twenty-seven are predicted genes, while 8 are named and annotated (Table 2); Five upregulated in the RA treated group and 3 down regulated. Half of the differentially expressed precursor microRNAs – *Mir6353*, *Mir290b*, *Mir5125*, and *Mir1993* – were poorly reported in the literature, with no results related to retinoic acid and/or the liver. *Mir466f-3*, downregulated on our array (FC -1.64 in the RA treated group), was highlighted as a negative regulator of insulin signalling in hepatocytes *in vitro* (106). Mir-126b-5p is a functional product of the precursor miRNA *Mir126b* that was upregulated 2.25-fold following RA. Mir-126b-5p has been linked to adipogenesis, and its overexpression exacerbated hepatic steatosis in mice on a high fat diet (107). Two separate miRNA microarrays identified *Mir6978* as significantly downregulated in mouse models of metabolic syndrome, although neither highlighted *Mir6978* as a key contributor to their findings (108, 109). Finally *Mir292b*, which was upregulated 2.55-fold in the RA treated group on our array, had been previously found downregulated in response to RA treatment in mouse embryonic stem cells (110); a difference that could be attributed to cell type. RBP1 was predicted as a target of Mir292b (Mouse Genome Informatics; Global Core Biodata Resource) and Mir-292b-5p was upregulated in the livers of mice fed a high-fat diet (111); upregulated in the livers of mice treated with antidiabetic hormone fibroblast growth factor 21 (112); and downregulated in the livers of a fibrosis-protected mouse model (113).

4.2.3 Pathway Analysis

To investigate the physiological significance of the DEGs, the coding and multiple complex gene list was analyzed through several database comparison methods. Firstly, over representation analysis (ORA) identified enriched molecular functions and biological processes: cellular actions in which more of the involved genes – as annotated to the GeneOntology (GO) database – appeared on the DEG list than would occur by random chance alone (FDR < 0.05). Fifty-four biological processes and 6 molecular functions were enriched by acute RA treatment (Table 3, Table 4).

Gene set enrichment analysis (GSEA) compared both the DEG list and each gene's reported fold-change to the KEGG Pathway database to provide insight on up and down regulated signalling pathways in response to RA. The ten most-enriched up and down-regulated pathways were identified ($p < 0.05$). Ordered by descending enrichment ratio: Retinol metabolism, Cytokine-cytokine receptor interaction, TNF signaling, Kaposi sarcoma-associated herpesvirus infection, TGF-beta signaling, Hematopoietic cell lineage, Human cytomegalovirus infection, Osteoclast differentiation, Herpes simplex infection and, HIF-1 signaling were upregulated; Steroid hormone biosynthesis, peroxisome proliferator-activated receptor (PPAR) signaling, Bile secretion, Aldosterone synthesis and secretion, Insulin signaling, PI3K-Akt signaling, Human immunodeficiency virus 1 infection, Phagosome Adipocytokine signaling, and [metabolic dysfunction associated steatotic liver disease] (MASLD; annotated as Non-alcoholic fatty liver disease) were downregulated (Figure 4A).

Finally, network topology analysis (NTA) integrated the DEG list with the Biological General Repository for Interaction Dataset (BioGRID): a database of known protein interactions

in intracellular pathways. This provides physiological insight on how DEGs may be interacting and can serve as a potential starting point for mechanistic investigation. Ten genes were identified as 'top-ranking neighbors' to the DEGs, representing genes that were not on the DEG list but are likely to interact with DEGs intracellularly: *GTF2IRD1*, *Fancd2*, *Foxp3*, *Ep300*, *Nr3c1*, *Dok1*, *Inpp5d*, *Ing4*, *Trim21*, and *Eed* (Figure 4B).

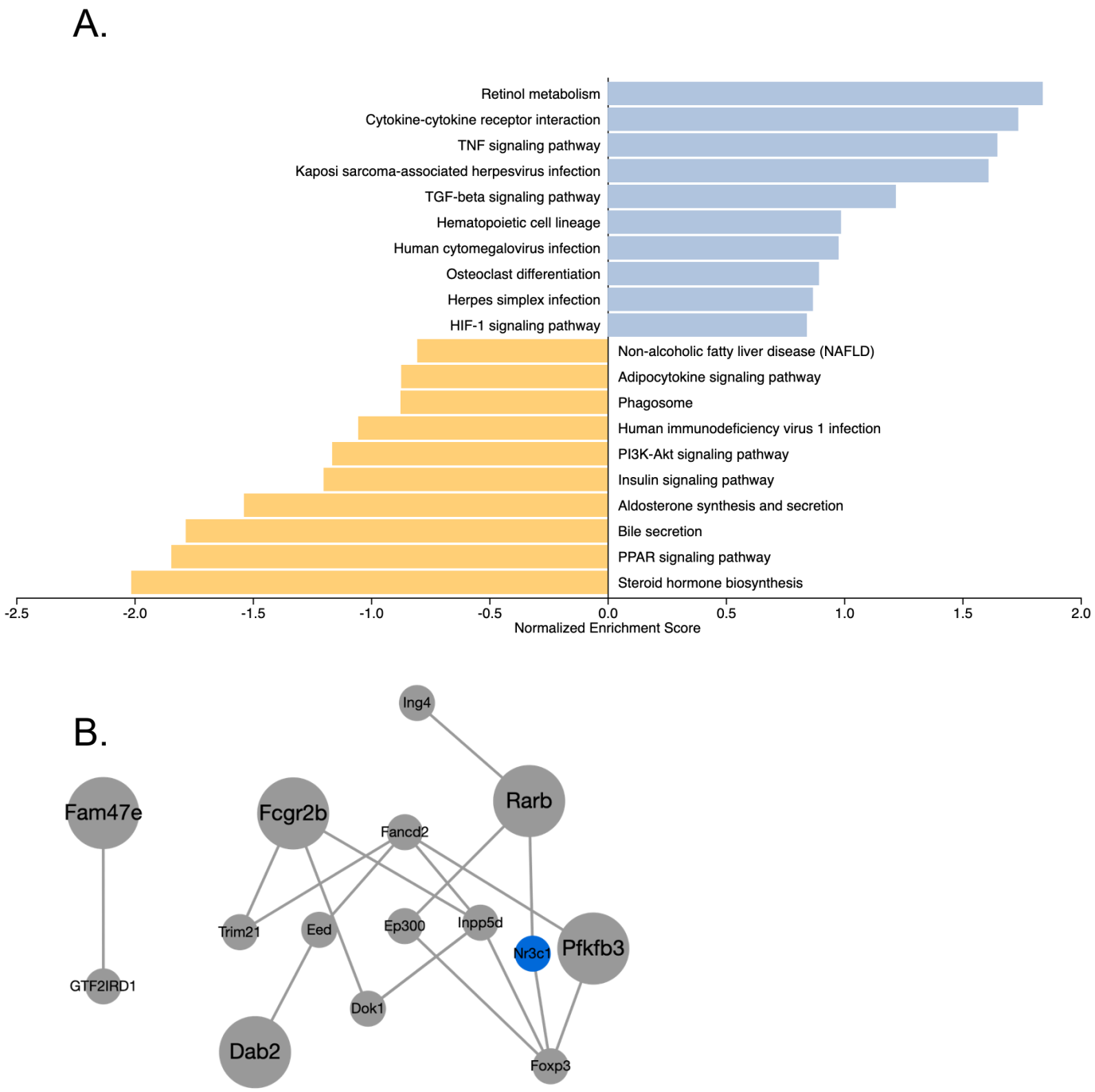

Figure 4. Pathway analysis of differentially expressed genes. A) Gene set enrichment analysis of differentially expressed gene list with Kegg pathway database, showing 10 most enriched up and downregulated pathways. B) Network topology analysis of differentially expressed gene list identified 10 top ranking neighbors (small circles). Gene of interest shown in blue.

4.3 Discussion

Although many gene responses to acute retinoic acid have been previously demonstrated, existing research has largely employed targeted methods of differential gene analysis such as quantitative polymerase chain reaction (qPCR) or immunohistochemistry (7). Such methods are often considered biased because the gene-target selection is hypothesis driven and may preferentially reinforce existing knowledge over the acquisition of novel insights (114). In contrast, data collection by RNA microarray avoids gene-selection bias, but important consideration must be given when isolating valid conclusions from background noise to avoid "over-fitting" the data to one's hypothesis. Integrating both targeted and genome-wide approaches for gene-expression analysis can overcome these limitations. Hence, the significance of specific genes and the pathway analysis outcomes are jointly discussed here.

The 301 DEGs identified by this study demonstrate that significant transcriptome remodeling occurs in the liver following exposure to RA. Consistent with the established negative feedback mechanism of RA hydrolysis, both hepatic retinoic acid specific hydrolases were upregulated. *Cyp26a1* had the largest expression change across the array, increasing 30-fold when mice were given RA. Interestingly, *Cyp26b1* ranked eighteenth with a 3.53-expression fold increase. The difference is likely a result of cell type specific expression patterns and uptake mechanisms. Hepatocytes primarily express CYP26A1, while CYP26B1 is predominantly expressed hepatic stellate cells (HSCs) which account for less than 10% of whole-liver cells (44, 9). RA administered by intraperitoneal injection is absorbed by the lymphatic system and reaches the liver through the circulation. Thus, it is possible that hepatocytes – which are both more abundant and more involved in xenobiotic metabolism than HSCs – buffered stellate cells from a substantial increase in RA concentration, resulting in a blunted response. Other genes in the

retinoid metabolome were modestly upregulated such as lecithin retinol acyltransferase (*Lrat*), which encodes the retinyl ester synthesising enzyme, and dehydrogenase/reductase 3 (*Dhrs3*), encoding the enzyme for retinol synthesis from retinaldehyde. Accordingly, gene set enrichment analysis (GSEA) identified retinol metabolism as the most upregulated pathway (Figure 4).

Several proinflammatory and immunity related genes were upregulated by RA, notably the second- and third-most upregulated genes: *Cxcl1*, a proinflammatory chemoattractant; and *Lcn2*, an innate immune molecule. An established function of RA in mucosa is supporting inflammation and innate immune cell recruitment during infection or after toxin exposure (115, 116). Immune cells are both present and physiologically significant in the liver, including Kupffer cells (liver resident macrophages), dendritic cells, B and T lymphocytes, and natural killer (NK) cells (117). These data suggest that RA may contribute to immune protection in the liver in a manner similar to that seen in mucosa, which is further supported by several enriched biological processes (Table 4) and pathways (Figure 4).

An unexpected finding by the microarray was down-regulation of the bile secretion pathway (Figure 4). CYP family 7, subfamily a, polypeptide 1 (CYP7A1) was the most down-regulated gene on this array, decreasing 18.63-fold. CYP7A1 catalyses the rate limiting step in the classical synthesis of bile acids from cholesterol, and inhibition of it significantly represses bile acid synthesis (118). It is unclear whether RA mediated down-regulation of *Cyp7a1* was through direct or indirect repression of its transcription. *In vivo*, regulation of bile acid synthesis is managed by transcriptional control of CYP7A1 expression through the farnesoid X receptor (FXR) and small heterodimer partner (SHP), which down-regulates *Cyp7a1* when bile acids are elevated (119). *Nr0b2*, the gene encoding SHP, was upregulated on the array and genomic binding of RARα to the *Nr0b2* has been observed (120). Bile acids are necessary for sufficient

intestinal absorption of fat-soluble nutrients (121). The negative regulation of bile acid synthesis by RA may be a mechanism to maximize vitamin A absorption during deficiency; low RA would reduce *Cyp7a1* inhibition to increase bile acid synthesis and support fat-soluble nutrient absorption.

Consistent with our hypothesis that RA alters lipid metabolism, [MASLD] (annotated as Non-alcoholic fatty liver disease), adipocytokine signaling, and PPAR signaling were identified as downregulated pathways (Figure 4). Phosphatidylinositol-3-kinase (PI3K)-Ak transforming (Akt; protein kinase B (PKB)) signalling and insulin signalling pathways were additionally repressed, supporting the proposal that the net effect of RA opposes that of insulin (Figure 4; 26). The downregulation of these pathways were driven by decreased expression of key lipogenic genes, suggesting several possible targets for elucidating the mechanism of RA's anti-obesogenic effects. Sterol regulatory element binding transcription factor 1 (*Srebf1*) decreased in expression 2.3-fold following RA treatment. *Srebf1* encodes both SREBP-1a and SREBP-1c using differential transcription, which subsequently activate a multitude of lipogenic and cholesterogenic (in the case of SREBP-1a) genes (122). Some of such genes were thus also downregulated, including fatty acid synthase (*Fasn*) which catalyzes the formation of palmitic acid from acetyl-CoA and malonyl-CoA; and 3-hydroxy-3-methylglutaryl-Coenzyme A reductase (*Hmgcr*), the rate-limiting enzyme in cholesterol synthesis (123). Peroxisome proliferative activated receptor, gamma, coactivator 1 alpha (*Ppargc1a*) encodes the PCG-1α protein and was down-regulated 1.8-fold on the array. PCG-1α is a transcriptional co-activator for the nuclear receptor PPARγ, which drives fatty acid uptake and triacylglycerol (TG) storage after feeding and is expressed primarily in adipocytes and at low levels in the liver (124). Significant effects on fatty acid uptake and β-oxidation pathways were not observed, which may

be due to the four-hour time course. Cumulatively, these data suggest that acutely decreased hepatic lipid accumulation in the presence of RA is primarily due to reduced fatty acid and TG synthesis.

The top-ranking neighbors identified by NTA represent genes that were not on the DEG list but are likely to interact with DEGs intracellularly. Hepatic expression and function of these genes were researched to determine if any were promising candidates for future investigation. Interestingly, the glucocorticoid receptor gene *Nr3c1* was highlighted as a top-ranking neighbor for RARβ. The glucocorticoid receptor itself has potent effects on metabolic state, glucose, and lipid metabolism, and interactions between retinoid and glucocorticoid signalling have been reported, although often with opposing effects (126, 127, 128). Similarly, the miRNAs differentially expressed on the array were linked to both lipogenic and lipolytic effects in the literature. Important roles for miRNAs in metabolic homeostasis are continuously emerging, such as miR-33 inhibition of cholesterol efflux (129). The RA-glucocorticoid signalling interaction and RA-responsive miRNAs may contribute to the complexity and nuance of retinoid-lipid signalling, and could be valuable avenues for further research.

Table 1 - Differentially Expressed Genes Used for Pathway Analysis

Gene Symbol	Experimental Avg (log2)	Control Avg (log2)	Fold Change	P-value	FDR P-value
Cyp26a1	16.56	11.62	30.62	1.08E-07	0.0012
Cxcl1	12.42	8.05	20.81	0.0008	0.1049
Lcn2	10.95	6.8	17.69	1.00E-05	0.0118
Saa2	17.64	14.12	11.44	0.0002	0.062
Rgs16	11.5	8.69	6.99	0.0042	0.2159
Saa1	18.03	15.32	6.52	0.0006	0.0931
Il1r1	14.43	11.91	5.7	0.0022	0.1613
Tacc2	9.64	7.14	5.66	0.0002	0.0565
Steap4	16.87	14.51	5.15	2.61E-05	0.0193
Pfkfb3	9.87	7.73	4.43	0.0011	0.1212
Mt2	19.9	17.75	4.42	0.0086	0.2942
Gm5828	8.34	6.28	4.17	0.0015	0.1366
Igfbp1	10.24	8.31	3.82	0.0257	0.4425
Gm7694	8.96	7.03	3.81	0.0001	0.0453
Lrrc32	9.06	7.14	3.78	2.51E-06	0.0068
Nos1ap	8.76	6.89	3.65	1.48E-05	0.0145
2010003K11Rik	9.03	7.17	3.63	4.99E-05	0.0268
Cyp26b1	9.23	7.41	3.53	0.0005	0.0842
Apcs	12.55	10.9	3.14	0.0081	0.2879
Trim24	11.02	9.46	2.94	5.51E-05	0.0282
Rlf	10.4	8.86	2.9	0.0001	0.0429
Slc25a47	15.9	14.41	2.82	7.72E-06	0.0102
E030018B13Rik	7.94	6.46	2.79	0.0165	0.3797

Orm3	10.82	9.34	2.78	0.0003	0.0632
Mt1	18.46	16.99	2.77	0.0016	0.1402
Prg4	14.94	13.48	2.75	0.0002	0.0548
Gm16363	13.38	11.93	2.73	7.69E-05	0.0338
Serpina3n	18.77	17.34	2.69	0.0002	0.0535
Fgl1	15.73	14.31	2.69	0.0028	0.1833
Gpcpd1	14.97	13.55	2.68	0.0001	0.0429
Txnip	13.34	11.98	2.56	0.0026	0.1768
Pim1	10.05	8.73	2.51	0.0022	0.1627
Cpne8	8.96	7.66	2.46	0.0001	0.0423
Mfsd2a	11.91	10.62	2.45	0.0162	0.3756
Fbf1	7.36	6.11	2.38	0.0004	0.075
Lilr4b	8.96	7.71	2.37	0.044	0.5189
Asns	7.63	6.39	2.37	0.0163	0.3775
Serpina10	16.14	14.89	2.36	0.0015	0.1362
Gm14420	15.39	14.15	2.36	0.0007	0.0986
Lpgat1	13.23	11.99	2.36	8.66E-06	0.0106
Slc39a14	12.81	11.57	2.35	0.0006	0.0921
Nedd4l	11.61	10.39	2.33	0.003	0.1872
Nr0b2	10.76	9.54	2.32	0.0044	0.2182
Tgm2	10.95	9.74	2.31	2.53E-09	0.0002
Tgm1	10.3	9.11	2.28	0.0007	0.1009
Litaf; Gm19955	9.55	8.36	2.28	6.73E-06	0.0098
Id2	16.85	15.66	2.27	0.0011	0.1207
Gm13086	10.56	9.37	2.27	0.0008	0.1058

Lrat	10.96	9.79	2.26	0.0002	0.0626
Lilrb4a	10.15	8.99	2.24	0.0449	0.5226
Id3	8.02	6.85	2.24	0.0005	0.0871
Hmox1	9.76	8.6	2.24	0.0207	0.4115
Alpk1	7.05	5.89	2.24	0.0004	0.0763
Bcl3	9.26	8.1	2.23	0.0002	0.0621
Slc37a1	7.1	5.97	2.2	0.0017	0.1449
Lbp	14.57	13.44	2.2	4.99E-05	0.0268
Retnlg	5.37	4.25	2.17	0.0006	0.0931
Gm14405	15.6	14.51	2.14	0.0007	0.0986
Gm12177	11.02	9.93	2.13	0.0008	0.1033
Pdk4	7.47	6.39	2.12	0.0003	0.0649
Mbd1	10.65	9.57	2.11	0.0053	0.2401
Olfr16	4.83	3.76	2.1	0.0106	0.3212
Pnpla2	11.94	10.87	2.1	4.32E-05	0.0257
Gm10011	10.24	9.17	2.1	0.0034	0.1975
Gm14421	14.48	13.42	2.09	0.001	0.113
Ell	10.75	9.7	2.08	5.17E-06	0.0082
Gm14436	14.78	13.73	2.08	0.0007	0.0986
Gm8016	9.45	8.39	2.08	2.07E-06	0.0068
Dnajc12	8.26	7.2	2.08	0.003	0.1872
Snx10	9.48	8.42	2.08	4.57E-05	0.0262
Bmp2	8.16	7.1	2.07	3.83E-05	0.0243
Lrg1	15.83	14.79	2.06	0.0008	0.1049
Angptl4	11	9.95	2.06	0.0004	0.077

Id1	8.23	7.21	2.04	0.0127	0.3443
Adgrf5	12.14	11.13	2.01	6.16E-07	0.003
Gm15035	13.26	12.25	2.01	0.0005	0.086
Gm14327	14.84	13.84	2.01	0.0006	0.0915
Gan	7.4	6.4	2	6.99E-05	0.033
Rarb	7.83	6.83	2	0.0003	0.0741
Lpin1	12.17	11.17	2	0.0166	0.3804
Gm7969	8.55	7.55	2	5.22E-06	0.0082
Neu3	6.58	5.59	1.99	5.51E-05	0.0282
Unidentified	8.54	7.55	1.99	3.01E-06	0.0068
Unidentified	8.54	7.55	1.99	3.01E-06	0.0068
Slc10a2	11.46	10.47	1.99	0.0008	0.1049
Rab30	9.43	8.45	1.98	0.0002	0.0532
Nrg4	9.08	8.09	1.98	0.0111	0.3266
Arhgef26	10.8	9.81	1.98	0.0014	0.1336
Ccl6	8.43	7.45	1.98	6.09E-07	0.003
Fbxo31	8.98	7.99	1.98	0.0002	0.0555
Gm11115	5.54	4.56	1.97	0.0178	0.388
Gm13295	12.65	11.67	1.97	0.0017	0.145
Olfr1036	7.85	6.87	1.96	4.96E-06	0.0082
Socs3	6.01	5.06	1.94	0.0036	0.2013
Slc41a2	11.96	11.01	1.94	0.0029	0.1867
Pim3	8.97	8.03	1.92	0.0019	0.1492
Zc3h13	9.07	8.13	1.92	0.0015	0.1368
Paqr9	13.64	12.7	1.91	0.0026	0.1753

Gm10309	5.2	4.28	1.89	0.009	0.299
Gm14431; Gm8898	14.88	13.98	1.87	0.0021	0.1595
Gm14431; Gm8898; Gm4245	14.88	13.98	1.87	0.0021	0.1595
Scara5	7.09	6.19	1.87	0.0097	0.308
Fmo5	15.39	14.49	1.87	0.0002	0.0492
Gm14431; Gm8898; Gm4723	14.44	13.54	1.86	0.0012	0.1251
Mettl20	12.89	12	1.86	0.0018	0.1474
Isyna1	7.83	6.94	1.85	0.0025	0.173
Tifa	8.36	7.47	1.85	0.0005	0.0871
Cmip	10.15	9.26	1.85	2.26E-06	0.0068
Gm14431; Gm8898	14.01	13.13	1.84	0.0029	0.1859
Slc30a5	12.01	11.13	1.84	0.0052	0.2363
Kcnk6	6.57	5.7	1.83	8.25E-06	0.0106
B3galt1	9.61	8.74	1.83	0.0218	0.4196
Apoa5	12.64	11.77	1.82	0.0009	0.1069
Marco	8.5	7.64	1.81	0.0052	0.2377
Gm5612	10.57	9.72	1.81	0.0001	0.0423
Dhrs3	13.13	12.27	1.81	2.17E-05	0.0178
Gm14405	12.36	11.51	1.81	0.002	0.1551
Stat3	11.32	10.48	1.8	0.0004	0.0763
Gm13606; RP23-27J1.3	11.17	10.32	1.8	0.0013	0.1315
Gm14301	7.48	6.63	1.8	0.0013	0.133
Gm14288; Gm14440	15.56	14.72	1.8	0.0009	0.1124
Tiparp	7.73	6.89	1.79	0.0002	0.0599

Gm14288; Gm14440	14.4	13.57	1.78	0.0008	0.1036
Mbl1	15.08	14.25	1.78	5.16E-06	0.0082
Ints7	10.19	9.35	1.78	3.70E-06	0.0069
Hoxa5	5.54	4.71	1.77	0.0002	0.0552
Pik3c2g	9.75	8.93	1.77	0.0002	0.0526
Gm13105	8.55	7.73	1.77	0.0078	0.2828
Cd93	7.81	6.99	1.77	7.26E-08	0.0012
Mustn1	7.62	6.81	1.76	0.0011	0.1229
Ttpal	8.46	7.65	1.76	0.0002	0.0532
Slc41a1	8.4	7.59	1.76	0.0008	0.1041
Gm14306	14.35	13.54	1.75	0.0012	0.1246
Tmem87b	9.56	8.75	1.75	4.58E-05	0.0262
Cd38	10.81	10.01	1.74	4.23E-07	0.0028
Gm17757; Gm18853	8.38	7.57	1.74	0.0079	0.2841
Bhlhe40	12.38	11.58	1.74	0.0182	0.3909
Olfr1034	9.4	8.61	1.73	0.0009	0.1112
Orm2	15.33	14.54	1.73	0.0054	0.2403
Pid1	10.24	9.46	1.73	0.0001	0.0472
Zfp125	11.82	11.04	1.72	0.0306	0.4742
Tapt1	13.95	13.17	1.72	0.0002	0.0572
Ranbp10	9.83	9.05	1.72	0.0005	0.0826
Myd88	9.52	8.73	1.72	0.0004	0.0763
LOC100861725	6.95	6.18	1.71	0.0028	0.1837
Osmr	7.34	6.57	1.71	0.0043	0.2159
Gm9992	9.66	8.89	1.7	1.25E-06	0.0048

Klf10	9.45	8.69	1.7	0.0134	0.3489
Ltc4s	4.6	3.84	1.7	0.003	0.1871
Zfp809	12.47	11.7	1.7	0.0183	0.3913
B4galt1	13.27	12.5	1.7	0.0006	0.0904
Pik3ap1	11.24	10.48	1.69	0.0014	0.1336
Plin2	14.72	13.96	1.69	0.0072	0.2745
Slc8b1	10.69	9.93	1.69	7.49E-05	0.0334
Itih3	16.99	16.23	1.69	0.003	0.1885
Il1rn	7.01	6.26	1.69	0.0002	0.061
Cebpb	9.1	8.35	1.68	0.0009	0.11
Etohi1	14.52	13.78	1.68	0.001	0.1189
Ctbs	8.76	8.02	1.68	0.0007	0.1023
Hspb8	13.63	12.88	1.68	0.0021	0.1576
Gse1	7.55	6.8	1.68	5.82E-06	0.0089
Cldn14	7.3	6.55	1.68	8.48E-05	0.0361
Mlxipl	14.27	13.52	1.67	0.0002	0.0584
Map4k3	10.98	10.25	1.67	1.17E-05	0.0133
Morc3	9.59	8.86	1.66	2.31E-05	0.0179
Gm527	6.75	6.02	1.66	0.0023	0.1659
Chac1	6.01	5.28	1.66	0.0143	0.3586
1810055G02Rik	9.57	8.84	1.66	0.0016	0.138
Gm14288; Gm14435	13.41	12.68	1.66	0.001	0.1142
Gm6485	11.76	11.03	1.66	2.33E-05	0.0179
Bmp6	7.83	7.11	1.65	1.80E-06	0.0063
Epb41	10.69	9.97	1.65	5.14E-05	0.0274

Zpr1	10.37	9.66	1.64	0.0142	0.3581
Acacb	10.09	9.38	1.64	0.0021	0.1579
Rbpms	9.53	8.82	1.64	3.94E-05	0.0245
Garem	10.48	9.77	1.63	0.0019	0.1517
H60b; Raet1a; Raet1b; Raet1c; Raet1d; Raet1e	9.23	8.53	1.63	0.0058	0.2508
Tlr13	5.21	4.51	1.63	0.0006	0.0922
Tnfrsf1a	10.06	9.35	1.63	0.0002	0.0565
Cyp2j9	9.3	8.6	1.63	0.0057	0.2492
Eif1a	10.94	10.25	1.62	0.0027	0.1798
2900026A02Rik	8.81	8.12	1.62	2.01E-05	0.0173
Cyp21a1	7.89	7.2	1.62	0.0041	0.2137
Unidentified	10.71	10.03	1.61	0.0044	0.2174
Trp53i11	7.98	7.29	1.61	1.43E-05	0.0144
Clpx	12.84	12.16	1.61	0.0125	0.3427
Cpt1a	15.38	14.7	1.6	0.0005	0.0886
Fkbp5	7.57	6.9	1.6	0.0023	0.1659
Zfp655	10.13	9.45	1.6	0.0323	0.4789
Smad9	7.29	6.62	1.6	2.19E-05	0.0178
Zkscan7	9	8.33	1.59	0.0002	0.0586
Gtf2ird1	8.04	7.37	1.59	0.0003	0.0688
Zfp36l1	12.36	11.69	1.59	0.0035	0.1975
Inf2	8.7	8.03	1.59	0.0007	0.0986
Mat2a	13.49	12.83	1.59	0.0005	0.086
Plek	6.45	5.79	1.58	0.0291	0.4653
F830016B08Rik	13.16	12.51	1.58	0.002	0.1555

Ada	5.97	5.31	1.58	3.59E-07	0.0028
Fgfr2	8.79	8.13	1.58	0.0005	0.086
Zfp36l2	10.38	9.73	1.57	0.0066	0.2642
Itih4	18.93	18.28	1.57	0.0002	0.0532
Fndc3b	9.67	9.02	1.57	0.0009	0.1106
Gas6	9.11	8.46	1.56	0.0142	0.3581
Gm15250; RP23-22L6.2	9.39	8.75	1.56	0.0092	0.302
Ppm1k	12.56	11.91	1.56	8.70E-06	0.0106
Gm2056	10.18	9.55	1.55	0.0074	0.2772
Bag3	8.4	7.77	1.55	0.0042	0.2159
Gm21857; LOC100861837; Mid1	8.92	8.3	1.55	0.0004	0.0771
Trak2	8.91	8.29	1.55	0.0028	0.1833
Olfr1033	7.6	6.97	1.54	0.0002	0.0532
Gm17530	6.83	6.21	1.54	0.0134	0.3489
Il17ra	8.34	7.72	1.54	0.0077	0.2813
Gvin1; Gm4070	9.47	8.85	1.54	0.0076	0.2792
Fas	9.8	9.18	1.54	4.56E-05	0.0262
Gm5859; Gm17081; LOC100862237	10.97	10.34	1.54	0.0059	0.2527
P2rx7	6.34	5.72	1.54	5.42E-05	0.0282
Rhob	7.79	7.18	1.53	0.0088	0.296
Gvin1; Gm4070; Gm17757; Gm18853	8.71	8.09	1.53	0.0067	0.2662
Rprd1a	10.57	9.96	1.53	0.0073	0.2749
Por	13.64	13.03	1.53	0.0014	0.1336

Stbd1	9.13	8.53	1.53	2.54E-05	0.019
C330013J21Rik	8.61	8	1.52	8.69E-05	0.0363
Clec9a	7.29	6.69	1.52	0.0003	0.0746
Unidentified	10.37	9.77	1.52	0.0033	0.1949
Cers6	8.8	8.2	1.52	0.0343	0.4869
Acpp	8.17	7.56	1.52	0.001	0.1133
Nrip1	8.27	7.67	1.52	6.96E-07	0.003
Map3k1	8.45	7.85	1.52	0.0036	0.2008
Grasp	7.12	6.52	1.51	0.0008	0.1049
Pik3c2g	8.1	7.51	1.51	0.0006	0.0931
Grn	12.92	12.32	1.51	0.0004	0.0775
Hp	18.67	18.08	1.5	0.0008	0.1035
Unc93a; Gm9992	8.66	8.08	1.5	4.83E-06	0.0082
Gfra1	12.98	12.39	1.5	0.0017	0.145
Hgf	8.89	8.31	1.5	0.0005	0.0846
Gm12399	6.14	6.72	-1.5	0.0016	0.1427
Irf6	7.48	8.07	-1.5	0.014	0.356
Cd55b	7.41	8	-1.51	7.12E-05	0.033
Cml5	7.78	8.38	-1.52	0.0324	0.4793
Slc22a29	6.42	7.02	-1.52	0.0004	0.0763
Car14	9.48	10.08	-1.52	0.0021	0.1583
Fmo1	13.54	14.14	-1.52	0.0006	0.0951
Afm	13.62	14.23	-1.53	0.003	0.187
Acsm5	12.93	13.54	-1.53	4.39E-05	0.0259
Acnat1	11.07	11.68	-1.53	0.0007	0.1023

Slc46a3	11.05	11.66	-1.53	0.0486	0.5355
Gm19945	8.68	9.3	-1.54	0.0009	0.11
Sult1c2	6.65	7.27	-1.54	0.0352	0.4897
Fcgr2b	8.05	8.67	-1.54	1.29E-05	0.0142
Tfrc	8.04	8.66	-1.54	0.047	0.5298
Svil	7.05	7.67	-1.54	0.0006	0.0949
Mcm10	6.12	6.75	-1.54	0.0037	0.2036
Slc19a2	12.04	12.67	-1.54	0.0004	0.0763
Hes6	8.26	8.9	-1.55	0.014	0.3566
Cutal	7.44	8.08	-1.56	0.0003	0.0658
Parp16	6.94	7.59	-1.57	0.0017	0.145
Nudt7	13.5	14.15	-1.57	0.0132	0.3472
Gm13139; Gm13251	7.18	7.83	-1.57	0.002	0.1553
Cited2	10.23	10.89	-1.58	0.012	0.3357
Dbp	11.77	12.43	-1.58	0.0431	0.5178
Prkd3	11.61	12.27	-1.58	0.0016	0.1379
Xlr4b	5.24	5.9	-1.58	0.0284	0.4601
Fam20c	7.82	8.47	-1.58	0.0005	0.0881
Dgat2	15.15	15.81	-1.58	7.88E-05	0.0342
Tmem25	7.34	8	-1.58	0.0007	0.1026
Ugp2	13.35	14.01	-1.58	1.36E-05	0.0144
Prkaa2	11.87	12.54	-1.59	0.002	0.1545
Tuba4a	13.38	14.06	-1.6	0.0002	0.0629
Clec14a	5.85	6.53	-1.6	0.0001	0.0443
Pdilt	8.38	9.06	-1.61	0.0013	0.1335

Stard4	9.88	10.57	-1.61	0.0072	0.2745
Keg1	13.07	13.76	-1.61	0.0025	0.1748
Anks4b	8.85	9.55	-1.62	0.0122	0.3391
Gm15371	10.69	11.39	-1.62	0.0016	0.14
Cyp2a5; Cyp2a4	16.63	17.32	-1.62	0.0011	0.1221
Slc17a3	10.68	11.38	-1.63	8.55E-05	0.0361
Calcrl	7.53	8.23	-1.63	2.10E-05	0.0177
Ces1d	13.95	14.66	-1.64	0.0013	0.1336
Dclk3	4.74	5.46	-1.65	0.0013	0.1308
Hmgcr	9.1	9.83	-1.65	0.0017	0.145
Insig1	12.98	13.71	-1.66	0.0013	0.1329
Cyp2a4	15.96	16.69	-1.66	0.0009	0.1107
Fkbp4	10.38	11.11	-1.66	0.0131	0.3472
Xlr4c	4.81	5.54	-1.66	0.023	0.4269
Gm8615	7.4	8.14	-1.66	0.0061	0.2562
Fam13a	7.59	8.33	-1.67	0.0002	0.052
Gm13248	9.25	10	-1.68	0.0049	0.23
Hsd3b5	14.33	15.08	-1.68	0.0058	0.2498
Gm15373	9.35	10.11	-1.68	0.0043	0.2168
Gm15369	9.98	10.74	-1.69	0.0014	0.1336
Xkr9	10.36	11.13	-1.7	0.0005	0.0846
Tbc1d30	7.03	7.79	-1.7	0.0459	0.5261
Atp1b1	10.27	11.07	-1.74	0.0036	0.2013
Osbpl8	9.73	10.53	-1.74	0.0007	0.1023
Gm15712	5.91	6.71	-1.74	0.0178	0.388

Hpgd	12.07	12.87	-1.75	0.0006	0.0931
Hsd17b6	13.25	14.06	-1.76	0.0007	0.0993
Sdr9c7	10.46	11.29	-1.77	0.0006	0.0943
Slc22a28	14.35	15.18	-1.78	1.58E-05	0.0147
Cyp2u1	8.86	9.69	-1.78	0.0055	0.2434
Fasn	11.7	12.54	-1.78	0.0364	0.4945
Slc22a30	15.07	15.91	-1.79	4.10E-05	0.0251
Ppargc1a	7.22	8.07	-1.81	0.0132	0.3472
Irs1	7.08	7.94	-1.81	0.0008	0.1052
Igfals	11.95	12.82	-1.82	0.0036	0.2008
Map2k6	7.24	8.11	-1.83	0.0056	0.2451
Abca8a	11.35	12.22	-1.83	5.27E-05	0.0278
Slc17a4	8.98	9.86	-1.84	0.0027	0.1788
Xlr4a	4.83	5.71	-1.84	0.021	0.4133
Hsph1	10.04	10.93	-1.85	0.0233	0.4289
Cd55	9.16	10.05	-1.86	3.10E-05	0.0215
Akr1c14	14.62	15.52	-1.87	0.0005	0.0846
Gnpda1	7.21	8.11	-1.88	0.0015	0.1368
Hsd3b3	15.41	16.33	-1.89	0.0004	0.0777
Adh6-ps1	11.03	11.97	-1.91	0.0026	0.1752
Ddc	9.71	10.68	-1.95	0.0014	0.1336
Olfml1	7.5	8.47	-1.96	0.0128	0.3452
Inmt	13.85	14.84	-1.99	0.0003	0.0682
Apol7a	9.75	10.76	-2.01	0.0016	0.1411
Sucnr1	10.08	11.16	-2.12	0.0007	0.1023

Etnppl	13.25	14.34	-2.13	0.0454	0.5249
Wee1	7.53	8.67	-2.21	0.0209	0.4121
Akr1c19	11.67	12.84	-2.25	0.001	0.1178
Srebf1; Mir6922	8.42	9.65	-2.33	0.0002	0.0599
Hsd3b2	10.57	11.83	-2.39	0.0004	0.0763
Egln3	10.61	11.98	-2.58	0.0093	0.3032
Clec2h	7.46	8.87	-2.66	0.0001	0.0429
Xlr3e-ps	5.37	6.97	-3.03	0.013	0.3465
Bcl6	6.75	8.48	-3.31	0.0251	0.4383
Xlr3b	5.42	7.15	-3.33	0.0063	0.2593
LOC215866	8.74	10.5	-3.38	0.0261	0.4457
Marcksl1-ps4	9.12	10.97	-3.6	0.0019	0.1492
Xlr3c	6.08	8.19	-4.32	0.0096	0.3072
Xlr3a	5.53	7.79	-4.79	0.0072	0.2734
Xlr3d-ps	5.28	8.06	-6.87	0.008	0.2856
Cyp7a1	10.02	14.24	-18.63	3.40E-05	0.0227

Table 2 - Micro RNAs differentially expressed following acute retinoic acid

Gene Symbol	Experimental Avg (log2)	Control Avg (log2)	Fold Change	P-value	FDR P-value
Mir292b	8.97	7.62	2.55	0.0010	0.1142
Mir126b	5.78	4.61	2.25	0.0055	0.2433
Mir6978	8.29	7.16	2.19	0.0009	0.1100
Mir6353	9.81	9.00	1.75	0.0174	0.3853
Mir290b	8.04	7.38	1.58	0.0187	0.3957
Mir5125	8.23	8.89	-1.58	0.0127	0.3446
Mir466f-3	13.11	13.83	-1.64	0.0013	0.1336
Mir1933	8.13	9.20	-2.11	0.0005	0.0860

Table 3 - Overrepresentation Analysis of Molecular Functions

Molecular Function	Enrichment Ratio	FDR P-Value	Genes
Pattern binding	10.53	0.027	Prg4; Gpcpd1; Mbl1; Stbd1
Steroid dehydrogenase activity	9.09	0.003	Hsd3b5; Hsd17b6; Akr1c14; Hsd3b3; Akr1c19; Hsd3b2
Divalent inorganic cation transmembrane transporter activity	8.65	0.049	Slc39a14; Slc41a2; Slc30a5; Slc41a1
Oxidoreductase activity, acting on CH-OH group of donors	5.27	3.98×10^{-4}	Bmp2; Dhrs3; Hmgcr; Hsd3b5; Hpgd; Hsd17b6; Sdr9c7; Fasn; Akr1c14; Hsd3b3; Akr1c19; Hsd3b2
Monooxygenase Activity	4.63	2.60×10^{-5}	Cyp26a1; Cyp26b1; Fmo5; Cyp2j9; Cyp21a1; Fmo1; Cyp2a4; Cyp2u1; Akr1c14; Akr1c19; Cyp7a1
Oxidoreductase activity, acting on paired donors, with incorporation or reduction of molecular oxygen	4.33	2.03×10^{-6}	Cyp26a1; Cyp26b1; Hmox1; Fmo5; Cyp2j9; Cyp21a1; Por; Fmo1; Pdilt; Cyp2a4; Cyp2u1; Akr1c14; Akr1c19; Egln3; Cyp7a1

Table 4 - Overrepresentation Analysis of Biological Processes

Biological Process	Enrichment Ratio	FDR P-Value	Genes
Response to stilbenoid	15.05	0.0013	Saa2;Fgl1;Cyp2a4;Hsd3b5;Ppargc1a
Oligosaccharide metabolic process	6.83	0.0424	Neu3;B3galt1;B4galt1;Ctbs
Acute inflammatory response	6.74	1.20×10^{-5}	Cxcl1;Saa2;Saa1;Lbp;Stat3;Orm2;B4galt1;Il1rn;Itih4;Hp;Cd55b;Fcgr2b;Cd55
Cellular ketone metabolic process	5.91	1.82×10^{-6}	Lpgat1;Pdk4;Bmp2;Apoa5;Mlxipl;Bmp6;Acacb;Cyp21a1;Cpt1a;Dgat2;Stard4;Hmgcr;Insig1;Ppargc1a;Irs1;Akr1c14;Cyp7a1
Steroid metabolic process	5.50	9.38×10^{-9}	Cyp26a1;Saa1;Cyp26b1;Fgl1;Bmp2;Apoa5;Tiparp;Bmp6;Cyp21a1;Por;Dgat2;Prkaa2;Stard4;Ces1d;Hmgcr;Insig1;Hsd3b5;Hsd17b6;Ppargc1a;Akr1c14;Hsd3b3;Akr1c19;Hsd3b2;Cyp7a1
Nucleoside bisphosphate metabolic process	5.37	0.0025	Pdk4;Acacb;Acsm5;Acnat1;Nudt7;Dgat2;Ces1d;Hmgcr;Fasn
Transition metal ion homeostasis	5.06	0.0018	Lcn2;Steap4;Mt2;Mt1;Slc39a14;Hmox1;Scara5;Slc30a5;Bmp6;Tfrc
Harbohydrate derivative transport	5.06	0.0244	Mfsd2a;Slc37a1;Lbp;Ada;Slc17a3;Slc17a4
Hormone metabolic process	4.56	1.27×10^{-4}	Cyp26a1;Cyp26b1;Lrat;Bmp2;Dhrs3;Tiparp;Bmp6;Cyp21a1;Por;Dgat2;Hsd3b5;Ppargc1a;Akr1c14;Hsd3b3;Hsd3b2
Isoprenoid metabolic process	4.46	0.0391	Cyp26a1;Cyp26b1;Lrat;Dhrs3;Dgat2;Hmgcr
Interleukin-6 production	4.39	0.0044	Prg4;Lbp;Stat3;Myd88;Il1rn;Cebpb;Tnfrsf1a;Gas6;P2rx7;Hgf

Regulation of carbohydrate metabolic process	4.02	0.0044	Fgl1;Pdk4;Stat3;Mlxipl;Acacb;Plek;P2rx7;Dgat2;Prkaa2;Ppargc1a;Irs1
Regulation of small molecule metabolic process	4.01	1.20 x 10^{-5}	Fgl1;Lpgat1;Pdk4;Bmp2;Apoa5;Stat3;Pid1;Mlxipl;Bmp6;Acacb;Cpt1a;Plek;P2rx7;Por;Dgat2;Prkaa2;Stard4;Insig1;Ppargc1a;Irs1;Cyp7a1
Regulation of lipid metabolic process	3.99	1.20 x 10^{-5}	Lpgat1;Id2;Pdk4;Pnpla2;Bmp2;Angptl4;Adgrf5;Socs3;Apoa5;Mlxipl;Bmp6;Acacb;Cpt1a;Por;Dgat2;Prkaa2;Stard4;Insig1;Ppargc1a;Irs1;Cyp7a1
Lipid homeostasis	3.89	0.0236	Pnpla2;Angptl4;Apoa5;Mlxipl;Dgat2;Prkaa2;Insig1;Cyp7a1
Fat cell differentiation	3.83	0.0014	Steap4;Id2;Bmp2;Lrg1;Adgrf5;Lpin1;Cebpb;Zfp36l1;Zfp36l2;Fndc3b;Nudt7;Insig1;Osbpl8;Ppargc1a
Carbohydrate catabolic process	3.83	0.0244	Neu3;Stat3;Ctbs;Mlxipl;P2rx7;Stbd1;Prkaa2;Ppargc1a
Response to interleukin-1	3.78	0.0417	Lcn2;Il1r1;Ccl6;Cd38;Myd88;Il1rn;Cebpb
Biomineral tissue development	3.77	0.0175	Snx10;Bmp2;Klf10;Cebpb;Bmp6;Fgfr2;Gas6;P2rx7;Fam20c
Fatty acid metabolic process	3.74	1.49 x 10^{-5}	Lpgat1;Pdk4;Lpin1;Apoa5;Mlxipl;Acacb;Tnfrsf1a;Cpt1a;Por;Acsm5;Acnat1;Dgat2;Prkaa2;Ces1d;Insig1;Cyp2a4;Hpgd;Fasn;Ppargc1a;Irs1;Akr1c14;Cyp7a1
Neutral lipid metabolic process	3.66	0.0466	Pnpla2;Lpin1;Apoa5;Cpt1a;Dgat2;Ces1d;Insig1
Regulation of inflammatory response	3.43	0.0010	Il1r1;Tgm2;Lbp;Socs3;Myd88;Pik3ap1;Cebpb;Tnfrsf1a;Ada;Il17ra;Hgf;Cd55b;Fcgr2b;Calcrl;Cd55;Sucnr1;Bcl6

Hepaticobiliary system development	3.43	0.0258	Asns;Hmox1;Rarb;Cebpb;Ada;Hp;Hgf;Cited2;Dbp
Muscle cell proliferation	3.40	0.0086	Pim1;Tgm2;Id2;Hmox1;Stat3;Myd88;Fgfr2;Cited2;Calcrl;Hmgcr;Hpgd;Ppargc1a
Lipid modification	3.39	0.0086	Pdk4;Socs3;B3galt1;Apoa5;Pik3c2g;Acacb;Cpt1a;Por;Dgat2;Stard4;Ppargc1a;Irs1
Cellular response to inorganic substance	3.38	0.0133	Mt2;Mt1;Cpne8;Id2;Hmox1;Slc41a1;Bmp6;Fas;Tfrc;Prkaa2;Ppargc1a
Drug catabolic process	3.35	0.0424	Ctbs;Cyp2j9;Ada;Por;Hp;Cyp2a4;Cyp2u1;Gnpda1
Response to tumor necrosis factor	3.29	0.0231	Lcn2;Ccl6;Pid1;Map4k3;Tnfrsf1a;Zfp36l1;Zfp36l2;Gas6;Fas;Ppargc1a
Cellular response to external stimulus	3.24	0.0022	Lcn2;Trim24;Pim1;Asns;Hmox1;Pdk4;Angptl4;Klf10;Bmp6;Tnfrsf1a;Gas6;Bag3;Fas;P2rx7;Tfrc;Prkaa2
Response to carbohydrate	3.07	0.0166	Txnip;Nr0b2;Pim3;Mlxipl;Zfp36l1;Gas6;Prkaa2;Calcrl;Hmgcr;Ppargc1a;Map2k6;Cyp7a1
Response to nutrient	3.04	0.0312	Cyp26b1;Trim24;Pim1;Lrat;Hmox1;Ada;Gas6;P2rx7;Por;Hmgcr
Organic hydroxy compound metabolic process	2.91	0.0011	Cyp26a1;Saa1;Cyp26b1;Fgl1;Lrat;Bmp2;Isyna1;Apoa5;Dhrs3;Bmp6;Plek;Por;Dgat2;Prkaa2;Stard4;Ces1d;Hmgcr;Insig1;Akr1c14;Ddc;Cyp7a1
Intracellular receptor signaling pathway	2.90	0.0413	Cyp26a1;Cyp26b1;Trim24;Pim1;Rarb;Tifa;Dhrs3;Stat3;Cited2;Fkbp4
Organic acid biosynthetic process	2.90	0.0060	Asns;Lpgat1;Pdk4;Apoa5;Stat3;Ltc4s;Mlxipl;Acacb;P2rx7;Acsm5;Prkaa2;Stard4;Insig1;Fasn;Ppargc1a;Cyp7a1

Cellular carbohydrate metabolic process	2.88	0.0173	Pfkfb3;Fgl1;Pdk4;Isyna1;Stat3;B4galt1;Acacb;Plek;Stbd1;Dgat2;Ugp2;Ppargc1a;Irs1
Carbohydrate homeostasis	2.86	0.0236	Pdk4;Adgrf5;Pim3;Stat3;Slc8b1;Mlxipl;Gas6;Prkaa2;Hmgcr;Ppargc1a;Sucnr1;Cyp7a1
Response to metal ion	2.86	0.0067	Mt2;Mt1;Txnip;Cpne8;Id2;Hmox1;Slc30a5;Slc41a1;Bmp6;Fas;P2rx7;Tfrc;Cutal;Prkaa2;Ppargc1a;Sucnr1
Response to acid chemical	2.80	0.0103	Cyp26a1;Cyp26b1;Asns;Lrat;Id3;Pdk4;Rarb;Cd38;Pid1;Cebpb;Bmp6;Cpt1a;Dgat2;Prkaa2;Ppargc1a
Protein localization to nucleus	2.77	0.0273	Txnip;Bcl3;Stat3;Morc3;Zpr1;Tnfrsf1a;Gas6;Bag3;Dclk3;Osbpl8;Irs1;Bcl6
Purine-containing compound metabolic process	2.76	0.0017	Pdk4;Stat3;Pid1;Mlxipl;Acacb;Clpx;Ada;P2rx7;Acpp;Acsm5;Acnat1;Nudt7;Fam20c;Dgat2;Prkaa2;Slc17a3;Ces1d;Hmgcr;Atp1b1;Fasn;Ppargc1a
Sulfur compound metabolic process	2.76	0.0275	Pdk4;Chac1;Acacb;Mat2a;Acpp;Acsm5;Acnat1;Sult1c2;Nudt7;Dgat2;Ces1d;Fasn
rhythmic process	2.73	0.0236	Id2;Id3;Bhlhe40;Klf10;Mat2a;Ada;Fas;Nrip1;Dbp;Prkaa2;Ppargc1a;Map2k6;Ddc
connective tissue development	2.73	0.0294	Fgl1;Id2;Bmp2;Rarb;Hoxa5;Mustn1;Tapt1;Bmp6;Smad9;Por;Dgat2;Ppargc1a
Lipid localization	2.70	0.0103	Mfsd2a;Lrat;Lbp;Pnpla2;Slc10a2;Apoa5;Bmp6;Acacb;P2rx7;Nrip1;Dgat2;Stard4;Osbpl8;Map2k6;Abca8a;Apol7a
Myeloid cell differentiation	2.60	0.0181	Apcs;Id2;Snx10;Adgrf5;Stat3;Hoxa5;Klf10;Cebpb;Zfp36l1;Fas;Tfrc;Cited2;Fam20c;Fasn;Bcl6

Cofactor metabolic process	2.59	0.0044	Hmox1;Pdk4;Stat3;Mlxipl;Chac1;Acacb;Mat2a;P2rx7;Hp;Fmo1;Acsm5;Acnat1;Nudt7;Dgat2;Prkaa2;Ces1d;Hmgcr;Fasn;Ppargc1a;Akr1c14
Lipid catabolic process	2.59	0.0413	Cyp26a1;Cyp26b1;Gpcpd1;Pnpla2;Lpin1;Neu3;Apoa5;Acacb;Cpt1a;Ces1d;Irs1;Cyp7a1
Ribose phosphate metabolic process	2.57	0.0086	Pdk4;Stat3;Pid1;Mlxipl;Acacb;Clpx;P2rx7;Acsm5;Acnat1;Nudt7;Fam20c;Dgat2;Prkaa2;Ces1d;Hmgcr;Atp1b1;Fasn;Ppargc1a
Leukocyte mediated immunity	2.57	0.0244	Cxcl1;Il1r1;Apcs;Hmox1;Bcl3;Mbl1;Myd88;Fas;P2rx7;Cd55b;Fcgr2b;Tfrc;Cd55;Bcl6
Homeostasis of number of cells	2.55	0.0424	Id2;Hmox1;Adgrf5;Stat3;Hoxa5;Zfp36l1;Ada;Fas;P2rx7;Fcgr2b;Cited2;Bcl6
Regulation of hemopoiesis	2.52	0.0231	Cxcl1;Cyp26b1;Apcs;Pim1;Id2;Stat3;Hoxa5;Klf10;Cebpb;Zfp36l1;Ada;Zfp36l2;Gas6;Fas;Bcl6
Multicellular organismal homeostasis	2.51	0.0103	Lcn2;Cyp26b1;Pdk4;Snx10;Adgrf5;Lpin1;Stat3;Cd38;Il1rn;Cebpb;Mlxipl;Bmp6;Acacb;P2rx7;Tfrc;Prkaa2;Ppargc1a;Map2k6
Adaptive immune response	2.39	0.0298	Il1r1;Apcs;Lilrb4a;Bcl3;Stat3;Mbl1;Myd88;Ada;Fas;P2rx7;Cd55b;Fcgr2b;Tfrc;Cd55;Bcl6
Regulation of leukocyte activation	2.36	0.0175	Lrrc32;Cyp26b1;Id2;Hmox1;Lbp;Adgrf5;Cd38;Myd88;Cebpb;Zfp36l1;Ada;Zfp36l2;Gas6;Fas;Fcgr2b;Tfrc;Hsph1;Bcl6

Chapter 5: Sex Differences in Hepatic Response to Acute Retinoic Acid Exposure and Long Term Dietary Vitamin A Manipulation

5.1 Overview

It has been well established that treatment with retinoic acid (RA) upregulates retinoid metabolism as means of maintaining homeostatic control (6). However, potential sex differences in this response remain poorly understood. Under our aim of constructing a *holistic* knowledgebase of retinoic acid responsive genes in the liver, we repeated the acute RA administration and examined a model of long-term dietary vitamin A manipulation in both female and male mice. Specifically, we sought to answer the questions 1) Does RA upregulate retinoid metabolism in females, as has been demonstrated in males; and 2) How do gene expression changes vary between acute, exogenous RA treatment and long term dietary vitamin A manipulation. The retinoid effect, sex effect, and interaction between the two were tested by two-way ANOVA, using RT-qPCR data generously collected, in part, by Nicole Applin.

5.2 Results

5.2.1 Sex Differences in Genes Responsive to Acute Retinoic Acid

Twelve female and twelve male mice, all four-months old, were injected with 30 mg/kg of all-*trans*-RA four hours prior to tissue collection. mRNA levels for twenty genes in the retinoid metabolic pathway (Figure 1) were quantified with RT-qPCR and are reported in Table 4. By student's T Test, an RA effect was identified in two genes: *Cyp26a1*, and *Cyp26b1* in females and five in males: the prior two plus *Rarb, Lrat,* and *Rarg*. The expression difference between RA treated females and males – representing a sex effect – was only significant for *Rarg* (Figure 5C). The retinoic acid specific hydrolase *Cyp26a1* increased in expression 3.39-fold and 4.53-fold in females and males respectively, while *Cyp26b1* – the primary retinoic acid

hydrolase in hepatic stellate cells (HSCs) – was upregulated 1.90-fold in females and 2.40-fold in males (Table 4). *Lrat*, which encodes the protein responsible to converting retinol to retinyl esters, increased 1.33 and 1.68-fold in females and males respectively (Table 4). Interestingly, no significance differences in RAR expression were observed in females while two of the three RAR isoforms – *Rarb* and *Rarg* – were upregulated in males (2.10 FC and 1.52 FC respectively; Table 4).

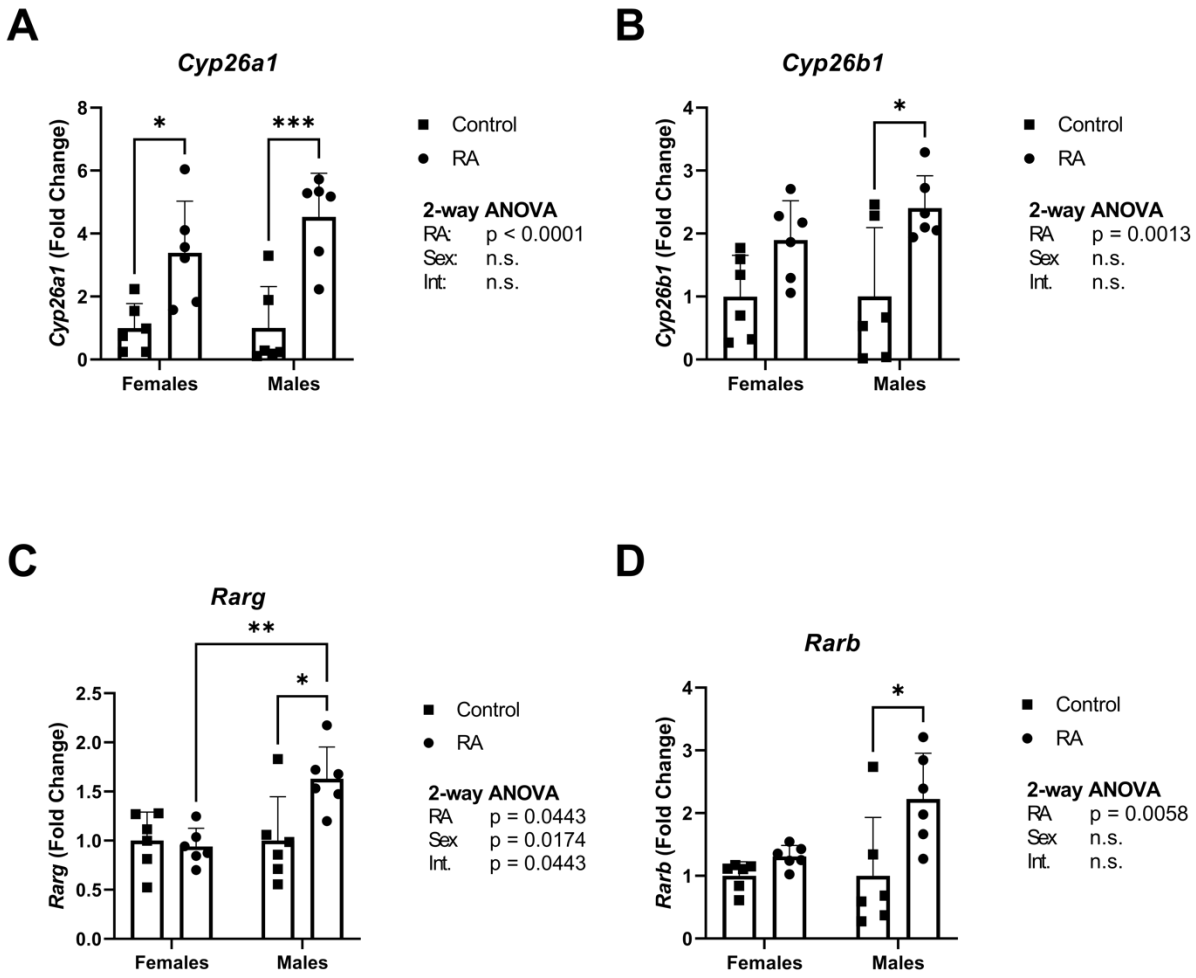

Figure 5. Gene fold changes in acute retinoic acid (RA) responsive genes in females and males. Fold change versus 18S Reference Gene. Group means (n = 6) are shown ± SEM. A) Acute RA induces *Cyp26a1* expression in female and male mice. B) Acute RA induces *Cyp26b1* in male mice. C) Acute RA induces *Rarg* in male mice; male *Rarg* expression is higher than female. D) Acute RA induces *Rarb* expression in male mice.

5.2.2 Effects of Dietary Vitamin A Manipulation in Female and Male Mice

To first confirm the model of dietary vitamin A manipulation, changes in retinoid status were quantified in mice following 120 days on 0, 4, or 25 IU/g Vitamin A diets. Hepatic and plasma retinol (ROH) and retinyl ester (RE) concentrations were measured by HPLC; dietary vitamin A manipulation caused significant changes in plasma ROH, liver RE, and liver ROH ($p < 0.0001$; Figure 6). As expected, mice fed a diet deficient in vitamin A (0 IU/g) had significantly reduced plasma ROH (0.40 ± 0.23 μM in females and 0.28 ± 0.094 μM in males) compared to mice on diets with 4 or 25 IU/g Vitamin A (1.15 ± 0.17 μM in females and 1.62 ± 0.08 μM in males; 1.22 ± 0.38 μM in females and 1.77 ± 0.18 μM in males for the 4 and 25 IU/g diet groups respectively; Figure 6). Because the liver buffers the body from changes in vitamin A availability, hepatic RE – and to some extent ROH – are widely considered to be the most accurate marker of vitamin A deficiency and excess. Both RE and ROH were significantly reduced in the livers of 0 IU/g vitamin A fed mice (females: 3.70 ± 3.71 nmol/g RE, males: 0 nmols/g RE; and females: 1.46 ± 0.33 nmol/g ROH, males: 2.21 ± 0.53 nmol/g ROH) and RE significantly increased in 25 IU/g vitamin A fed mice (females: 1552.86 ± 1065.61 nmol/g RE, males: 1234.79 ± 446.30 nmol/g RE) when compared to mice consuming 4 IU/g vitamin A (females: 205.52 ± 42.63 nmol/g RE, males: 102.19 ± 76.16 nmol/g RE; females 2.72 ± 0.56 nmol/g ROH, males: 2.91 ± 0.89 nmol/g ROH; Figure 6).

Following validation of the dietary manipulation model, RT-qPCR was applied to probe for changes in gene expression. In addition to the twenty retinoid-metabolic genes tested in the acute-sex effect study, the ten most up and downregulated genes (with sufficient expression for RT-qPCR) identified by the microarray were assessed in the 0, 4, and 25 IU/g vitamin A fed mice to support comparison between the acute and chronic models and maintain our goal of an

unbiased analysis of vitamin A responsive genes. The most striking effect was seen in *Cyp26a1* expression, which was significantly downregulated in mice receiving 0 IU/g vitamin A group (0.048-FC in females and 0.039-FC in males) and upregulated in mice receiving 25 IU/g vitamin A (6.93-FC in females and 9.22-FC in males, compared to the 4 IU/g group (Figure 7). *Cyp26b1*, *Lrat*, and *Rarb* were significantly downregulated in female and male mice on 0 IU/g vitamin A diet but were not upregulated by 25 IU/g consumption. *Rxra* expression decreased in female 0 IU/g fed mice but was unchanged in males, and *Bco1* was expressed at significantly lower levels in 25 IU/g fed male versus female mice, but was not associated with a diet effect within the same sex.

Of the other genes tested that were identified as upregulated by the array, only *Rgs16* was upregulated by high dietary vitamin A in females and males. In the male 25 IU/g diet *Steap4*, *Pfkfb3*, *Il1r1*, and *Tacc2* expression also increased. Unexpectedly, none of the genes downregulated by acute RA treatment were suppressed by dietary vitamin A and, in fact, *Hsd3b2* and *Inmt* expression increased in males consuming 25 IU/g vitamin A. In total, a diet effect was recorded in 13 of 39 genes tested, a sex effect in 10, and an interaction in 8.

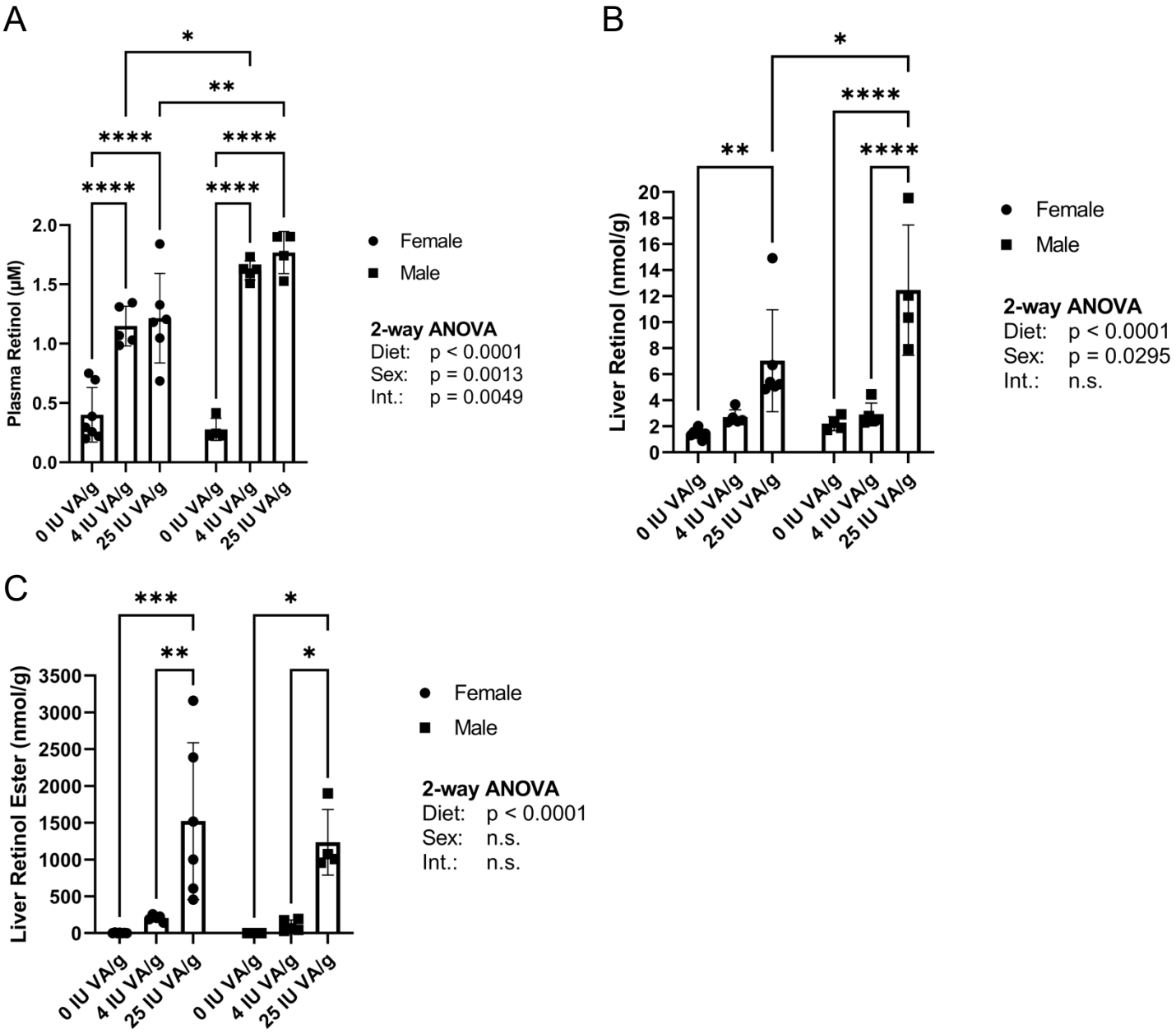

Figure 6. Retinoid changes after dietary vitamin A manipulation. Female and male mice consumed diet with 0, 4, or 25 IU/g Vitamin A for 120 days and retinoid levels were quantified by HPLC. Plasma retinol (A), liver retinol (B), and liver retinyl ester (C) concentration increased with high dietary vitamin A and decreased with dietary vitamin A deficiency, compare to 4 IU/g vitamin A diet.

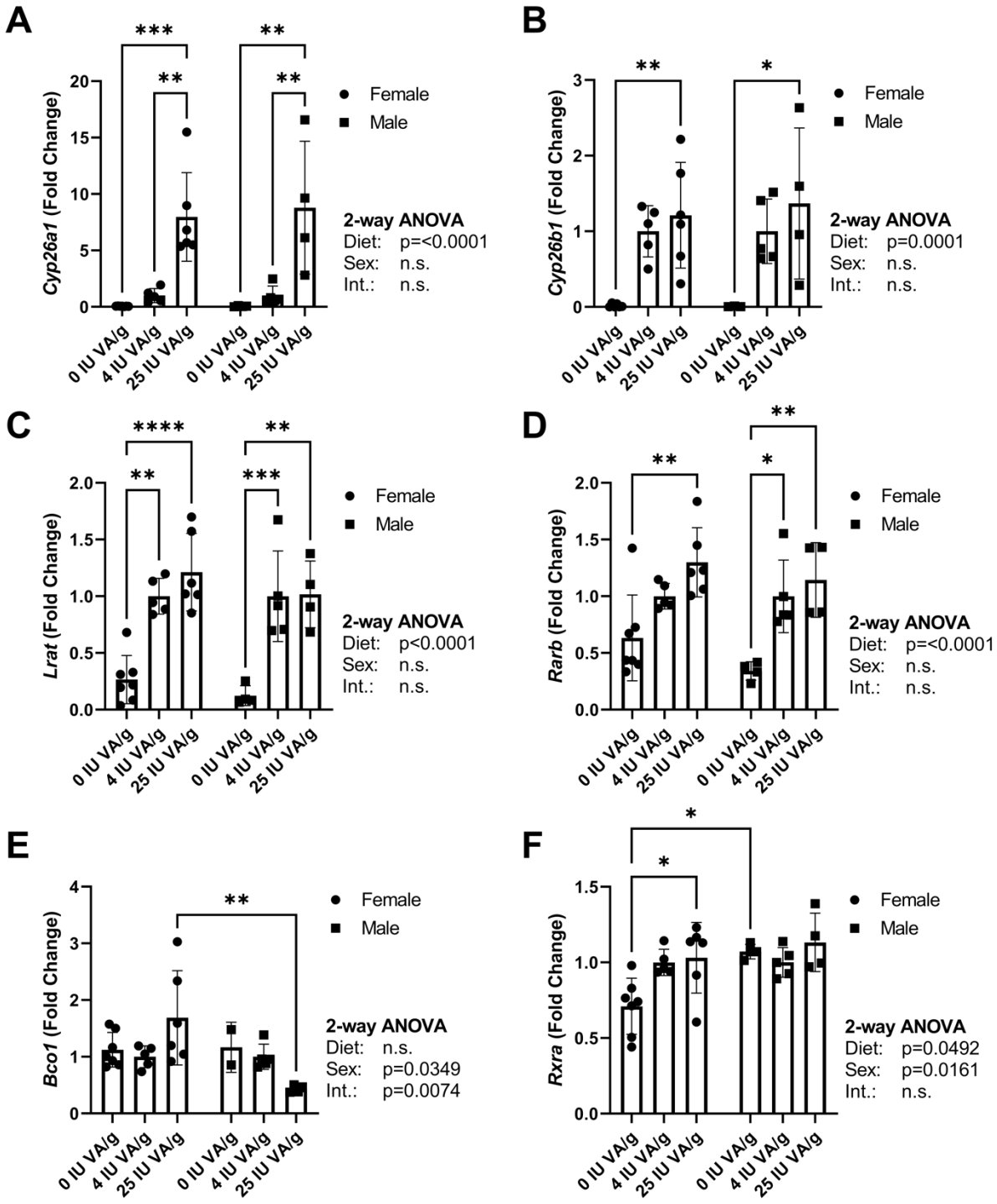

Figure 7. mRNA changes after dietary vitamin A manipulation. Changes in retinoid metabolic genes were quantified by RT-qPCR relative to B2M reference gene. A) Dietary vitamin A concentration directly modulated *Cyp26a1* expression. Cyp26b1 (B), Lrat (C), and Rarb (D) expression decreased with dietary vitamin A deficiency. Bco1 expression (E) was higher in female mice; Rxra expression (F) was lower compared to male mice.

5.3 Discussion

Of the twenty retinoid metabolic genes tested in both models, only *Cyp26a1* was induced by both acute RA and high dietary vitamin A. When normalised by average daily food consumption and body weight, the 30 mg/kg dose of all-*trans*-RA represents ~30-times the retinol activity equivalents of the 25 IU/g diet. This highlights the efficacy of *Cyp26a1* induction. In fact, *in vitro*, *Cyp26a1* expression can increase more than 3000-fold in hepatocytes exposed to retinoic acid (130). *Cyp26b1* and *Lrat* were induced by acute RA but not high dietary vitamin A, however they were suppressed by vitamin A deficiency. The observed difference likely reflects the physiological capacity to cope with these two states. The 25 IU Vitamin A per gram of food diet represents a plentiful, but not toxic dose of retinol; as high as 1000 IU/g diets have been reported in the literature without serious deleterious effects (131, 132, 133). It is possible that increased CYP26A1 attenuated gene expression changes in mice on 25 IU/g diet. On the contrary, the 0 IU/g diet necessitated that mice maximize hepatic RE stores established prior to weaning to maintain growth and development. Hence, retinoid channeling towards storage by LRAT and breakdown by CYP26A1 and CYP26B1 were decreased. Although not assessed in this study, because the specific enzyme responsible is yet unidentified, RE hydrolase activity also increases in vitamin A deficient mice to support the mobilisation of stored retinoids to RA signalling (134). Collectively, these data demonstrate that RA drives hepatic retinoid metabolism in both females and males, and in response to both exogenous RA and dietary vitamin A.

The absence of gene repression by dietary vitamin A suggests that negative regulation of RA responsive genes is less sensitive than gene induction and/or that there is a temporal difference in short-term and long-term responsive genes. A total of four genes were upregulated in females and twelve in males, in response to either exogenous RA or 25 IU/g dietary vitamin

A. The decrease in the number of DEGs and the pattern of gene fold-changes trending lower in females may suggest that the effects of RA are attenuated in females versus males; be a result of significantly lower liver retinol in females on 25 IU/g compared to males; or be a symptom of applying gene-list selection based on microarray data exclusively from male mice. Both our observation that hepatic and plasma retinol were lower in female vitamin A consuming mice, and the lower number of DEGs (compared to males) are consistent with literature proposing estrogen induces retinol but not retinaldehyde dehydrogenase, but this has not been validated in the liver (Chapter 2.4; 91, 95). It appears likely that modest sex differences exist in the transcriptomic response to RA, but the details would be better elucidated by repeating the genome-wide RNA microarray in female mice.

Table 4. Gene expression changes in female and male mice after retinoic acid treatment

Gene Symbol	Female Fold Change	Male Fold Change	RA Effect	Sex Effect	Interaction
Cyp26a1	**3.39**	**4.53**	**p < 0.0001**	n.s.	n.s.
Cyp26b1	**1.90**	**2.40**	**p = 0.0002**	n.s.	n.s.
Rara	0.70	1.18	n.s.	n.s.	n.s.
Rarb	**1.24**	**2.10**	**p = 0.0058**	n.s.	n.s.
Rarg	**0.97**	**1.52**	**0.0443**	**0.0174**	**0.0174**
Dhrs3	**0.72**	**1.27**	n.s.	**p = 0.030**	**p = 0.030**
Dhrs4	0.94	0.97	n.s.	n.s.	n.s.
Raldh1	0.66	0.94	n.s.	n.s.	n.s.
Lrat	**1.09**	**1.60**	**p = 0.0215**	n.s.	n.s.
Rbp1	0.57	1.17	n.s.	n.s.	n.s.
Rbp4	0.93	0.92	n.s.	n.s.	n.s.
Rdh1	0.83	0.92	n.s.	n.s.	n.s.
Rdh10	0.92	1.00	n.s.	n.s.	n.s.
Rdh11	0.72	0.94	n.s.	n.s.	n.s.

Gene Symbol	Female Fold Change	Male Fold Change	RA Effect	Sex Effect	Interaction
Rxra	1.28	1.13	n.s.	n.s.	n.s.
Rxrb	0.97	1.06	n.s.	n.s.	n.s.
Rxrg	0.58	1.08	n.s.	n.s.	n.s.
Stra6l	1.15	1.20	n.s.	n.s.	n.s.
Bco1	1.42	0.88	n.s.	n.s.	n.s.
Bco2	0.70	0.97	n.s.	n.s.	n.s.

Chapter 6: Hepatocyte Specific Knock-in of Dominant Negative Retinoic Acid Receptor Alters Retinoid and Triacylglycerol Homeostasis

6.1 Overview

To examine the effects of impaired retinoic acid (RA) signalling, we expressed a dominant negative retinoic acid receptor (RAR) in hepatocytes of mice (Alb-cre$^{+/-}$:RARdn$^{fl/-}$). We hypothesised that impaired RA signalling would alter hepatic retinoid status and, consequently, whole-body retinoid homeostasis and hepatic lipid homeostasis. To test this, we quantified mRNA, retinoid, and triacylglycerol (TG) levels using RT-qPCR, HPLC, and colorimetric assays respectively, and applied the results to our two overall research aims. For our first aim, we used the RT-qPCR data to validate our putative knowledgebase of hepatic RA responsive genes. Secondly, we aimed to describe the phenotype of this novel mouse model and determine the changes in whole body retinoid and TG homeostasis driven specifically by hepatic RAR signalling. We compared two cohorts – unfasted and fasted – of mice because TG accumulates in the liver in the fasted state, and we sought to better understand how impaired RA signalling effects hepatic steatosis.

6.2 Results

6.2.1 Physical Characteristics and Model Validation of Alb-cre$^{+/-}$:RARdn$^{fl/-}$ Mice

Mice were genotyped by PCR of the of ear notch, with bands visible by gel electrophoresis at 374bp for Alb-cre$^{+/-}$ mice, 210bp for RARdn$^{fl/-}$ mice, or both for Alb-cre$^{+/-}$:RARdn$^{fl/-}$ mice. Twenty-six male mice (5 wild-type, 5 Alb-cre$^{+/-}$, 7 RARdn$^{fl/-}$, and 9 Alb-cre$^{+/-}$:RARdn$^{fl/-}$) were 'unfasted' with free access to food and water until tissue collection. Twenty-two male mice (8 RARdn$^{fl/-}$ and 14 Alb-cre$^{+/-}$:RARdn$^{fl/-}$) were fasted 18 hours overnight prior to tissue collection midmorning. RT-qPCR analysis confirmed expression of the dominant negative

RAR isoform (RARaT403) only in offspring with both transgenes (Alb-cre$^{+/-}$:RARdn$^{fl/-}$), and not in the Alb-cre$^{+/-}$ or RARdn$^{fl/-}$ mice (Figure 8). Further, there were no differences between the Alb-cre$^{+/-}$ and RARdn$^{fl/-}$ groups in any parameters measured, nor were there differences between these mice and wild-type. This supports the validity of Alb-cre$^{+/-}$ and RARdn$^{fl/-}$ mice as control mice, which were selected instead of wild-type littermates to eliminate the possibility of confounding effects caused by the presence of either transgene alone. Alb-cre$^{+/-}$ and RARdn$^{fl/-}$ mice were combined to form the 'control' group for analyses.

Alb-cre$^{+/-}$:RARdn$^{fl/-}$ mice are generally healthy mice with typical maturation. Alb-cre$^{+/-}$:RARdn$^{fl/-}$ mice have an increased liver:body weight ratio compared to Alb-cre$^{+/-}$and RARdn$^{fl/-}$ mice, without an increase in overall body mass (Figure 9). Other metabolic parameters such as food consumption, basal metabolic rate, oxygen consumption, and basal body temperature have not yet been analysed but may be of interest in follow up studies.

Finally, the following tissues were tested for RARaT403 expression by RT-qPCR to validate the liver specific knock-in model: white adipose (WAT), brown adipose (BAT), lung, kidney, heart, intestine, stomach, muscle, spleen, and brain. RARaT403 was high in the liver and undetectable in all other tissues examined (Figure 8).

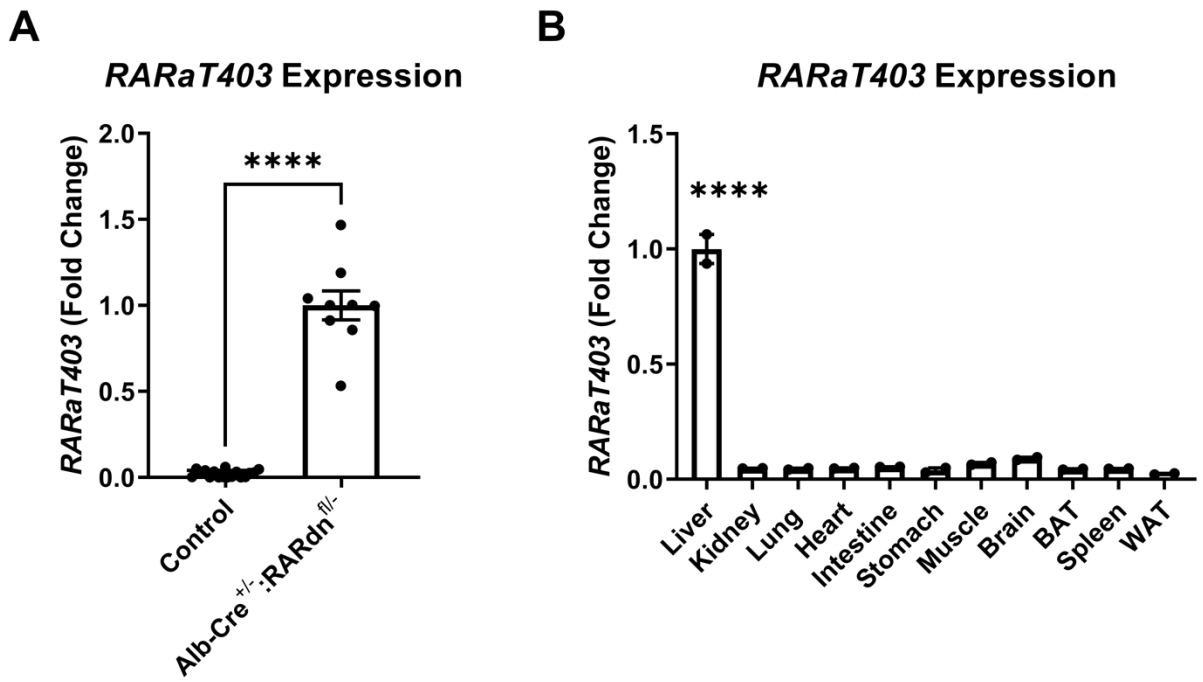

Figure 8. mRNA expression of dominant negative isoform of retinoic acid receptor alpha (RARaT403). A) Control litermates were not expressing RARaT403 mutation. B) RARaT403 is only expressed in the liver.

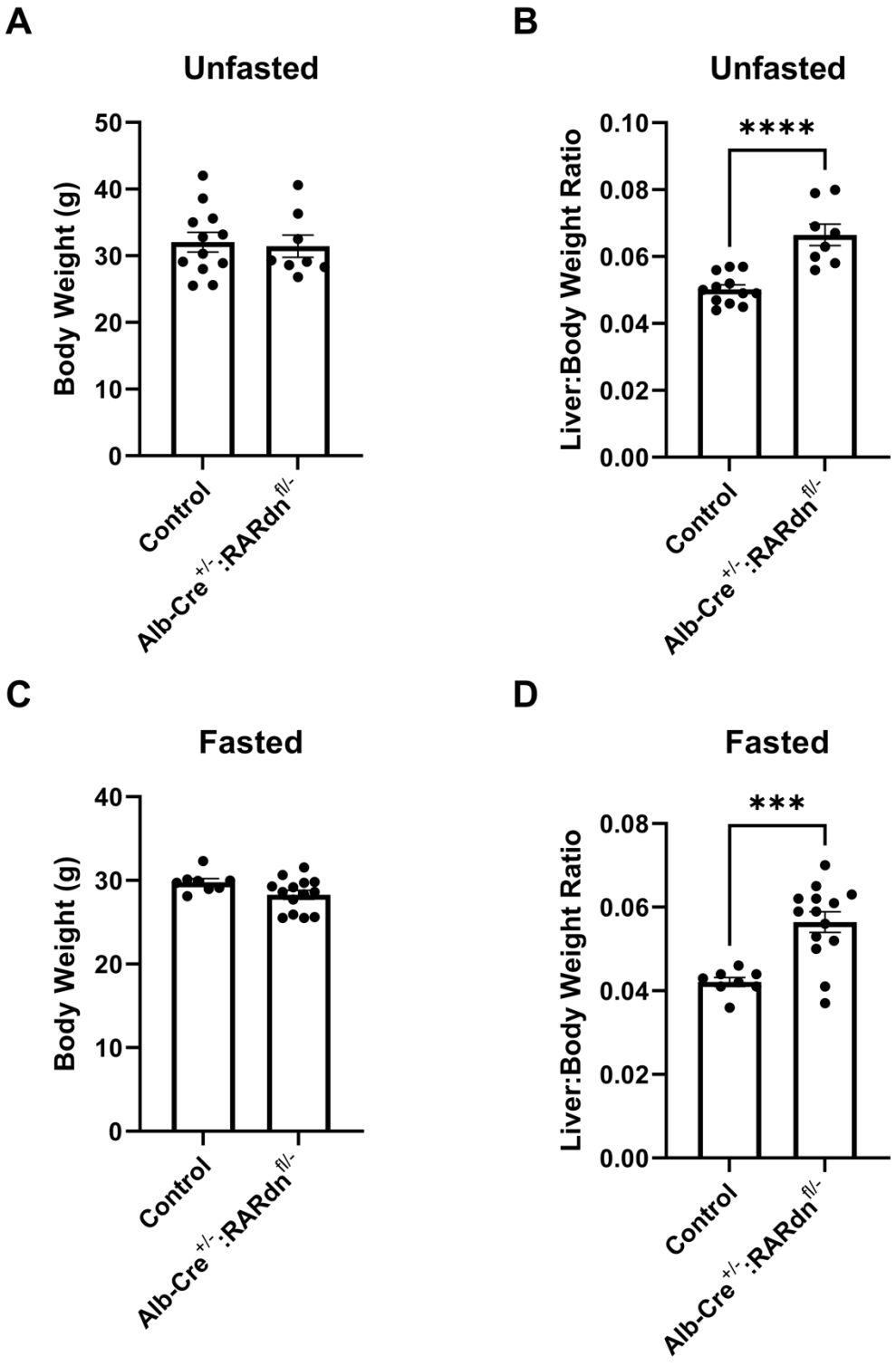

Figure 9. Body and liver weight in Alb-cre$^{+/-}$:RARdn$^{fl/-}$ mice. A) and C) No difference in body weight between Alb-cre$^{+/-}$:RARdn$^{fl/-}$ and control mice in both the unfasted and fasted states. B) and D) Alb-cre$^{+/-}$:RARdn$^{fl/-}$ mice have increased liver weight relative to body weight in both unfasted and fasted states.

6.2.2 Altered Expression of Retinoid Metabolic Genes in Alb-cre$^{+/-}$:RARdn$^{fl/-}$ Mice

Expression changes in retinoid-related genes were assessed by RT-qPCR in unfasted Alb-cre$^{+/-}$:RARdn$^{fl/-}$ mice. *Cyp26a1* was profoundly downregulated in the Alb-cre$^{+/-}$:RARdn$^{fl/-}$ mice while *Cyp26b1* was upregulated (Figure 10). *Rbp4*, retinol dehydrogenase 10 (*Rdh10*), and *Lrat* increased in Alb-cre$^{+/-}$:RARdn$^{fl/-}$ mice by 1.6, 1.5, and 1.9 -fold respectively. Retinol binding protein 1 (*Rbp1*) was decreased in Alb-cre$^{+/-}$:RARdn$^{fl/-}$ mice (fold change = 0.3 compared to control). All other genes tested (*Rarβ*, dehydrogenase/reductase 3 (*Dhrs3*), stimulated by retinoic acid 6 (*Stra6*)) were unchanged.

6.2.3 Altered Retinoid Homeostasis in Alb-cre$^{+/-}$:RARdn$^{fl/-}$ Mice

Both unfasted and fasted Alb-cre$^{+/-}$:RARdn$^{fl/-}$ mice had significantly increased plasma retinol concentrations: 2.84μM and 3.38μM compared to 1.96μM and 1.78μM in the control group for the unfasted and fasted states respectively (Figure 11, Figure 12). This was corroborated by increased plasma RBP4 concentration: 8.60μM in unfasted Alb-cre$^{+/-}$:RARdn$^{fl/-}$ versus 3.84μM in unfasted controls (Figure 11).

Liver retinol decreased in the unfasted Alb-cre$^{+/-}$:RARdn$^{fl/-}$ group, however liver retinol was elevated compared to control genotypes when Alb-cre$^{+/-}$:RARdn$^{fl/-}$ mice were fasted (8.96 versus 15.67 nmol ROH/g Liver and 25.15 versus 17.21 nmol ROH/g liver respectively; Figure 11, Figure 12).

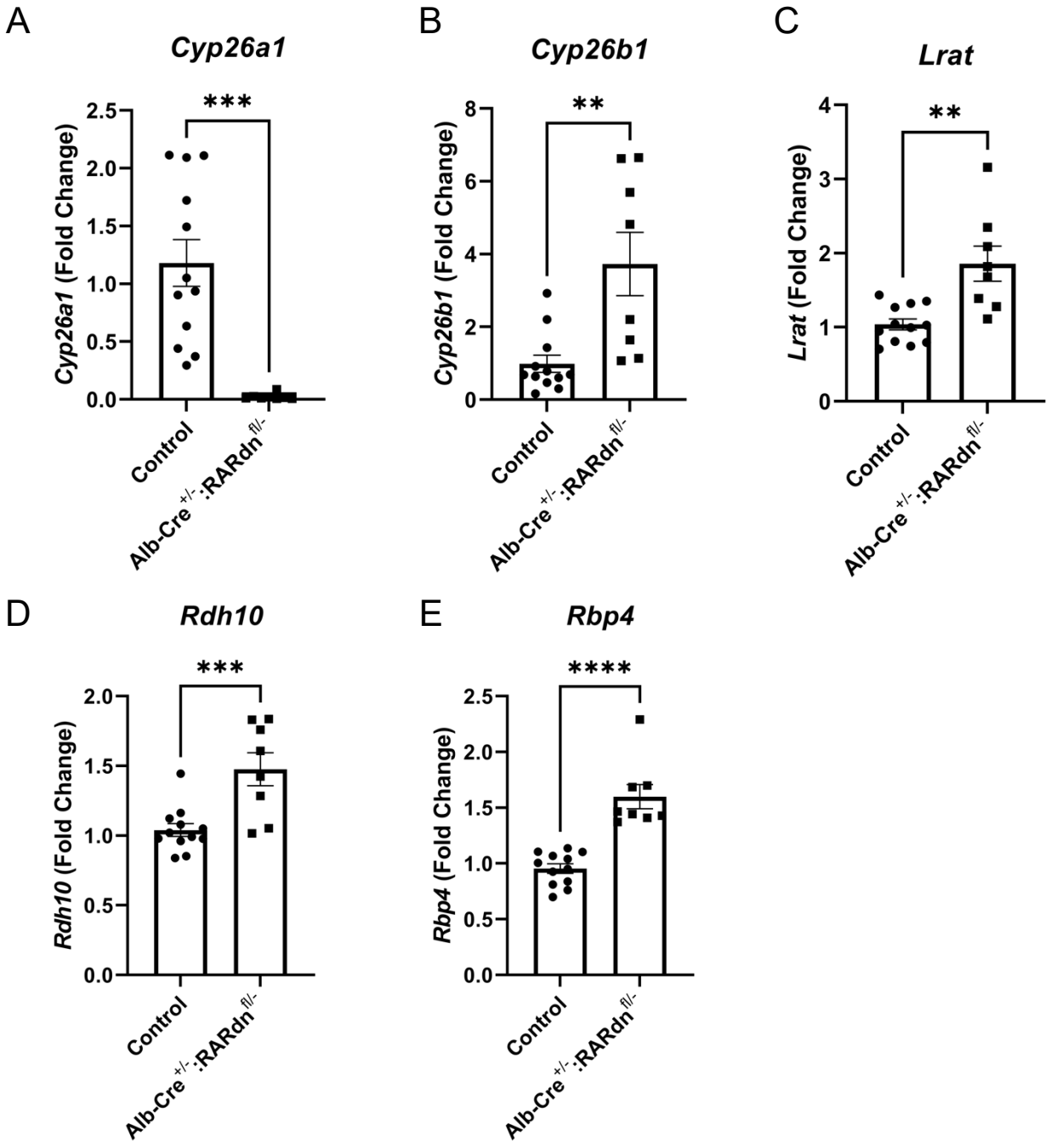

Figure 10. Gene expression changes in unfasted Alb-cre$^{+/-}$:RARdn$^{fl/-}$ mice. A) *Cyp26a1* expression is profoundly downregulated in Alb-cre$^{+/-}$:RARdn$^{fl/-}$ mice. B-E) *Cyp26b1*, *Lrat*, *Rdh10*, and *Rbp4* are upregulated in Alb-cre$^{+/-}$:RARdn$^{fl/-}$ mice. Analysed by unpaired T test **** = $p < 0.0001$; *** = $p < 0.0005$; ** = $p < 0.005$.

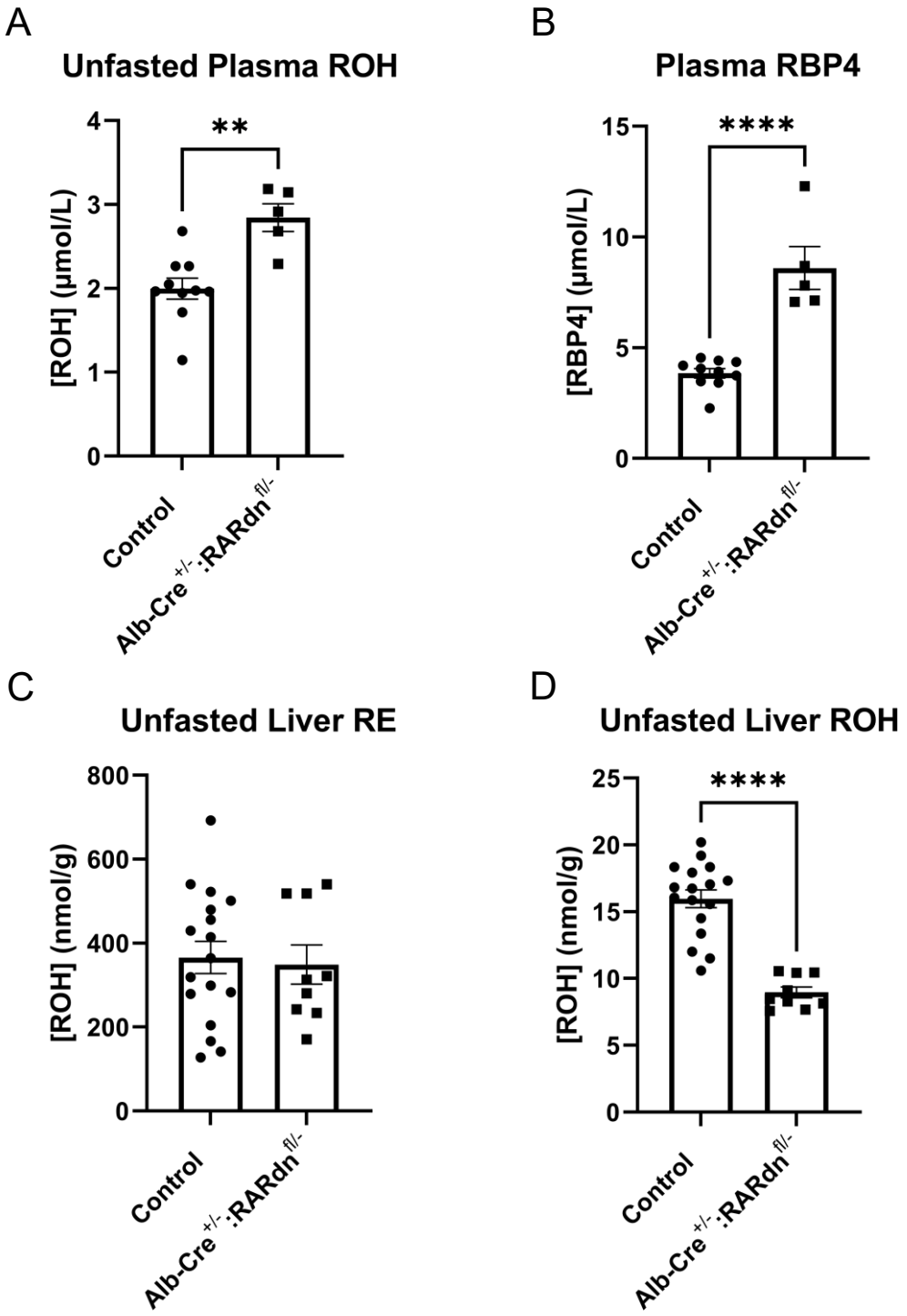

Figure 11. Retinoid homeostasis changes in unfasted Alb-cre$^{+/-}$:RARdn$^{fl/-}$ mice. Retinol (ROH) and retinyl ester (RE) were quantified by HPLC. Retinol binding protein 4 (RBP4) was measured by ELISA. Analysed by unpaired T test **** = $p < 0.0001$; *** = $p < 0.0005$; ** = $p < 0.005$.

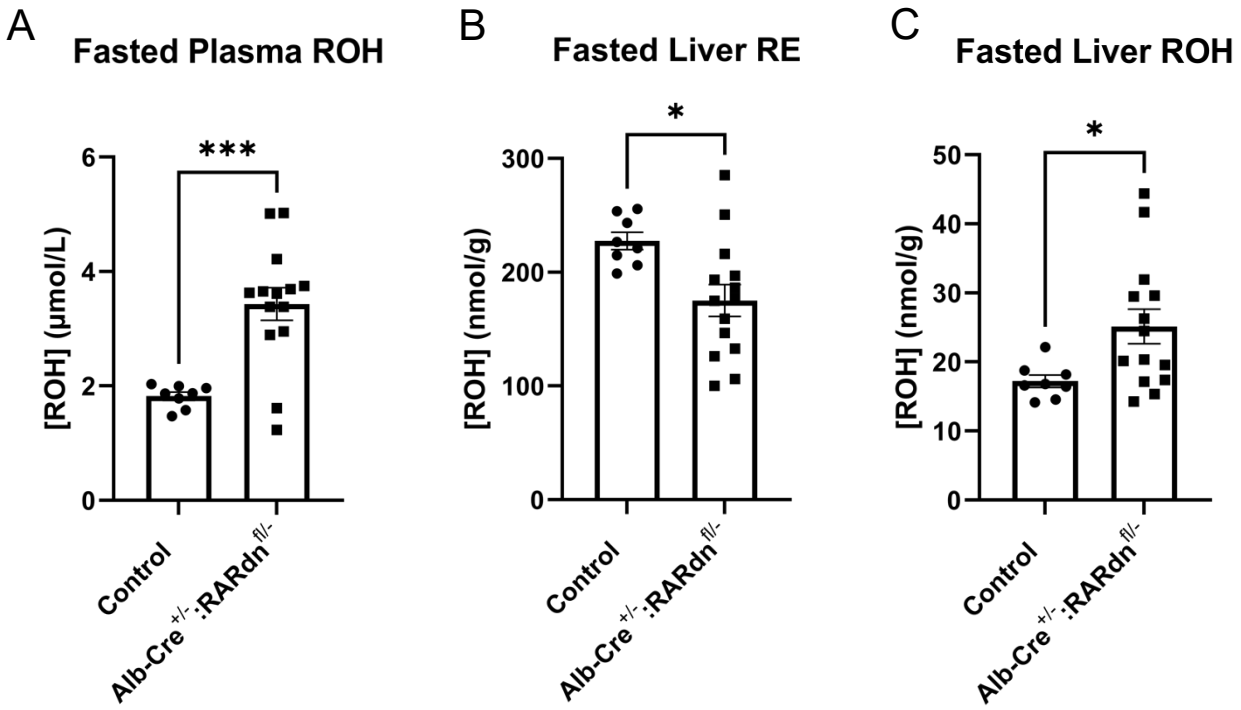

Figure 12. Retinoid homeostasis changes in fasted Alb-cre$^{+/-}$:RARdn$^{fl/-}$ mice. Retinol (ROH) and retinyl ester (RE) were quantified by HPLC. A) Fasted Alb-cre$^{+/-}$:RARdn$^{fl/-}$ mice have increased circulating retinol. B) Fasted Alb-cre$^{+/-}$:RARdn$^{fl/-}$ mice have decreased liver retinyl esters and increased liver retinol (C). Analysed by unpaired T test **** = $p < 0.0001$; *** = $p < 0.0005$; ** = $p < 0.005$.

Retinyl ester stores in the liver decreased from 227.52 nmol RE/g in controls to 175.14 nmol RE/g liver in fasted Alb-cre$^{+/-}$:RARdn$^{fl/-}$ mice (Figure 10, Figure 11), however hepatic RE were unchanged in the unfasted Alb-cre$^{+/-}$:RARdn$^{fl/-}$ group (Figure 10, Figure 11). Corresponding with the increased circulating retinol, lung retinyl ester stores increased from 120.93 nmol RE/g lung in controls to 220.48 nmol RE/g lung in Alb-cre$^{+/-}$:RARdn$^{fl/-}$ mice. There were no changes to retinol or retinyl ester concentrations in white adipose tissue in either the unfasted or fasted mice.

6.2.4 Altered Triacylglycerol Homeostasis in Alb-cre$^{+/-}$:RARdn$^{fl/-}$ Mice

To begin examining the effect of RAR signalling on TG metabolism, plasma and liver triglyceride concentration were determined by colorimetric assay in unfasted and fasted transgenic mice. Plasma triglyceride concentration decreased in both the unfasted (21.97mg/dL) and fasted (36.69mg/dL) Alb-cre$^{+/-}$:RARdn$^{fl/-}$ mice compared to controls (81.58mg/dL and 100.73mg/dL for unfasted and fasted controls respectively; Figure 12). Consistent with the hypothesis that RAR signalling is protective against steatotic liver, hepatic triglycerides increased in the unfasted Alb-cre$^{+/-}$:RARdn$^{fl/-}$ mice (12.94 mg TG/g liver versus 5.86 mg TG/g liver in control mice). However, when mice were fasted to test the effect of impaired RAR signalling on hepatic TG accumulation, the expected fasting-induced increase in hepatic TG was abolished by the Alb-cre$^{+/-}$:RARdn$^{fl/-}$ genotype (Figure 13). Fasted Alb-cre$^{+/-}$:RARdn$^{fl/-}$ mice had an average of 12.79 mg TG/g liver, compared to 20.94 mg TG/g liver in control mice.

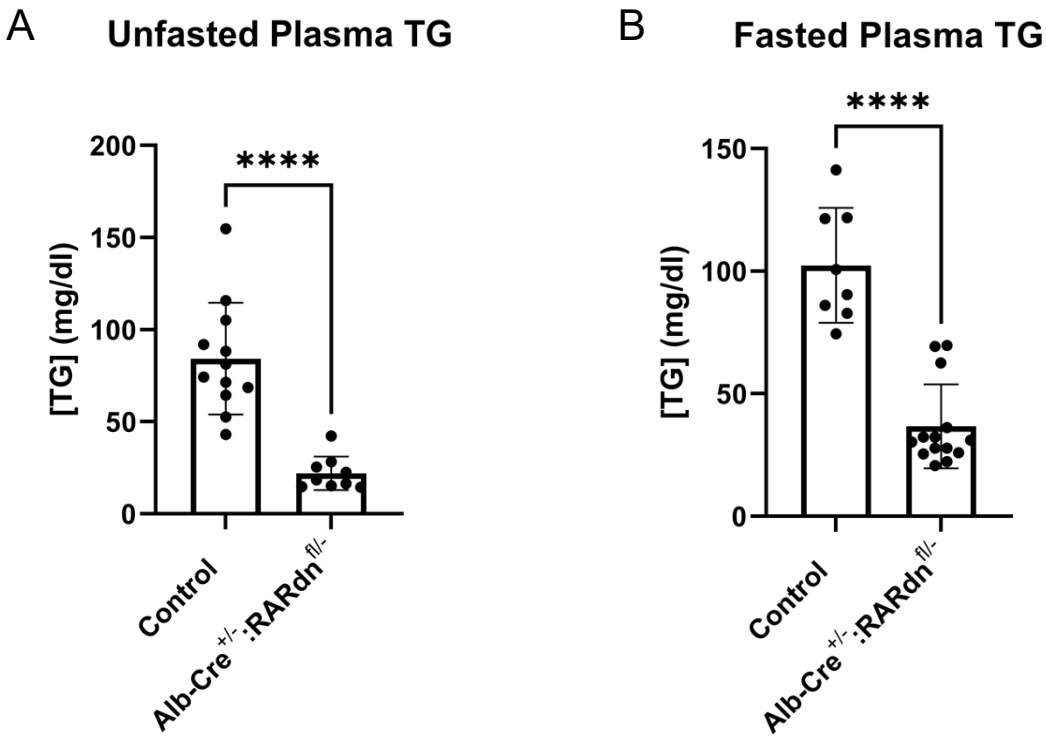

Figure 13. Plasma triacylglycerol in unfasted and fasted Alb-cre$^{+/-}$:RARdn$^{fl/-}$ mice. Alb-cre$^{+/-}$:RARdn$^{fl/-}$ mice have decreased circulating triacylglycerol (TG) relative to control, in both the unfasted (A) and fasted (B) metabolic states. Quantified by HPLC. **** = $p < 0.0001$.

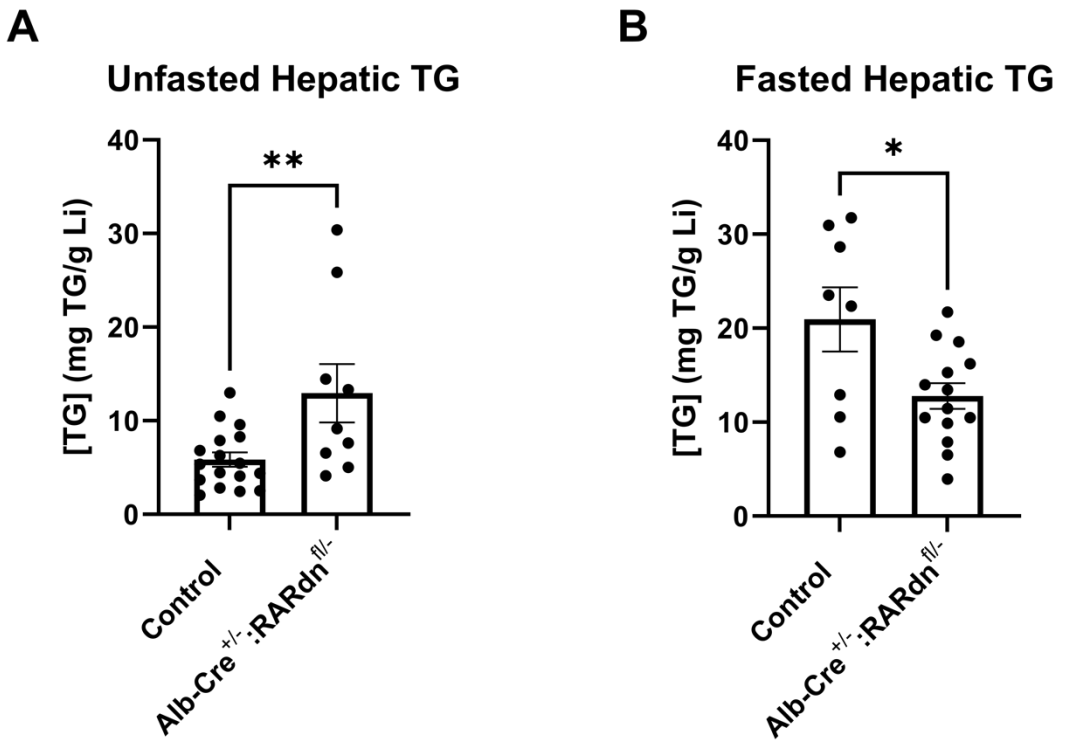

Figure 14. Hepatic triacylglycerol in unfasted and fasted Alb-cre$^{+/-}$:RARdn$^{fl/-}$ mice. A) Alb-cre$^{+/-}$:RARdn$^{fl/-}$ mice have elevated hepatic TG. B) Alb-cre$^{+/-}$:RARdn$^{fl/-}$ mice fail to demonstrate fasting induced hepatic steatosis. Quantified by HPLC and unpaired T test; ** = $p < 0.005$; * = $p < 0.05$.

6.3 Discussion

Since the original development of RAR transgenic mice, various germline, adult-onset, whole-body, and tissue-specific models have been studied to investigate the effects of genetic interference of RA signalling (22, 23). Despite this, certain gaps have persisted in the literature that we sought to address through the Alb-cre$^{+/-}$:RARdn$^{fl/-}$ mouse model. Hepatocyte-specific RARα knockout, for example, does not account for the compensatory upregulation and physiological redundancy of RAR beta and gamma (135, 53). Although the liver has long been known as the central hub of whole-body vitamin A homeostasis, the extent to which hepatocyte specific RAR signalling drives whole-body retinoid homeostasis had not been quantified. Further, the RA-mediated repression of lipogenic genes and pathways raised the question if ablation of RAR signalling in hepatocytes would cause steatosis.

Consistent with our findings in vitamin A deficient mice, the profound decrease in *Cyp26a1* expression in Alb-cre$^{+/-}$:RARdn$^{fl/-}$ mice both validates it as an RA target gene and suggests that an alternative, RAR-independent mechanism of *Cyp26a1* induction is not present in hepatocytes. The pathway of RA breakdown by CYP26A1 is responsible for the vast majority of all retinoid clearance from the body, and hepatocyte specific knockdown of CYP26A1 causes significantly increased intracellular RA concentration (99, 105). Thus, these data propose that RAR signalling is necessary to maintain intracellular RA within homeostatic levels.

Further evidence that hepatic RA is elevated in hepatocytes of Alb-cre$^{+/-}$:RARdn$^{fl/-}$ mice is the induction of *Cyp26b1*. CYP26B1 is predominantly expressed hepatic stellate cells (HSCs) and, like the A1 isoform, is RA responsive. LRAT, which synthesises RE in HSCs for storage, was also upregulated. Compensatory upregulation of *Cyp26b1* and *Lrat* is possible because the

albumin-promoter linked RARaT403 is not expressed in HSCs, leaving endogenous RAR signalling intact. It is debated whether retinol binding protein 4 (RBP4) is expressed by both hepatocytes and HSCs or only by hepatocytes (136). Increased hepatic *Rbp4* expression in Alb-cre$^{+/-}$:RARdn$^{fl/-}$ mice, along with the increased plasma RBP4 and retinol demonstrate that retinol:RBP4 export from the liver is not dependent on hepatocyte RAR, either because it is mediated by HSCs or by the presence of a RAR independent mechanism.

The efflux of hepatic retinol in Alb-cre$^{+/-}$:RARdn$^{fl/-}$ mice is reminiscent of early vitamin A deficiency, in which the liver mobilises stored retinoids to supply extrahepatic tissues; and early MASLD, which is associated with increased circulating RBP4 (137, 138). HPLC quantification revealed that hepatic RE stores were unchanged in unfasted Alb-cre$^{+/-}$:RARdn$^{fl/-}$ mice compared to controls. Thus, ablation of RAR signalling in hepatocytes induces a pseudo-vitamin A deficiency phenotype, in which the liver appears to interpret the absence of RAR activation as low retinol availability. Since the mRNA changes imply that RA itself is elevated, these data propose that hepatocyte RAR activation is the hepatic sensor for vitamin A availability rather than RA or RE levels directly.

Plasma and liver TG concentrations were measured in Alb-cre$^{+/-}$:RARdn$^{fl/-}$ mice to test our understanding of hepatic lipid metabolism regulation by the RAR. Corroborating our microarray finding that RA represses lipogenic gene expression in the liver, unfasted Alb-cre$^{+/-}$:RARdn$^{fl/-}$ mice had elevated hepatic TG compared to control genotypes. However, both unfasted and fasted Alb-cre$^{+/-}$:RARdn$^{fl/-}$ mice had significantly decreased plasma TG. RA treatment is known to decrease hepatic TG secretion and plasma TG concentration in a retinoid X receptor (RXR) dependent mechanism (73, 120). Adipocyte lipoprotein lipase (LPL) is not induced by RA (139). Therefore, it is unlikely that increased plasma retinol in Alb-cre$^{+/-}$

:RARdn$^{fl/-}$ mice caused the reduction in plasma TG by RA-driven increased peripheral clearance. Alternatively, elevated RA may decrease hepatic TG secretion and plasma TG concentration in Alb-cre$^{+/-}$:RARdn$^{fl/-}$ mice through a hepatocyte RAR-independent mechanism.

One cohort of mice were fasted prior to tissue collection to test how RAR signaling affects hepatic TG accumulation, which is induced by fasting (59). Based on the hypothesis that RA is protective against hepatic steatosis, we expected fasted Alb-cre$^{+/-}$:RARdn$^{fl/-}$ mice to have increased hepatic TG relative to both unfasted Alb-cre$^{+/-}$:RARdn$^{fl/-}$ and fasted control mice. Surprisingly, hepatic TG concentration in fasted Alb-cre$^{+/-}$:RARdn$^{fl/-}$ mice was unchanged from unfasted Alb-cre$^{+/-}$:RARdn$^{fl/-}$ mice and substantially lower than fasted control mice, indicating that RAR activation is necessary for fasting induced hepatic steatosis.

Typically, hepatic RA concentration increases modestly during fasting, driven by nuclear FOXO1 induction of retinol dehydrogenase (RDH) and regulated by CYP26A1 mediated breakdown (97, 98, 99). In Alb-cre$^{+/-}$:RARdn$^{fl/-}$ mice however, *Cyp26a1* is profoundly downregulated. I hypothesise that RA, which already appears to be elevated in unfasted Alb-cre$^{+/-}$:RARdn$^{fl/-}$ mice compared to controls, may be significantly increased in these mice after fasting and, consequently, that high RA prevents fasting induced hepatic steatosis through a RAR-independent mechanism.

Though debated, evidence of non-canonical action by RA is present in the literature, and the kinetics of RA binding to lower-affinity proteins would be assisted by high RA concentration (19, 140, 141). Fatty acid binding protein 5 (FABP5) can bind cytosolic RA with nanomolar affinity, which is particularly relevant when cellular retinoic acid binding protein 2 (CRABP2) expression is low (142). CRABP2 itself is a RAR target gene and, although not measured here,

could be repressed in Alb-cre$^{+/-}$:RARdn$^{fl/-}$ mice (143). FABP5-bound RA is delivered to the nuclear receptor peroxisome proliferator activated receptor beta/delta (PPARβ/δ), where RA may activate PPARβ/δ mediated transcription of lipolytic and fatty acid oxidative genes (124, 144-146).

Chapter 7: Conclusions and Future Directions

7.1 Summary

Vitamin A is an essential dietary micronutrient and its active metabolite all-*trans* retinoic acid (RA) is a key regulator of both hepatic retinoid and hepatic lipid homeostasis. As metabolic-dysfunction associated steatotic liver disease (MASLD) is highly prevalent and vitamin A deficiency persists world-wide, understanding the interaction between retinoid signalling and hepatic steatosis is critically important (1-4, 11-14). Yet significant gaps – particularly pertaining to the tissue, dose, and sex dependent variation in retinoid signalling – remain in our understanding of fundamental vitamin A metabolism and the mechanism for retinoid regulation of lipid metabolism is unknown. This research project was developed to answer some of these outstanding questions with the overall goal of building a more holistic understanding of vitamin A signalling and the specific aims of 1) Building a knowledgebase of retinoic acid responsive genes in the liver; and 2) Describing the phenotype of the novel Alb-cre$^{+/-}$:RARdn$^{fl/-}$ mouse model. Retinoid responsive genes were identified in the livers of mice following acute RA treatment (Chapter 4, Chapter 5.2.1), long-term dietary vitamin A manipulation (Chapter 5.2.2), and genetic ablation of retinoic acid receptor (RAR) signalling (Chapter 6.2.2); mRNA changes that developed our understanding of the RA-lipid metabolism interaction were highlighted (Chapters 4.3, 5.3, and 6.3). The effects of a hepatocyte-specific dominant negative RAR (Alb-cre$^{+/-}$:RARdn$^{fl/-}$) on retinoid and lipid homeostasis were quantified (Chapter 6.2), and potential mechanisms were proposed to explain our observations.

7.2 Overall Conclusions

The RA specific hydrolase CYP26A1 emerged as the most prominent RA-responsive gene across all models tested. *Cyp26a1* was induced by acute RA treatment and high dietary vitamin A consumption, and repressed by a vitamin A deficient diet and expression of the dominant negative RAR. While the essential role of CYP26A1 during embryogenesis is clear, its postnatal contributions are often overlooked (42, 100). The physiological significance of CYP26A1 in the adult liver was demonstrated here in its induction by high dietary vitamin A – which appeared to buffer the liver from a significant increase in the concentration of RA, diminishing further mRNA changes – and the consequences when its expression was blocked – wherein Alb-cre$^{+/-}$:RARdn$^{fl/-}$ mice had dysregulated retinoid and triacylglycerol (TG) balance.

The effect of *Cyp26a1* repression without vitamin A deficiency, as demonstrated by the Alb-cre$^{+/-}$:RARdn$^{fl/-}$ mice, was an apparent increase in hepatic RA concentration. This was particularly evident after mice were fasted, when CYP26A1 typically restricts the physiological rise in RA driven by low insulin (97, 98). Interestingly, the apparent rise in hepatic RA concentration was associated with altered TG homeostasis – namely decreased plasma TG and no fasting-induce hepatic steatosis – despite the absence of functional RAR. When considered alongside RA's downregulation of lipogenic pathways by (Chapter 4.3, Figure 3), these data support our original hypothesis that RA is protective against steatosis yet, surprisingly, suggest that the effects of RA are not exclusively mediated by the RAR.

7.3 Limitations and Future Directions

The proposed mechanism by which fasting-induced hepatic steatosis was abolished in Alb-cre$^{+/-}$:RARdn$^{fl/-}$ mice is founded on the assumption that intracellular RA concentration is elevated. Thus, RA should be directly quantified – which can only be done by liquid chromatography-mass spectrometry – to begin testing this hypothesis. RA binding to FABP5 could be examined by quantifying colocalization of a fluorescent RA analogue with immunofluorescent stained FABP5 on microscopy in Alb-cre$^{+/-}$:RARdn$^{fl/-}$ and control mice (147). Activation of PPARβ/δ could be tested by luciferase reporter assay, in which the fluorescent luciferase gene would be linked to the PPARβ/δ promoter; our hypothesis would predict that PPARβ/δ activation is higher in Alb-cre$^{+/-}$:RARdn$^{fl/-}$ mice (140). Binding inhibitors for FABP5 and PPARβ/δ could also be applied *in vivo* to test if the control phenotype would be restored without this pathway (148).

The Alb-cre$^{+/-}$:RARdn$^{fl/-}$ mouse is an intriguing model for future studies. The fasted experiment conducted here were selected as a preliminary test to probe for effects on hepatic lipid accumulation. A true model of MASLD in Alb-cre$^{+/-}$:RARdn$^{fl/-}$ mice could be tested by placing mice on a prolonged high fat or high fat-high cholesterol diet (149). Based on these data, I hypothesise that Alb-cre$^{+/-}$:RARdn$^{fl/-}$ mice would be protected against diet-induced hepatic steatosis.

A significant limitation of the reported sex-differences in gene induction by RA was the gene-list selection based on microarray data from exclusively male mice (Chapter 5). Although qPCR identified fewer genes responsive to RA in females rather than males, this may be indicative of a divergent, rather than reduced, response to RA in females. Thus, repeating a

genome wide expression assay in females would be a valuable future direction. The apparent significance of hepatocyte versus hepatic stellate cell (HSC) responsive genes was prominent across all models tested here. To elucidate these differences, the study should be repeated with single-cell RNA sequencing, rather than whole liver microarray, in female and male mice.

7.4 Significance

Treatment options for MASLD remain limited and, despite RA's seeming protective effect, pharmaceutical administration of systemic RA is not a viable treatment due to its broad and potent affects. The identification by this project of a pathway through which RA may diminish hepatic steatosis opens new avenues for clinical investigation.

References

1. Christensen K, Lawler T, Mares J. Dietary Carotenoids and Non-Alcoholic Fatty Liver Disease among US Adults, NHANES 2003–2014. Nutrients. 2019 May 17;11(5):1101. doi: 10.3390/nu11051101. PMID: 31108934; PMCID: PMC6566688.
2. Terao J. Revisiting carotenoids as dietary antioxidants for human health and disease prevention. Food Funct. 2023 Aug 29;14(17):7799-7824. doi: 10.1039/d3fo02330c. PMID: 37593767.
3. Ahmed M, Praneet Ng A, L'Abbe MR. Nutrient intakes of Canadian adults: results from the Canadian Community Health Survey (CCHS)-2015 Public Use Microdata File. Am J Clin Nutr. 2021 Sep 1;114(3):1131-1140. doi: 10.1093/ajcn/nqab143. PMID: 34020449; PMCID: PMC8408873.
4. Song P, Adeloye D, Li S, Zhao D, Ye X, Pan Q, Qiu Y, Zhang R, Rudan I; Global Health Epidemiology Research Group (GHERG). The prevalence of vitamin A deficiency and its public health significance in children in low- and middle-income countries: A systematic review and modelling analysis. J Glob Health. 2023 Aug 11;13:04084. doi: 10.7189/jogh.13.04084. PMID: 37565390; PMCID: PMC10416138.
5. Neidecker-Gonzales O, Nestel P, Bouis H. Estimating the global costs of vitamin A capsule supplementation: a review of the literature. Food Nutr Bull. 2007 Sep;28(3):307-16. doi: 10.1177/156482650702800307. PMID: 17974364.
6. Isoherranen, N. and Zhong, G. (2019). Biochemical and physiological importance of the CYP26 retinoic acid hydroxylases. Pharmacology and Therapeutics. https://doi.org/10.1016/j.pharmthera.2019.107400.
7. Balmer, J. E., & Blomhoff, R. (2002). Gene expression regulation by retinoic acid. Journal of Lipid Research 43, 1773-1808.
8. Mangelsdorf DJ, Evans RM. The RXR heterodimers and orphan receptors. Cell. 1995 Dec 15;83(6):841-50. doi: 10.1016/0092-8674(95)90200-7. PMID: 8521508.
9. Blaner WS, O'Byrne SM, Wongsiriroj N, Kluwe J, D'Ambrosio DM, Jiang H, Schwabe RF, Hillman EM, Piantedosi R, Libien J. Hepatic stellate cell lipid droplets: a specialized lipid droplet for retinoid storage. Biochim Biophys Acta. 1791(6):467-73, 2009.

10. Rinella ME, Lazarus JV, Ratziu V, Francque SM, Sanyal AJ, Kanwal F, Romero D, Abdelmalek MF, Anstee QM, Arab JP, Arrese M, Bataller R, Beuers U, Boursier J, Bugianesi E, Byrne CD, Castro Narro GE, Chowdhury A, Cortez-Pinto H, Cryer DR, Cusi K, El-Kassas M, Klein S, Eskridge W, Fan J, Gawrieh S, Guy CD, Harrison SA, Kim SU, Koot BG, Korenjak M, Kowdley KV, Lacaille F, Loomba R, Mitchell-Thain R, Morgan TR, Powell EE, Roden M, Romero-Gómez M, Silva M, Singh SP, Sookoian SC, Spearman CW, Tiniakos D, Valenti L, Vos MB, Wong VW, Xanthakos S, Yilmaz Y, Younossi Z, Hobbs A, Villota-Rivas M, Newsome PN; NAFLD Nomenclature consensus group. A multisociety Delphi consensus statement on new fatty liver disease nomenclature. J Hepatol. 2023 Dec;79(6):1542-1556. doi: 10.1016/j.jhep.2023.06.003. Epub 2023 Jun 24. PMID: 37364790.
11. Loomba R, Friedman SL, Shulman GI. Mechanisms and disease consequences of nonalcoholic fatty liver disease. Cell. 2021 May 13;184(10):2537-2564. doi: 10.1016/j.cell.2021.04.015. PMID: 33989548.
12. Younossi Z, Anstee QM, Marietti M, Hardy T, Henry L, Eslam M, George J, Bugianesi E. Global burden of NAFLD and NASH: trends, predictions, risk factors and prevention. Nat Rev Gastroenterol Hepatol. 2018 Jan;15(1):11-20. doi: 10.1038/nrgastro.2017.109. Epub 2017 Sep 20. PMID: 28930295.
13. Sookoian S, Pirola CJ. Genetic predisposition in nonalcoholic fatty liver disease. Clin Mol Hepatol. 2017 Mar;23(1):1-12. doi: 10.3350/cmh.2016.0109. Epub 2017 Mar 9. PMID: 28268262; PMCID: PMC5381829.
14. Vusirikala A, Thomas T, Bhala N, Tahrani AA, Thomas GN, Nirantharakumar K. Impact of obesity and metabolic health status in the development of non-alcoholic fatty liver disease (NAFLD): A United Kingdom population-based cohort study using the health improvement network (THIN). BMC Endocr Disord. 2020 Jun 30;20(1):96. doi: 10.1186/s12902-020-00582-9. PMID: 32605642; PMCID: PMC7325099.
15. Dowman JK, Tomlinson JW, Newsome PN. Pathogenesis of non-alcoholic fatty liver disease. QJM. 2010 Feb;103(2):71-83. doi: 10.1093/qjmed/hcp158. Epub 2009 Nov 13. PMID: 19914930; PMCID: PMC2810391.
16. Feldstein AE, Werneburg NW, Canbay A, Guicciardi ME, Bronk SF, Rydzewski R, Burgart LJ, Gores GJ. Free fatty acids promote hepatic lipotoxicity by stimulating TNF-

alpha expression via a lysosomal pathway. Hepatology. 2004 Jul;40(1):185-94. doi: 10.1002/hep.20283. PMID: 15239102.

17. Chaves GV, Pereira SE, Saboya CJ, Spitz D, Rodrigues CS, Ramalho A. Association between liver vitamin A reserves and severity of nonalcoholic fatty liver disease in the class III obese following bariatric surgery. Obes Surg. 2014 Feb;24(2):219-24. doi: 10.1007/s11695-013-1087-8. PMID: 24101088.
18. Hirsova P, Ibrahim SH, Verma VK, Morton LA, Shah VH, LaRusso NF, Gores GJ, Malhi H. Extracellular vesicles in liver pathobiology: Small particles with big impact. Hepatology. 2016 Dec;64(6):2219-2233. doi: 10.1002/hep.28814. Epub 2016 Oct 20. PMID: 27628960; PMCID: PMC5115968.
19. Berry DC, Noy N. All-trans-retinoic acid represses obesity and insulin resistance by activating both peroxisome proliferation-activated receptor beta/delta and retinoic acid receptor. Mol Cell Biol. 2009 Jun;29(12):3286-96. doi: 10.1128/MCB.01742-08. Epub 2009 Apr 13. PMID: 19364826; PMCID: PMC2698724.
20. Kim SC, Kim CK, Axe D, Cook A, Lee M, Li T, Smallwood N, Chiang JY, Hardwick JP, Moore DD, Lee YK. All-trans-retinoic acid ameliorates hepatic steatosis in mice by a novel transcriptional cascade. Hepatology. 2014 May;59(5):1750-60. doi: 10.1002/hep.26699. Epub 2014 Mar 26. PMID: 24038081; PMCID: PMC4008145.
21. Cassim Bawa FN, Xu Y, Gopoju R, Plonski NM, Shiyab A, Hu S, Chen S, Zhu Y, Jadhav K, Kasumov T, Zhang Y. Hepatic retinoic acid receptor alpha mediates all-trans retinoic acid's effect on diet-induced hepatosteatosis. Hepatol Commun. 2022 Jul 19. doi: 10.1002/hep4.2049. Epub ahead of print. PMID: 35852305.
22. Li E, Sucov HM, Lee KF, Evans RM, Jaenisch R. Normal development and growth of mice carrying a targeted disruption of the alpha 1 retinoic acid receptor gene. Proc Natl Acad Sci U S A. 1993 Feb 15;90(4):1590-4. Doi: 10.1073/pnas.90.4.1590. PMID: 7679509; PMCID: PMC45920.
23. Lufkin T, Lohnes D, Mark M, Dierich A, Gorry P, Gaub MP, LeMeur M, Chambon P. High postnatal lethality and testis degeneration in retinoic acid receptor alpha mutant mice. Proc Natl Acad Sci U S A. 1993 Aug 1;90(15):7225-9. doi: 10.1073/pnas.90.15.7225. PMID: 8394014; PMCID: PMC47109.

24. Damm K, Heyman RA, Umesono K, Evans RM. Functional inhibition of retinoic acid response by dominant negative retinoic acid receptor mutants. Proc Natl Acad Sci U S A. 1993 Apr 1;90(7):2989-93. doi: 10.1073/pnas.90.7.2989. PMID: 8096643; PMCID: PMC46222.
25. Lee SA, Jiang H, Feranil JB, Brun PJ, Blaner WS. Adipocyte-specific expression of a retinoic acid receptor α dominant negative form causes glucose intolerance and hepatic steatosis in mice. Biochem Biophys Res Commun. 2019 Jul 5;514(4):1231-1237. doi: 10.1016/j.bbrc.2019.05.075. Epub 2019 May 17. PMID: 31109648.
26. Napoli JL. Retinoic Acid: Sexually Dimorphic, Anti-Insulin and Concentration-Dependent Effects on Energy. Nutrients. 2022 Apr 8;14(8):1553. doi: 10.3390/nu14081553. PMID: 35458115; PMCID: PMC9027308.
27. Burra P, Bizzaro D, Gonta A, Shalaby S, Gambato M, Morelli MC, Trapani S, Floreani A, Marra F, Brunetto MR, Taliani G, Villa E; Special Interest Group Gender in Hepatology of the Italian Association for the Study of the Liver (AISF). Clinical impact of sexual dimorphism in non-alcoholic fatty liver disease (NAFLD) and non-alcoholic steatohepatitis (NASH). Liver Int. 2021 Aug;41(8):1713-1733. doi: 10.1111/liv.14943. Epub 2021 Jun 8. PMID: 33982400.
28. McCollum EV, Davis M: The necessity of certain lipins in the diet during growth. J Biol Chem 1913;15:167–175
29. O'Byrne SM, Blaner WS. Retinol and retinyl esters: biochemistry and physiology. J Lipid Res. 2013 Jul;54(7):1731-43. doi: 10.1194/jlr.R037648. Epub 2013 Apr 26. PMID: 23625372; PMCID: PMC3679378.
30. Cooper AD. Hepatic uptake of chylomicron remnants. J Lipid Res. 1997 Nov;38(11):2173-92. PMID: 9392416.
31. Kane MA, Folias AE, Napoli JL. HPLC/UV quantitation of retinal, retinol, and retinyl esters in serum and tissues. Anal Biochem. 2008 Jul 1;378(1):71-9. doi: 10.1016/j.ab.2008.03.038. Epub 2008 Mar 25. PMID: 18410739; PMCID: PMC2483537.
32. Harrison EH, Gad MZ, Ross AC. Hepatic uptake and metabolism of chylomicron retinyl esters: probable role of plasma membrane/endosomal retinyl ester hydrolases. J Lipid Res. 1995 Jul;36(7):1498-506. PMID: 7595074.

33. Hessel S, Eichinger A, Isken A, Amengual J, Hunzelmann S, Hoeller U, Elste V, Hunziker W, Goralczyk R, Oberhauser V, von Lintig J, Wyss A. CMO1 deficiency abolishes vitamin A production from beta-carotene and alters lipid metabolism in mice. J Biol Chem. 2007 Nov 16;282(46):33553-33561. doi: 10.1074/jbc.M706763200. Epub 2007 Sep 12. PMID: 17855355.
34. Kanai M, Raz A, Goodman DS. Retinol-binding protein: the transport protein for vitamin A in human plasma. J Clin Invest. 1968 Sep;47(9):2025-44. doi: 10.1172/JCI105889. PMID: 5675424; PMCID: PMC297364.
35. Blaner WS, Dixon JL, Moriwaki H, Martino RA, Stein O, Stein Y, Goodman DS. Studies on the in vivo transfer of retinoids from parenchymal to stellate cells in rat liver. Eur J Biochem. 1987 Apr 15;164(2):301-7. doi: 10.1111/j.1432-1033.1987.tb11058.x. PMID: 3569264.
36. Yamada M, Blaner WS, Soprano DR, Dixon JL, Kjeldbye HM, Goodman DS. Biochemical characteristics of isolated rat liver stellate cells. Hepatology. 1987 Nov-Dec;7(6):1224-9. doi: 10.1002/hep.1840070609. PMID: 2824313.
37. Weng W, Li L, van Bennekum AM, Potter SH, Harrison EH, Blaner WS, Breslow JL, Fisher EA. Intestinal absorption of dietary cholesteryl ester is decreased but retinyl ester absorption is normal in carboxyl ester lipase knockout mice. Biochemistry. 1999 Mar 30;38(13):4143-9. doi: 10.1021/bi981679a. PMID: 10194330.
38. Mello T, Nakatsuka A, Fears S, Davis W, Tsukamoto H, Bosron WF, Sanghani SP. Expression of carboxylesterase and lipase genes in rat liver cell-types. Biochem Biophys Res Commun. 2008 Sep 26;374(3):460-4. doi: 10.1016/j.bbrc.2008.07.024. Epub 2008 Jul 17. PMID: 18639528; PMCID: PMC2566784.
39. Pang W, Zhang Y, Wang S, Jia A, Dong W, Cai C, Hua Z, Zhang J. The mPlrp2 and mClps genes are involved in the hydrolysis of retinyl esters in the mouse liver. J Lipid Res. 2011 May;52(5):934-41. doi: 10.1194/jlr.M010082. Epub 2011 Feb 21. PMID: 21339507; PMCID: PMC3073471.
40. Thatcher JE, Isoherranen N. The role of CYP26 enzymes in retinoic acid clearance. Expert Opin Drug Metab Toxicol. 2009 Aug;5(8):875-86. doi: 10.1517/17425250903032681. PMID: 19519282; PMCID: PMC2730205.

41. Xi J, Yang Z. Expression of RALDHs (ALDH1As) and CYP26s in human tissues and during the neural differentiation of P19 embryonal carcinoma stem cell. Gene Expr Patterns. 2008 Jul;8(6):438-442. doi: 10.1016/j.gep.2008.04.003. Epub 2008 Apr 22. PMID: 18502188.
42. Abu-Abed S, Dollé P, Metzger D, Beckett B, Chambon P, Petkovich M. The retinoic acid-metabolizing enzyme, CYP26A1, is essential for normal hindbrain patterning, vertebral identity, and development of posterior structures. Genes Dev. 2001 Jan 15;15(2):226-40. doi: 10.1101/gad.855001. PMID: 11157778; PMCID: PMC312609.
43. Yashiro K, Zhao X, Uehara M, Yamashita K, Nishijima M, Nishino J, Saijoh Y, Sakai Y, Hamada H. Regulation of retinoic acid distribution is required for proximodistal patterning and outgrowth of the developing mouse limb. Dev Cell. 2004 Mar;6(3):411-22. doi: 10.1016/s1534-5807(04)00062-0. PMID: 15030763.
44. D'Ambrosio DN, Walewski JL, Clugston RD, Berk PD, Rippe RA, Blaner WS. Distinct populations of hepatic stellate cells in the mouse liver have different capacities for retinoid and lipid storage. PLoS One. 2011;6(9):e24993. doi: 10.1371/journal.pone.0024993. Epub 2011 Sep 16. PMID: 21949825; PMCID: PMC3174979.
45. de Thé H, Vivanco-Ruiz MM, Tiollais P, Stunnenberg H, Dejean A. Identification of a retinoic acid responsive element in the retinoic acid receptor beta gene. Nature. 1990 Jan 11;343(6254):177-80. doi: 10.1038/343177a0. PMID: 2153268.
46. Kurokawa R, DiRenzo J, Boehm M, Sugarman J, Gloss B, Rosenfeld MG, Heyman RA, Glass CK. Regulation of retinoid signalling by receptor polarity and allosteric control of ligand binding. Nature. 1994 Oct 6;371(6497):528-31. doi: 10.1038/371528a0. PMID: 7935766.
47. Shimada T, Ross AC, Muccio DD, Brouillette WJ, Shealy YF. Regulation of hepatic lecithin:retinol acyltransferase activity by retinoic acid receptor-selective retinoids. Arch Biochem Biophys. 1997 Aug 1;344(1):220-7. doi: 10.1006/abbi.1997.0209. PMID: 9244401.
48. Elizondo G, Corchero J, Sterneck E, Gonzalez FJ. Feedback inhibition of the retinaldehyde dehydrogenase gene ALDH1 by retinoic acid through retinoic acid receptor

alpha and CCAAT/enhancer-binding protein beta. J Biol Chem. 2000 Dec 15;275(50):39747-53. doi: 10.1074/jbc.M004987200. PMID: 10995752.

49. Elizondo G, Medina-Díaz IM, Cruz R, Gonzalez FJ, Vega L. Retinoic acid modulates retinaldehyde dehydrogenase 1 gene expression through the induction of GADD153-C/EBPbeta interaction. Biochem Pharmacol. 2009 Jan 15;77(2):248-57. doi: 10.1016/j.bcp.2008.10.011. Epub 2008 Oct 17. PMID: 18992716; PMCID: PMC2790144.
50. Li E, Sucov HM, Lee KF, Evans RM, Jaenisch R. Normal development and growth of mice carrying a targeted disruption of the alpha 1 retinoic acid receptor gene. Proc Natl Acad Sci U S A. 1993 Feb 15;90(4):1590-4. doi: 10.1073/pnas.90.4.1590. PMID: 7679509; PMCID: PMC45920.
51. Ghyselinck NB, Dupé V, Dierich A, Messaddeq N, Garnier JM, Rochette-Egly C, Chambon P, Mark M. Role of the retinoic acid receptor beta (RARbeta) during mouse development. Int J Dev Biol. 1997 Jun;41(3):425-47. PMID: 9240560
52. Subbarayan V, Kastner P, Mark M, Dierich A, Gorry P, Chambon P. Limited specificity and large overlap of the functions of the mouse RAR gamma 1 and RAR gamma 2 isoforms. Mech Dev. 1997 Aug;66(1-2):131-42. doi: 10.1016/s0925-4773(97)00098-1. PMID: 9376317.
53. Manshouri T, Yang Y, Lin H, Stass SA, Glassman AB, Keating MJ, Albitar M. Downregulation of RAR alpha in mice by antisense transgene leads to a compensatory increase in RAR beta and RAR gamma and development of lymphoma. Blood. 1997 Apr 1;89(7):2507-15. PMID: 9116296.
54. Calder PC. Bioactive lipids in foods. Biochem Soc Trans. 1996 Aug;24(3):814-24. doi: 10.1042/bst0240814. PMID: 8878854.
55. Mu H, Høy CE. The digestion of dietary triacylglycerols. Prog Lipid Res. 2004 Mar;43(2):105-33. doi: 10.1016/s0163-7827(03)00050-x. PMID: 14654090.
56. Redgrave TG. Chylomicron metabolism. Biochem Soc Trans. 2004 Feb;32(Pt 1):79-82. doi: 10.1042/bst0320079. PMID: 14748717.
57. Kraemer FB, Shen WJ. Hormone-sensitive lipase: control of intracellular tri-(di-)acylglycerol and cholesteryl ester hydrolysis. J Lipid Res. 2002 Oct;43(10):1585-94. doi: 10.1194/jlr.r200009-jlr200. PMID: 12364542.

58. Cerk IK, Wechselberger L, Oberer M. Adipose Triglyceride Lipase Regulation: An Overview. Curr Protein Pept Sci. 2018;19(2):221-233. doi: 10.2174/1389203718666170918160110. PMID: 28925902; PMCID: PMC7613786.
59. Guan HP, Goldstein JL, Brown MS, Liang G. Accelerated fatty acid oxidation in muscle averts fasting-induced hepatic steatosis in SJL/J mice. J Biol Chem. 2009 Sep 4;284(36):24644-52. doi: 10.1074/jbc.M109.034397. Epub 2009 Jul 6. PMID: 19581301; PMCID: PMC2782053.
60. Ruppert PMM, Kersten S. Mechanisms of hepatic fatty acid oxidation and ketogenesis during fasting. Trends Endocrinol Metab. 2023 Nov 6:S1043-2760(23)00215-1. doi: 10.1016/j.tem.2023.10.002. Epub ahead of print. PMID: 37940485.
61. Kawano Y, Cohen DE. Mechanisms of hepatic triglyceride accumulation in non-alcoholic fatty liver disease. J Gastroenterol. 2013 Apr;48(4):434-41. doi: 10.1007/s00535-013-0758-5. Epub 2013 Feb 9. PMID: 23397118; PMCID: PMC3633701.
62. Delarue J, Magnan C. Free fatty acids and insulin resistance. Curr Opin Clin Nutr Metab Care. 2007 Mar;10(2):142-8. doi: 10.1097/MCO.0b013e328042ba90. PMID: 17285001.
63. Ferré P, Foufelle F. Hepatic steatosis: a role for de novo lipogenesis and the transcription factor SREBP-1c. Diabetes Obes Metab. 2010 Oct;12 Suppl 2:83-92. doi: 10.1111/j.1463-1326.2010.01275.x. PMID: 21029304.
64. Li S, Brown MS, Goldstein JL. Bifurcation of insulin signaling pathway in rat liver: mTORC1 required for stimulation of lipogenesis, but not inhibition of gluconeogenesis. Proc Natl Acad Sci U S A. 2010 Feb 23;107(8):3441-6. doi: 10.1073/pnas.0914798107. Epub 2010 Feb 1. PMID: 20133650; PMCID: PMC2840492.
65. Yecies JL, Zhang HH, Menon S, Liu S, Yecies D, Lipovsky AI, Gorgun C, Kwiatkowski DJ, Hotamisligil GS, Lee CH, Manning BD. Akt stimulates hepatic SREBP1c and lipogenesis through parallel mTORC1-dependent and independent pathways. Cell Metab. 2011 Jul 6;14(1):21-32. doi: 10.1016/j.cmet.2011.06.002. Erratum in: Cell Metab. 2011 Aug 3;14(2):280. PMID: 21723501; PMCID: PMC3652544.
66. Ter Horst KW, Vatner DF, Zhang D, Cline GW, Ackermans MT, Nederveen AJ, Verheij J, Demirkiran A, van Wagensveld BA, Dallinga-Thie GM, Nieuwdorp M, Romijn JA, Shulman GI, Serlie MJ. Hepatic Insulin Resistance Is Not Pathway Selective in Humans

With Nonalcoholic Fatty Liver Disease. Diabetes Care. 2021 Feb;44(2):489-498. doi: 10.2337/dc20-1644. Epub 2020 Dec 8. PMID: 33293347; PMCID: PMC7818337.

67. Longuet C, Sinclair EM, Maida A, Baggio LL, Maziarz M, Charron MJ, Drucker DJ. The glucagon receptor is required for the adaptive metabolic response to fasting. Cell Metab. 2008 Nov;8(5):359-71. doi: 10.1016/j.cmet.2008.09.008. PMID: 19046568; PMCID: PMC2593715.
68. Sidossis LS, Stuart CA, Shulman GI, Lopaschuk GD, Wolfe RR. Glucose plus insulin regulate fat oxidation by controlling the rate of fatty acid entry into the mitochondria. J Clin Invest. 1996 Nov 15;98(10):2244-50. doi: 10.1172/JCI119034. PMID: 8941640; PMCID: PMC507673.
69. Schmid AI, Szendroedi J, Chmelik M, Krssák M, Moser E, Roden M. Liver ATP synthesis is lower and relates to insulin sensitivity in patients with type 2 diabetes. Diabetes Care. 2011 Feb;34(2):448-53. doi: 10.2337/dc10-1076. Epub 2011 Jan 7. PMID: 21216854; PMCID: PMC3024365.
70. Satapati S, Sunny NE, Kucejova B, Fu X, He TT, Méndez-Lucas A, Shelton JM, Perales JC, Browning JD, Burgess SC. Elevated TCA cycle function in the pathology of diet-induced hepatic insulin resistance and fatty liver. J Lipid Res. 2012 Jun;53(6):1080-92. doi: 10.1194/jlr.M023382. Epub 2012 Apr 9. PMID: 22493093; PMCID: PMC3351815.
71. Pessayre D, Fromenty B. NASH: a mitochondrial disease. J Hepatol. 2005 Jun;42(6):928-40. doi: 10.1016/j.jhep.2005.03.004. Epub 2005 Mar 26. PMID: 15885365.
72. Ginsberg HN, Fisher EA. The ever-expanding role of degradation in the regulation of apolipoprotein B metabolism. J Lipid Res. 2009 Apr;50 Suppl(Suppl):S162-6. doi: 10.1194/jlr.R800090-JLR200. Epub 2008 Dec 2. PMID: 19050312; PMCID: PMC2674708.
73. Zhou F, Wu X, Pinos I, Abraham BM, Barrett TJ, von Lintig J, Fisher EA, Amengual J. β-Carotene conversion to vitamin A delays atherosclerosis progression by decreasing hepatic lipid secretion in mice. J Lipid Res. 2020 Nov;61(11):1491-1503. doi: 10.1194/jlr.RA120001066. Epub 2020 Sep 22. PMID: 32963037; PMCID: PMC7604725.
74. Fabbrini E, Mohammed BS, Magkos F, Korenblat KM, Patterson BW, Klein S. Alterations in adipose tissue and hepatic lipid kinetics in obese men and women with

nonalcoholic fatty liver disease. Gastroenterology. 2008 Feb;134(2):424-31. doi: 10.1053/j.gastro.2007.11.038. Epub 2007 Nov 28. PMID: 18242210; PMCID: PMC2705923.

75. Donnelly KL, Smith CI, Schwarzenberg SJ, Jessurun J, Boldt MD, Parks EJ. Sources of fatty acids stored in liver and secreted via lipoproteins in patients with nonalcoholic fatty liver disease. J Clin Invest. 2005 May;115(5):1343-51. doi: 10.1172/JCI23621. PMID: 15864352; PMCID: PMC1087172.
76. Kuri-Harcuch W. Differentiation of 3T3-F442A cells into adipocytes is inhibited by retinoic acid. Differentiation. 1982;23(2):164-9. doi: 10.1111/j.1432-0436.1982.tb01279.x. PMID: 7166214.
77. Valmaseda A, Carmona MC, Barberá MJ, Viñas O, Mampel T, Iglesias R, Villarroya F, Giralt M. Opposite regulation of PPAR-alpha and -gamma gene expression by both their ligands and retinoic acid in brown adipocytes. Mol Cell Endocrinol. 1999 Aug 20;154(1-2):101-9. doi: 10.1016/s0303-7207(99)00081-7. PMID: 10509805.
78. Sawada Y, Noda M. An adipogenic basic helix-loop-helix-leucine zipper type transcription factor (ADD1) mRNA is expressed and regulated by retinoic acid in osteoblastic cells. Mol Endocrinol. 1996 Oct;10(10):1238-48. doi: 10.1210/mend.10.10.9121491. PMID: 9121491.
79. Zhong G, Kirkwood J, Won KJ, Tjota N, Jeong H, Isoherranen N. Characterization of Vitamin A Metabolome in Human Livers With and Without Nonalcoholic Fatty Liver Disease. J Pharmacol Exp Ther. 2019 Jul;370(1):92-103. doi: 10.1124/jpet.119.258517. Epub 2019 May 1. PMID: 31043436; PMCID: PMC6548984.
80. Liu C, Sun X, Peng J, Yu H, Lu J, Feng Y. Association between dietary vitamin A intake from different sources and non-alcoholic fatty liver disease among adults. Sci Rep. 2024 Jan 22;14(1):1851. doi: 10.1038/s41598-024-52077-5. PMID: 38253816; PMCID: PMC10803811.
81. Amengual J, Ribot J, Bonet ML, Palou A. Retinoic acid treatment enhances lipid oxidation and inhibits lipid biosynthesis capacities in the liver of mice. Cell Physiol Biochem. 2010;25(6):657-66. doi: 10.1159/000315085. Epub 2010 May 18. PMID: 20511711.

82. Shiota G, Tuchiya H. [Mouse NASH model using retinoic acid receptor alpha]. Nihon Rinsho. 2006 Jun;64(6):1049-55. Japanese. PMID: 16768108.
83. Palomer X, Barroso E, Pizarro-Delgado J, Peña L, Botteri G, Zarei M, Aguilar D, Montori-Grau M, Vázquez-Carrera M. PPARβ/δ: A Key Therapeutic Target in Metabolic Disorders. Int J Mol Sci. 2018 Mar 20;19(3):913. doi: 10.3390/ijms19030913. PMID: 29558390; PMCID: PMC5877774.
84. Seif El-Din SH, El-Lakkany NM, El-Naggar AA, Hammam OA, Abd El-Latif HA, Ain-Shoka AA, Ebeid FA. Effects of rosuvastatin and/or β-carotene on non-alcoholic fatty liver in rats. Res Pharm Sci. 2015 Jul-Aug;10(4):275-87. PMID: 26600855; PMCID: PMC4623617.
85. Ni Y, Nagashimada M, Zhan L, Nagata N, Kobori M, Sugiura M, Ogawa K, Kaneko S, Ota T. Prevention and reversal of lipotoxicity-induced hepatic insulin resistance and steatohepatitis in mice by an antioxidant carotenoid, β-cryptoxanthin. Endocrinology. 2015 Mar;156(3):987-99. doi: 10.1210/en.2014-1776. Epub 2015 Jan 6. PMID: 25562616.
86. Chang WH, Reddy SP, Di YP, Yoneda K, Harper R, Wu R. Regulation of thioredoxin gene expression by vitamin A in human airway epithelial cells. Am J Respir Cell Mol Biol. 2002 May;26(5):627-35. doi: 10.1165/ajrcmb.26.5.4276. PMID: 11970916.
87. Terao J. Revisiting carotenoids as dietary antioxidants for human health and disease prevention. Food Funct. 2023 Aug 29;14(17):7799-7824. doi: 10.1039/d3fo02330c. PMID: 37593767.
88. Blaner WS, Shmarakov IO, Traber MG. Vitamin A and Vitamin E: Will the Real Antioxidant Please Stand Up? Annu Rev Nutr. 2021 Oct 11;41:105-131. doi: 10.1146/annurev-nutr-082018-124228. Epub 2021 Jun 11. PMID: 34115520.
89. Bhupathiraju SN, Wedick NM, Pan A, Manson JE, Rexrode KM, Willett WC, Rimm EB, Hu FB. Quantity and variety in fruit and vegetable intake and risk of coronary heart disease. Am J Clin Nutr. 2013 Dec;98(6):1514-23. doi: 10.3945/ajcn.113.066381. Epub 2013 Oct 2. PMID: 24088718; PMCID: PMC3831537.
90. Zhao Y, Vuckovic M, Yoo HS, Fox N, Rodriguez A, McKessy K, Napoli JL. Retinoic acid exerts sexually dimorphic effects on muscle energy metabolism and function. J Biol

Chem. 2021 Sep;297(3):101101. doi: 10.1016/j.jbc.2021.101101. Epub 2021 Aug 19. PMID: 34419449; PMCID: PMC8441203.

91. Li XH, Kakkad B, Ong DE. Estrogen directly induces expression of retinoic acid biosynthetic enzymes, compartmentalized between the epithelium and underlying stromal cells in rat uterus. Endocrinology. 2004 Oct;145(10):4756-62. doi: 10.1210/en.2004-0514. Epub 2004 Jun 17. PMID: 15205379.
92. Gushchina LV, Yasmeen R, Ziouzenkova O. Moderate vitamin A supplementation in obese mice regulates tissue factor and cytokine production in a sex-specific manner. Arch Biochem Biophys. 2013 Nov 15;539(2):239-47. doi: 10.1016/j.abb.2013.06.020. Epub 2013 Jul 11. PMID: 23850584; PMCID: PMC3818464.
93. Karastergiou K, Smith SR, Greenberg AS, Fried SK. Sex differences in human adipose tissues - the biology of pear shape. Biol Sex Differ. 2012 May 31;3(1):13. doi: 10.1186/2042-6410-3-13. PMID: 22651247; PMCID: PMC3411490.
94. Yasmeen R, Reichert B, Deiuliis J, Yang F, Lynch A, Meyers J, Sharlach M, Shin S, Volz KS, Green KB, Lee K, Alder H, Duester G, Zechner R, Rajagopalan S, Ziouzenkova O. Autocrine function of aldehyde dehydrogenase 1 as a determinant of diet- and sex-specific differences in visceral adiposity. Diabetes. 2013 Jan;62(1):124-36. doi: 10.2337/db11-1779. Epub 2012 Aug 28. PMID: 22933113; PMCID: PMC3526050.
95. Petrosino JM, Disilvestro D, Ziouzenkova O. Aldehyde dehydrogenase 1A1: friend or foe to female metabolism? Nutrients. 2014 Mar 3;6(3):950-73. doi: 10.3390/nu6030950. PMID: 24594504; PMCID: PMC3967171.
96. Ley CJ, Lees B, Stevenson JC. Sex- and menopause-associated changes in body-fat distribution. Am J Clin Nutr. 1992 May;55(5):950-4. doi: 10.1093/ajcn/55.5.950. PMID: 1570802.
97. Obrochta KM, Krois CR, Campos B, Napoli JL. Insulin regulates retinol dehydrogenase expression and all-trans-retinoic acid biosynthesis through FoxO1. J Biol Chem. 2015 Mar 13;290(11):7259-68. doi: 10.1074/jbc.M114.609313. Epub 2015 Jan 27. PMID: 25627686; PMCID: PMC4358144.
98. Siddle K. Signalling by insulin and IGF receptors: supporting acts and new players. J Mol Endocrinol. 2011 Jun 17;47(1):R1-10. doi: 10.1530/JME-11-0022. PMID: 21498522.

99. Yoo HS, Rodriguez A, You D, Lee RA, Cockrum MA, Grimes JA, Wang JC, Kang S, Napoli JL. The glucocorticoid receptor represses, whereas C/EBPβ can enhance or repress *CYP26A1* transcription. iScience. 2022 Jun 9;25(7):104564. doi: 10.1016/j.isci.2022.104564. PMID: 35789854; PMCID: PMC9249609.

100. Reeves PG, Nielsen FH, Fahey GC Jr. AIN-93 purified diets for laboratory rodents: final report of the American Institute of Nutrition ad hoc writing committee on the reformulation of the AIN-76A rodent diet. J Nutr. 1993 Nov;123(11):1939-51. doi: 10.1093/jn/123.11.1939. PMID: 8229312.

101. Rocke AW, Clarke TG, Dalmer TRA, McCluskey SA, Rivas JFG, Clugston RD. Low maternal vitamin A intake increases the incidence of teratogen induced congenital diaphragmatic hernia in mice. Pediatr Res. 2022 Jan;91(1):83-91. doi: 10.1038/s41390-021-01409-6. Epub 2021 Mar 2. PMID: 33654278; PMCID: PMC8770141.

102. Rosselot C, Spraggon L, Chia I, Batourina E, Riccio P, Lu B, Niederreither K, Dolle P, Duester G, Chambon P, Costantini F, Gilbert T, Molotkov A, Mendelsohn C. Non-cell-autonomous retinoid signaling is crucial for renal development. Development. 2010 Jan;137(2):283-92. doi: 10.1242/dev.040287. PMID: 20040494; PMCID: PMC2799161.

103. Kim YK, Quadro L. Reverse-phase high-performance liquid chromatography (HPLC) analysis of retinol and retinyl esters in mouse serum and tissues. Methods Mol Biol. 2010;652:263-75. doi: 10.1007/978-1-60327-325-1_15. PMID: 20552434; PMCID: PMC3716261.

104. Folch J, Lees M, Sloane Stanley GH. A simple method for the isolation and purification of total lipides from animal tissues. J Biol Chem. 1957 May;226(1):497-509. PMID: 13428781.

105. Yoo HS, Cockrum MA, Napoli JL. Cyp26a1 supports postnatal retinoic acid homeostasis and glucoregulatory control. J Biol Chem. 2023 May;299(5):104669. doi: 10.1016/j.jbc.2023.104669. Epub 2023 Apr 1. PMID: 37011860; PMCID: PMC10176252.

106. Zhang Q, Sun X, Xiao X, Zheng J, Li M, Yu M, Ping F, Wang Z, Qi C, Wang T, Wang X. Maternal chromium restriction induces insulin resistance in adult mice offspring

through miRNA. Int J Mol Med. 2018 Mar;41(3):1547-1559. doi: 10.3892/ijmm.2017.3328. Epub 2017 Dec 18. PMID: 29286159; PMCID: PMC5819906.

107. Shen L, He J, Zhao Y, Niu L, Chen L, Tang G, Jiang Y, Hao X, Bai L, Li X, Zhang S, Zhu L. MicroRNA-126b-5p Exacerbates Development of Adipose Tissue and Diet-Induced Obesity. Int J Mol Sci. 2021 Sep 23;22(19):10261. doi: 10.3390/ijms221910261. PMID: 34638602; PMCID: PMC8508536.

108. Zhang C, Seo J, Murakami K, Salem ESB, Bernhard E, Borra VJ, Choi K, Yuan CL, Chan CC, Chen X, Huang T, Weirauch MT, Divanovic S, Qi NR, Thomas HE, Mercer CA, Siomi H, Nakamura T. Hepatic Ago2-mediated RNA silencing controls energy metabolism linked to AMPK activation and obesity-associated pathophysiology. Nat Commun. 2018 Sep 10;9(1):3658. doi: 10.1038/s41467-018-05870-6. PMID: 30201950; PMCID: PMC6131149.

109. Shu L, Zhao H, Huang W, Hou G, Song G, Ma H. Resveratrol Upregulates mmu-miR-363-3p via the PI3K-Akt Pathway to Improve Insulin Resistance Induced by a High-Fat Diet in Mice. Diabetes Metab Syndr Obes. 2020 Feb 14;13:391-403. doi: 10.2147/DMSO.S240956. PMID: 32104036; PMCID: PMC7027849.

110. Stachowiak M. Genome-wide microRNA transcriptome profiles in pluripotent mouse Embryonic Stem Cells and during Retinoic Acid-induced differentiation. Gene Expression Omnibus. 2015 Feb 6.

111. Yang WM, Min KH, Lee W. MicroRNA expression analysis in the liver of high fat diet-induced obese mice. Data Brief. 2016 Dec 1;9:1155-1159. doi: 10.1016/j.dib.2016.11.081. PMID: 27995171; PMCID: PMC5153443.

112. Hochreuter MY, Altıntaş A, Garde C, Emanuelli B, Kahn CR, Zierath JR, Vienberg S, Barrès R. Identification of two microRNA nodes as potential cooperative modulators of liver metabolism. Hepatol Res. 2019 Dec;49(12):1451-1465. doi: 10.1111/hepr.13419. Epub 2019 Sep 11. PMID: 31408567; PMCID: PMC6972499.

113. Crespo Yanguas S, da Silva TC, Pereira IVA, Maes M, Willebrords J, Shestopalov VI, Goes BM, Sayuri Nogueira M, Alves de Castro I, Romualdo GR, Barbisan LF, Gijbels E, Vinken M, Cogliati B. Genetic ablation of pannexin1 counteracts liver fibrosis in a chemical, but not in a surgical mouse model. Arch Toxicol. 2018

Aug;92(8):2607-2627. doi: 10.1007/s00204-018-2255-3. Epub 2018 Jul 9. PMID: 29987408; PMCID: PMC6139022.

114. Bianchi F, Nicassio F, Di Fiore PP. Unbiased vs. biased approaches to the identification of cancer signatures: the case of lung cancer. Cell Cycle. 2008 Mar 15;7(6):729-34. doi: 10.4161/cc.7.6.5591. Epub 2008 Jan 14. PMID: 18239450.

115. Sun CM, Hall JA, Blank RB, Bouladoux N, Oukka M, Mora JR, Belkaid Y. Small intestine lamina propria dendritic cells promote de novo generation of Foxp3 T reg cells via retinoic acid. J Exp Med. 2007 Aug 6;204(8):1775-85. doi: 10.1084/jem.20070602. Epub 2007 Jul 9. PMID: 17620362; PMCID: PMC2118682.

116. Kim MH, Taparowsky EJ, Kim CH. Retinoic Acid Differentially Regulates the Migration of Innate Lymphoid Cell Subsets to the Gut. Immunity. 2015 Jul 21;43(1):107-19. doi: 10.1016/j.immuni.2015.06.009. Epub 2015 Jun 30. PMID: 26141583; PMCID: PMC4511719.

117. Freitas-Lopes MA, Mafra K, David BA, Carvalho-Gontijo R, Menezes GB. Differential Location and Distribution of Hepatic Immune Cells. Cells. 2017 Dec 7;6(4):48. doi: 10.3390/cells6040048. PMID: 29215603; PMCID: PMC5755505.

118. Miao J, Choi SE, Seok SM, Yang L, Zuercher WJ, Xu Y, Willson TM, Xu HE, Kemper JK. Ligand-dependent regulation of the activity of the orphan nuclear receptor, small heterodimer partner (SHP), in the repression of bile acid biosynthetic CYP7A1 and CYP8B1 genes. Mol Endocrinol. 2011 Jul;25(7):1159-69. doi: 10.1210/me.2011-0033. Epub 2011 May 12. PMID: 21566081; PMCID: PMC3125094.

119. Goodwin B, Jones SA, Price RR, Watson MA, McKee DD, Moore LB, Galardi C, Wilson JG, Lewis MC, Roth ME, Maloney PR, Willson TM, Kliewer SA. A regulatory cascade of the nuclear receptors FXR, SHP-1, and LRH-1 represses bile acid biosynthesis. Mol Cell. 2000 Sep;6(3):517-26. doi: 10.1016/s1097-2765(00)00051-4. PMID: 11030332.

120. He Y, Gong L, Fang Y, Zhan Q, Liu HX, Lu Y, Guo GL, Lehman-McKeeman L, Fang J, Wan YJ. The role of retinoic acid in hepatic lipid homeostasis defined by genomic binding and transcriptome profiling. BMC Genomics. 2013 Aug 28;14:575. doi: 10.1186/1471-2164-14-575. PMID: 23981290; PMCID: PMC3846674.

121. Chiang JY. Regulation of bile acid synthesis: pathways, nuclear receptors, and mechanisms. J Hepatol. 2004 Mar;40(3):539-51. doi: 10.1016/j.jhep.2003.11.006. PMID: 15123373.

122. SREBF1 [Internet]. Bethesda (MD): National Library of Medicine (US), National Center for Biotechnology Information; 2004 – [cited 2023 Feb 15]. Available from: https://www.ncbi.nlm.nih.gov/gene/6720

123. Eberlé D, Hegarty B, Bossard P, Ferré P, Foufelle F. SREBP transcription factors: master regulators of lipid homeostasis. Biochimie. 2004 Nov;86(11):839-48. doi: 10.1016/j.biochi.2004.09.018. PMID: 15589694.

124. Wang Y, Nakajima T, Gonzalez FJ, Tanaka N. PPARs as Metabolic Regulators in the Liver: Lessons from Liver-Specific PPAR-Null Mice. Int J Mol Sci. 2020 Mar 17;21(6):2061. doi: 10.3390/ijms21062061. PMID: 32192216; PMCID: PMC7139552.

125. PFKFB3 [Internet]. Bethesda (MD): National Library of Medicine (US), National Center for Biotechnology Information; 2004 – [cited 2023 Feb 15]. Available from: https://www.ncbi.nlm.nih.gov/gene/5209

126. Tóth K, Sarang Z, Scholtz B, Brázda P, Ghyselinck N, Chambon P, Fésüs L, Szondy Z. Retinoids enhance glucocorticoid-induced apoptosis of T cells by facilitating glucocorticoid receptor-mediated transcription. Cell Death Differ. 2011 May;18(5):783-92. doi: 10.1038/cdd.2010.136. Epub 2010 Nov 12. PMID: 21072052; PMCID: PMC3131916.

127. Bakke O. Antagonistic effect of glucocorticoids on retinoic acid induced growth inhibition and morphological alterations of a human cell line. Cancer Res. 1986 Mar;46(3):1275-9. PMID: 3753660.

128. Subramaniam N, Campión J, Rafter I, Okret S. Cross-talk between glucocorticoid and retinoic acid signals involving glucocorticoid receptor interaction with the homoeodomain protein Pbx1. Biochem J. 2003 Mar 15;370(Pt 3):1087-95. doi: 10.1042/BJ20020471. PMID: 12487626; PMCID: PMC1223238.

129. Rayner KJ, Suárez Y, Dávalos A, Parathath S, Fitzgerald ML, Tamehiro N, Fisher EA, Moore KJ, Fernández-Hernando C. MiR-33 contributes to the regulation of cholesterol homeostasis. Science. 2010 Jun 18;328(5985):1570-3. doi:

10.1126/science.1189862. Epub 2010 May 13. PMID: 20466885; PMCID: PMC3114628.

130. Topletz AR, Tripathy S, Foti RS, Shimshoni JA, Nelson WL, Isoherranen N. Induction of CYP26A1 by metabolites of retinoic acid: evidence that CYP26A1 is an important enzyme in the elimination of active retinoids. Mol Pharmacol. 2015;87(3):430-41. doi: 10.1124/mol.114.096784. Epub 2014 Dec 9. Erratum in: Mol Pharmacol. 2020 Jan;97(1):1. PMID: 25492813; PMCID: PMC4352583.

131. Yokota S, Shirahata T, Yusa J, Sakurai Y, Ito H, Oshio S. Long-term dietary intake of excessive vitamin A impairs spermatogenesis in mice. J Toxicol Sci. 2019;44(4):257-271. doi: 10.2131/jts.44.257. PMID: 30944279.

132. Weiss K, Mihály J, Liebisch G, Marosvölgyi T, Garcia AL, Schmitz G, Decsi T, Rühl R. Effect of high versus low doses of fat and vitamin A dietary supplementation on fatty acid composition of phospholipids in mice. Genes Nutr. 2014 Jan;9(1):368. doi: 10.1007/s12263-013-0368-0. Epub 2013 Dec 4. PMID: 24306959; PMCID: PMC3896631.

133. Felipe F, Mercader J, Ribot J, Palou A, Bonet ML. Effects of retinoic acid administration and dietary vitamin A supplementation on leptin expression in mice: lack of correlation with changes of adipose tissue mass and food intake. Biochim Biophys Acta. 2005 May 30;1740(2):258-65. doi: 10.1016/j.bbadis.2004.11.014. Epub 2004 Dec 10. PMID: 15949693.

134. Gao Y, Lu W, Sun Q, Yang X, Liu J, Ge W, Yang Y, Zhao Y, Xu X, Zhang J. Pancreatic lipase-related protein 2 is responsible for the increased hepatic retinyl ester hydrolase activity in vitamin A-deficient mice. FEBS J. 2019 Nov;286(21):4232-4244. doi: 10.1111/febs.14958. Epub 2019 Jun 28. PMID: 31199585.

135. Cassim Bawa FN, Xu Y, Gopoju R, Plonski NM, Shiyab A, Hu S, Chen S, Zhu Y, Jadhav K, Kasumov T, Zhang Y. Hepatic retinoic acid receptor alpha mediates all-trans retinoic acid's effect on diet-induced hepatosteatosis. Hepatol Commun. 2022 Oct;6(10):2665-2675. doi: 10.1002/hep4.2049. Epub 2022 Jul 19. PMID: 35852305; PMCID: PMC9512485.

136. Blaner WS, Li Y, Brun PJ, Yuen JJ, Lee SA, Clugston RD. Vitamin A Absorption, Storage and Mobilization. Subcell Biochem. 2016;81:95-125. doi: 10.1007/978-94-024-0945-1_4. PMID: 27830502.

137. Cho YM, Youn BS, Lee H, Lee N, Min SS, Kwak SH, Lee HK, Park KS. Plasma retinol-binding protein-4 concentrations are elevated in human subjects with impaired glucose tolerance and type 2 diabetes. Diabetes Care. 2006 Nov;29(11):2457-61. doi: 10.2337/dc06-0360. PMID: 17065684.

138. Kwanbunjan K, Panprathip P, Phosat C, Chumpathat N, Wechjakwen N, Puduang S, Auyyuenyong R, Henkel I, Schweigert FJ. Association of retinol binding protein 4 and transthyretin with triglyceride levels and insulin resistance in rural thais with high type 2 diabetes risk. BMC Endocr Disord. 2018 May 10;18(1):26. doi: 10.1186/s12902-018-0254-2. PMID: 29747616; PMCID: PMC5946392.

139. Oliver JD, Rogers MP. Effects of retinoic acid on lipoprotein lipase activity and mRNA level in vitro and in vivo. Biochem Pharmacol. 1993 Feb 9;45(3):579-83. doi: 10.1016/0006-2952(93)90130-o. PMID: 8442757.

140. Shaw N, Elholm M, Noy N. Retinoic acid is a high affinity selective ligand for the peroxisome proliferator-activated receptor beta/delta. J Biol Chem. 2003 Oct 24;278(43):41589-92. doi: 10.1074/jbc.C300368200. Epub 2003 Sep 8. PMID: 12963727.

141. Rieck M, Meissner W, Ries S, Müller-Brüsselbach S, Müller R. Ligand-mediated regulation of peroxisome proliferator-activated receptor (PPAR) beta/delta: a comparative analysis of PPAR-selective agonists and all-trans retinoic acid. Mol Pharmacol. 2008 Nov;74(5):1269-77. doi: 10.1124/mol.108.050625. Epub 2008 Aug 13. PMID: 18701617.

142. Schug TT, Berry DC, Shaw NS, Travis SN, Noy N. Opposing effects of retinoic acid on cell growth result from alternate activation of two different nuclear receptors. Cell. 2007 May 18;129(4):723-33. doi: 10.1016/j.cell.2007.02.050. PMID: 17512406; PMCID: PMC1948722.

143. Ghaffari H, Petzold LR. Identification of influential proteins in the classical retinoic acid signaling pathway. Theor Biol Med Model. 2018 Oct 16;15(1):16. doi: 10.1186/s12976-018-0088-7. PMID: 30322383; PMCID: PMC6190658.

144. Schug TT, Berry DC, Toshkov IA, Cheng L, Nikitin AY, Noy N. Overcoming retinoic acid-resistance of mammary carcinomas by diverting retinoic acid from PPARbeta/delta to RAR. Proc Natl Acad Sci U S A. 2008 May 27;105(21):7546-51. doi: 10.1073/pnas.0709981105. Epub 2008 May 21. PMID: 18495924; PMCID: PMC2396692.

145. Tong L, Wang L, Yao S, Jin L, Yang J, Zhang Y, Ning G, Zhang Z. PPARδ attenuates hepatic steatosis through autophagy-mediated fatty acid oxidation. Cell Death Dis. 2019 Feb 27;10(3):197. doi: 10.1038/s41419-019-1458-8. PMID: 30814493; PMCID: PMC6393554.

146. Chen J, Montagner A, Tan NS, Wahli W. Insights into the Role of PPARβ/δ in NAFLD. Int J Mol Sci. 2018 Jun 27;19(7):1893. doi: 10.3390/ijms19071893. PMID: 29954129; PMCID: PMC6073272.

147. Chisholm DR, Tomlinson CWE, Zhou GL, Holden C, Affleck V, Lamb R, Newling K, Ashton P, Valentine R, Redfern C, Erostyák J, Makkai G, Ambler CA, Whiting A, Pohl E. Fluorescent Retinoic Acid Analogues as Probes for Biochemical and Intracellular Characterization of Retinoid Signaling Pathways. ACS Chem Biol. 2019 Mar 15;14(3):369-377. doi: 10.1021/acschembio.8b00916. Epub 2019 Feb 13. PMID: 30707838.

148. Meyers E. Targeting FABP5 with Small-Molecule Inhibitors and Assessing the Impact on Retinoic Acid (RA)-Resistant Cancers. Case Western Reserve University. 2020 Jan.

149. Echeverría F, Valenzuela R, Bustamante A, Álvarez D, Ortiz M, Espinosa A, Illesca P, Gonzalez-Mañan D, Videla LA. High-fat diet induces mouse liver steatosis with a concomitant decline in energy metabolism: attenuation by eicosapentaenoic acid (EPA) or hydroxytyrosol (HT) supplementation and the additive effects upon EPA and HT co-administration. Food Funct. 2019 Sep 1;10(9):6170-6183. doi: 10.1039/c9fo01373c. Epub 2019 Sep 10. PMID: 31501836.